ECOLOGICAL EFFECTS AND IN-SITU DETECTION OF PARTICULATE CONTAMINANTS IN AQUEOUS ENVIRONMENTS

A Dissertation

by

CHRISTOPHER BYRON FULLER

Submitted to the Office of Graduate Studies of
Texas A&M University
in partial fulfillment of the requirements for the degree of

DOCTOR OF PHILOSOPHY

May 2011

Major Subject: Civil Engineering

Ecological Effects and In-Situ Detection of Particulate Contaminants in

Aqueous Environments

ECOLOGICAL EFFECTS AND IN-SITU DETECTION OF PARTICULATE CONTAMINANTS IN AQUEOUS ENVIRONMENTS

A Dissertation

by

CHRISTOPOHER BYRON FULLER

Submitted to the Office of Graduate Studies of
Texas A&M University
in partial fulfillment of the requirements for the degree of

DOCTOR OF PHILOSOPHY

Approved by:

Chair of Committee,	Robin Autenrieth
Committee Members,	James S. Bonner
	Anthony Cahill
	Thomas McDonald
Head of Department,	John Niedzwecki

May 2011

Major Subject: Civil Engineering

ABSTRACT

Ecological Effects and In-situ Detection of Particulate Contaminants in Aqueous Environments. (May 2011)

Christopher Byron Fuller, B.S., Texas A&M University;

M.S., Texas A&M University-Kingsville

Chair of Advisory Committee: Dr. Robin L. Autenrieth

The ecological effects and mechanistic efficiency of chemical oil spill countermeasures must be evaluated prior to their ethical application during real spill response scenarios. Equally important is the ability to monitor the effectiveness of any spill response in real time, permitting informed response management. In-situ sensors are key components of such event based monitoring and continuous monitoring programs. This project investigates crude oil toxicity as a particulate suspension, suitability of in-situ instrumentation to measure crude oil suspensions, and the applicability of using acoustic backscatter to measure suspended solids and sub-surface oil droplet suspension concentrations.

The ecological effects to inter- and sub-tidal sediment dwelling organisms exposed to crude oil, both treated with a chemical dispersant and un-treated, was evaluated. . Elevated toxicity, expressed as percent mortality and reduced luminescence, and oil concentrations were observed in inter-tidal sediments receiving oil only treatments compared to oil-plus-dispersant treatments. Sub-tidal sediments showed

heterogeneous distribution of crude oil with elevated amphipod mortality compared to no oil controls suggesting an oil-sediment aggregation mechanism. A separate laboratory scale study found that the soluble crude oil fractions were responsible for the observed mortality in pelagic species while the more dominant oil droplet fractions were relatively non-toxic.

Subsequent studies focused on the in-situ detection of crude oil and particle suspensions in aqueous environments. The first showed that both in-situ fluorescence spectroscopy and Laser In-Situ Scattering Transmissometry (LISST) can effectively measure crude oil concentrations in aqueous environments. The applicability of the LISST implies that crude oil in an aqueous medium can be measured as a particle suspension. Acoustic backscatter (ABS) was investigated for its applicability as a surrogate measurement technology for aqueous particle suspensions. This study showed a log linear correlation between ABS and volume concentration (VC) over a variable particle size distribution. This correlation is due to the dependency of both ABS and VC to the particle size distribution. Log-linear ABS responses to oil-droplet suspension volume concentrations were also demonstrated. However, the inability to reproduce response factors suggest that more work is required to produce viable calibrations that may be used for sub-surface oil plume detection.

DEDICATION

I dedicate this work to my children, Jacob and Cayley Fuller, and hope this achievement demonstrates to them the value of perseverance. I also dedicate this work to my parents, Byron and Carolyn Fuller, and my sister, Michelle Walker, for their unyielding love and encouragement throughout the duration of my graduate work.

ACKNOWLEDGEMENTS

I would like to thank my committee chair, Dr. Robin Autenrieth, and my committee members, Dr. James Bonner, Dr. Anthony Cahill, and Dr. Tom McDonald, for their guidance and support throughout the course of this research.

Special thanks is extended to Dr. James Bonner who served as my principal advisor throughout my graduate experience. He has taught me that anything is possible with perseverance. Completion of this project was made possible only through his continuous encouragement.

I would like to thank Robin Jamail at the Texas General Land Office and Mr. John Cronin at the Beacon Institute, Beacon, New York for their financial support.

I would like to extend a special thanks to my colleagues, Dr. Cheryl Page, Dr. Shahidul Islam, and Mr. John Perez, for their academic guidance and critical reviews of my research. More importantly, their friendship and moral support during difficult times enabled me to continue with this work even when I believed its completion was impossible.

I would also like to thank the numerous support staff who helped me throughout the duration of this work.

TABLE OF CONTENTS

CHAPTER Page

CHAPTER Page

CHAPTER Page

LIST OF FIGURES

FIGURE Page

FIGURE Page

FIGURE Page

LIST OF TABLES

CHAPTER I

INTRODUCTION

Statement of Purpose

Coastal regions are important to the global economy as demonstrated in the U.S with more than half the population residing in coastal counties with an additional growth of 12 million expected by the year 2015 (Crosset et al. 2004). Spatially, areas affected by coastal processes can extend far inland such as the Hudson River, NY where tidal influences are observed 247 km inland (Wall et al. 2006). In oil-rich regions, concentrated human impacts extend to the outer continental shelf in water depths exceeding 1,524 meters (MMS 2008). As such, coastal areas include diverse and sensitive ecosystems that must be protected and in some cases remediated from the deleterious effects of ever growing anthropogenic activity.

In coastal systems, environmental change resulting from environmental activity occurs during a small fraction of time and may be characterized as a series of episodic events (Bonner et al. 2003a). These events may originate as natural processes or human activity, both of which have a capacity for catastrophic effects as recently demonstrated along the U.S. Gulf Coast by Hurricane Ike and the Deepwater Horizon oil spill, respectively. Selection of appropriate response actions to damaging environmental

---

This dissertation follows the style of *Environmental Monitoring and Assessment.*

events require that both the positive and negative effects be assessed with respect to ecological impacts and overall effectiveness. Any comprehensive assessment requires a foundation of fundamental effects (e.g. toxicity) data from which a selected response technology can be compared against other known response actions. It is equally important to monitor real world applications of the selected response to ensure the mitigation strategy achieves the desired result. Considering the temporal and spatial scales of episodic marine events requires that new sensor technology and protocols be developed to accurately define the event's intensity and extent, and be capable of monitoring the efficacy of the selected response action.

Background

Concerns persist in the oil spill response community regarding both the effectiveness and ecological effects of chemical dispersants as recently demonstrated during British Petroleum's response to the Deep Water Horizon oil spill, a Spill of National Significance (SONS), which occurred April 20, 2010 (Gibbs 2010). Previous to this event, the Texas General Land Office (TGLO) and the Marine Spill Response Corporation (MSRC) commissioned the design and construction of a meso-scale test facility to evaluate oil spill chemical-counter-measure effectiveness and subsequent ecological impacts on affected coastlines. Following successful prototype testing in 1993, construction of the full scale facility the Coastal Oil-Spill Simulation System (COSS) was completed in 1997 (Kitchen et al. 1997). In 1999, COSS was transferred to the Texas A&M University System and the name was changed to the Shoreline

Environmental Research Facility (SERF) signifying an expansion of the research initiatives to include other environmentally important processes affecting coastal systems.

Initial SERF research efforts paralleled the TGLO's objective to evaluate and develop oil spill response technology for near shore applications with an emphasis on chemical dispersants. Petroleum related activities (production, refining, and transportation) are more concentrated in near shore regions and thus more susceptible to accidental releases than locations farther at sea. However, as observed in the recent BP Deep Water Horizon oil spill, coastal margins may also be threatened when oil slicks originating from off-shore spills are transported by wind and ocean currents. Coastal margins include sensitive wetlands that serve as nurseries for our fisheries and provide habitat many other species (Wood et al. 1997). These areas are susceptible to significant damage resulting from subsequent remedial actions including physical removal processes and *in-situ* burning. In these situations bioremediation may be the best response option (Barataria-Terrebonne National Estuary Program 2010). The significant role biological processes play in reducing the petroleum contaminant burden and ultimate recovery of oil impacted wetlands has been demonstrated in many studies (Harris et al. 1999; Mills et al. 2003, 2004; Mueller et al. 1999, 2003; Simon et al. 1999, 2004; Townsend et al. 2000). In contrast to biological treatments, the use of a chemical shoreline cleaner did not significantly improve the removal of petroleum from wetland test plots (Bizzell et al. 1999). These studies indicate that natural processes are important to wetland recovery following impact by oil and further suggest that remedial

actions are limited to optimizing the conditions for biodegradation.

Chemical dispersants

Considering the limited spill response alternatives following landfall emphasizes the need to prevent oil spilled at off-shore locations from reaching sensitive coastal habitats. Chemical dispersants are one response technology developed to address this need. These are surface active agents designed to enhance oil entrainment in the water column via the formation of oil-surfactant micelles that may be easily diluted in dynamic marine systems. Studies have shown that chemically dispersed oil is readily consumed by oil degrading bacterial colonies (MacNaughton et al. 2003; Harris et al. 2001). Furthermore, chemical dispersant applications have been shown to reduce oil accumulations in both wetlands and in simulated sandy beaches (Page et al. 2000a, 2002a). Despite the potential benefits of dispersant use, existing regulations restrict chemical dispersant applications within 3 nautical miles from shore and in water depths less than 10 meters (RRT-6 2005) due to ecological concerns of both the dispersant and the resultant oil suspensions.

The acute toxicity of dispersants and dispersed oil on various marine species has been evaluated extensively with widely different results. Dispersants have been reported to adversely affect the respiratory and nervous systems in a wide range of marine species (Scarlett et al. 2005; Khan and Payne 2005). Other studies have demonstrated that dispersants result in elevated crude oil concentration, bioavailability, and toxicity compared to no dispersant (Kanga et al. 1997; Couillard et al. 2005; Ramachandran et al.

2004). Conversely, a comparative study showed that the dispersant applications did not increase the crude oil toxicity (Long and Holdway 2002).

While many studies have characterized the harmful effects of dispersant and dispersed oil on marine organisms they do not necessarily predict the effects resulting from realistic spill response exposures. Page et al. (2000b) showed that chemically dispersed oil exists primarily as a colloidal suspension while truly soluble fractions make a minor contribution to the total oil concentration. The colloidal fractions are subject to the combined mechanisms of aggregation and subsequent resurfacing via Stoke's settling (Sterling et al. 2004a). The soluble fractions are subject other transport mechanisms including diffusion and volatilization. The combined effect of these mechanisms is a declining exposure from a pulsed input (i.e. oil spill). This observation has been recognized by a group of researchers (Chemical Response to Oil Spills Ecological Effects Research Forum, CROSERF) who implemented a declining exposure toxicity protocol to evaluate oil spill toxicity and have shown reduced toxic effects relative to standard continuous exposure evaluations (Singer et al. 1991, 1993; Bragin et al. 1994; Fuller et al. 2004; Pace et al. 1995).

The two basic oil fractions (i.e. soluble and colloidal) may also differ substantially in there respective toxicities. Early studies showed that the crude oil fractions responsible for the observed toxicity are the more soluble lower-molecular weight polycyclic aromatic hydrocarbons (PAH) (Anderson et al. 1974; Couillard et al. 2005). Fuller et al. (2004) showed it was the soluble crude oil fractions that were responsible for the observed mortality not the more prevalent colloidal fractions. These

observations illustrate the need to recognize dispersed oil exposures as a multi-phase system with each phase differing in their respective transport mechanisms and biological effects.

While laboratory scale bioassays provide a means to evaluate the relative environmental risks of various contaminants (i.e. oils and dispersants), they fail to accurately emulate real world exposures. To address this deficiency, researchers must rely on field-scale or meso-scale evaluations. Field trials involving planned and intentional oil releases have been conducted on a limited bases in both the United States (Page et al. 2002a; Mills et al. 2004), and Europe (Merlin 2008). However, existing regulatory environments typically restrict full field scale evaluation to "spills of opportunity". The difficulty in conducting scientific studies during actual spill responses is hindered by the logistics required to mobilize scientific equipment and human resources in a timely manner to often remote locations. Additionally, it is difficult to establish sufficient experimental control and replication during an emergency response. To address these deficiencies, a mass balance experimental approach was developed to evaluate chemically dispersed oil exposures under scaled hydrodynamic conditions (Bonner et al. 2003b). These methods were used to evaluate the behavior of chemically dispersed oil and whole oil in meso-scale oil spill simulations (Page et al. 2000a). Companion studies evaluated the toxicity of the simulated oil spills in the various environmental compartments with representative indicator organisms (Fuller et al. 1999; Bragin et al. 1999).

Oil spill monitoring

While laboratory- and meso-scale studies provide useful guidelines for dispersant use during actual spill response applications, quantitative field observations are needed to provide spill responders with valid feed back information required to make informed operational decisions. To address these needs, the U.S. Coast Guard developed the Special Monitoring of Applied Response Technologies (SMART) protocol, to monitor dispersant application effectiveness during spill responses (U.S. Coast Guard 2006). The primary sensor used in this protocol is an *ex-situ* single-wave length fluorometer. The fact that this sensor is *ex-situ* posed limitations and special requirements for deployment on board response vessels at sea. Instrument set up and calibration during emergency response scenarios were presented as significant deficiencies by the on scene response parties including the U.S. Coast Guard. To address these concerns and further advance the development of an event based monitoring program for dispersant use in near shore waters, the TGLO charged our research team with the establishment of a vessel-based monitoring system using *in-situ* sensors to be mobilized during an actual spill of opportunity (Ojo et al. 2007a). In addition to the vessel-based monitoring program, fixed monitoring stations were established to provide real time environmental data (Bonner et al. 2003a). The fixed platforms provide observations with high temporal resolutions and are important to indicate when and where episodic events have occurred while mobile platform deployments are useful to define an event's spatial extent. In addition to this system's value as an oil spill monitoring tool, it has proven to be valuable in the development of a constituent transport model and helped to define the effect of shear

augmented and turbulent diffusion processes in an estuary (Ojo et al. 2006a, 2006b, 2007b).

In addition to oil and chemical spills, many environmentally significant events, for example hypoxia, water column stratification, flooding, particle resuspension, etc., can be characterized as episodic events. Characterizing the fundamental processes controlling such events is limited by insufficient data at the required spatial density and temporal frequency (Montgomery et al. 2007). To address these needs, integrated real-time observatory systems including IOOS (Integrated Ocean Observing System) and WATers (WATer and Environmental Research Systems) have been established by NOAA (National Oceanographic and Atmospheric Administration) and NSF (National Science Foundation), respectively (NOAA 2010a; Montgomery et al. 2007). Our previously established sensor network including both mobile and stationary environmental monitoring platforms in Corpus Christi Bay, a designated National Estuary, was selected as a WATERs test bed (WATERs Network 2005). As such, the applicability of this monitoring system was extended beyond oil spill monitoring. The initial research objective addressed with the Corpus Christi Bay test bed was an annually recurring hypoxic event (Montagna and Kalke 1992). Data collected from the stationary platforms identified water column stratification as a possible mechanism responsible for estuarine hypoxia (Islam et al. 2010a). The original mobile profiling system developed by Ojo et al. (2007a) was revised and used to characterize water column stratification stability (Islam et al. 2011a). Finally, data from the fixed and mobile sensing platforms was integrated to capture a low oxygen condition in an area with no previous record of

hypoxia (Islam et al. 2011b). These examples demonstrate sensor network applicability for environmental disturbance monitoring and characterizing the fundamental processes affecting the overall system (i.e. bay) health.

The ability to establish environmental observatory networks is dependent on the implementation of *in-situ* instrumentation. Single wavelength fluorescence instruments have demonstrated their applicability for oil spill monitoring as made evident by their broad commercial availability. Among the benefits provided by fluorometry include large detection limit ranges and analyte specificity (Guilbault 1990). However, interferences including background fluorescence, stray light, and light scattering in turbid waters may preclude its use (Lakowicz 1999).

Considering crude oil plumes as particulate suspensions, as opposed to a molecular solution, opens the possibility of measuring crude oil suspension using optical methods generally used to measure suspended solids including optical transmittance and volume concentration determinations. Both measures are dependent on the particle (droplet) size distribution (Agrawal and Pottsmith 1994). Measuring oil droplet volume concentration has been used successfully to measure crude oil droplet aggregation kinetics (Sterling et al. 2004b). It is important to recognize that during aggregation processes, mass is conserved while volume is not (Sterling et al. 2004b). Considering the dependence of optical transmittance and volume concentration determinations on the size distributions suggest that changes to the particle size distribution can affect the observed transmittance and/or volume concentration with no change in the mass concentration.

In addition to existing as discrete droplets, oil-droplets will interact with other suspended solids to form oil-particle aggregates. The formation of these oil-particle-complexes and their subsequent effects on oil transport mechanisms has been investigated (Sterling et al. 2004c; Page et al. 2000b, 2002b; Le Floch et al. 2002). Other poorly soluble contaminants have also been shown to form oil-sediment aggregates. For example, heavy metals, pesticides and polychlorinated biphenyls demonstrate a propensity to adsorb to sediment particles in aqueous environments (Kuwabara et al. 1989; Garton et al. 1996). Considering the particulate nature of many environmentally important contaminants, opens the possibility for surrogate detection methods.

Acoustic backscatter has received considerable interest as a surrogate suspended solids measurement technology (Wall et al. 2006, Gartner 2004; Hoitink and Hoekstra 2005). The physical laws of attenuation and backscatter that apply to optical sensors also apply to acoustic measurement devices (Reichel and Nachtnebel 1994). Acoustic based suspended solids determination methods have inherent advantages over optical methods including the ability be deployed as *in-situ* remote sensing devices with its sensing range limited by the range of the acoustic signal. Conversely, optical sensors are essentially point source measurement devices and thus restricted in the spatial resolution provided by a single instrument (Hoitink and Hoekstra 2005). Additionally, acoustic methods are less affected by biological fouling and sedimentation than optical methods (Hamilton et al. 1998). Therefore, they are well suited to deployment in areas characterized by high biological productivity and/or those that receive heavy sediment

loads.

The above characteristics suggest that acoustic backscatter is a viable technology to estimate aqueous particle suspension concentrations. In natural systems, acoustic backscatter calibrations to suspended solids have demonstrated spatial and temporal dependencies due to variations in particle size distributions (Hoitink and Hoekstra 2005). As such, site specific acoustic backscatter-suspended sediment concentration relationships have been used to reasonably estimate the suspended solids mass concentrations (Wall et al. 2006). However, the methodology is unable to determine the effects due to changes in the suspended particle sizes (Reichel and Nachtnebel 1994). The common objective in the previous citations was to estimate the suspended solids mass concentration with the acoustic backscatter. However, Rayleigh scattering theory gives the acoustic target strength as function of the particle size distribution, number concentration, acoustic wavelength, and intensity (Urick 1983). This suggests that acoustic backscatter response should correlate with particle volume concentration which is also inferred from the particle size distribution (Agrawal and Pottsmith 1994).

Considering that dispersed oil plumes exist primarily as droplet suspensions suggests that acoustic backscatter methodology may be extended to quantify sub-surface oil plumes. The need to develop this technology was demonstrated during the recent British Petroleum-Deepwater Horizon oil spill where a sub-surface oil plume was detected using autonomous underwater vehicles and ship-cabled samplers (Camilli et al. 2010). The applicability of acoustic backscatter detection of sub-surface oil plumes has been demonstrated in field experiments where echo sounders were used to track sub-

surface oil and gas releases (Adams and Socolofsky 2005). While it is clear that oil droplet suspensions will result in acoustic backscatter responses, further testing is required to evaluate if this technology can be used for quantitative determinations.

Objectives

This project will investigate the ecological effects of chemical oil spill countermeasures and quantitative methods to characterize contaminant suspensions in aqueous environments. The specific objectives addressed in this study include the following:

1. Evaluate the toxicity of beach sediments exposed to oil suspensions generated in a meso-scale experiment with and without chemical dispersants. Dispersant applications were expected to reduce oil accumulation on the beach sediment substrates and lead to reduced toxicity relative to no dispersant use.
2. The toxicity of oil, dispersant, and oil plus dispersant were evaluated under continuous and declining exposures. The declining exposures were expected to result in decreased toxic responses relative to the continuous exposure.
3. *In-situ* optical sensors were evaluated for their ability to quantify crude oil suspensions in artificial sea water. This study was expected to provide information regarding applicability of relevant excitation and emission spectra detection limits for the fluorescence sensors tested. Considering the particulate nature of oil suspensions, it was also expected that laser *in-situ* scattering could be used as a viable detection alternative.

4. Acoustic backscatter was evaluated in a laboratory test tank as a surrogate technology for quantitative suspended solids measurements. Considering that acoustic backscatter is a function of the particle size distribution it was expected that acoustic back scatter would correlate with volume concentration over a variable particle size distribution.
5. The acoustic backscatter response to oil droplet suspensions was evaluated as a quantitative subsurface oil plume detection technology. The acoustic backscatter response was further evaluated as a function of variable particle size distribution to evaluate the effects of interfering ambient particles.

CHAPTER II

COMPARATIVE TOXICITY OF SIMULATED BEACH SEDIMENTS IMPACTED WITH BOTH WHOLE AND CHEMICAL DISPERSIONS OF WEATHERED ARABIAN MEDIUM CRUDE

Overview

The ecological impact on sediment dwelling organisms exposed to crude oil, both treated with a chemical dispersant and un-treated, was evaluated in simulated beach sediments at the Shoreline Environmental Research Facility in Corpus Christi, TX. Both inter- and sub-tidal sediment samples collected during a meso-scale dispersant effects study were evaluated for toxicity using the amphipod, *Leptocheirus plumulosus.* Inter-tidal sediment elutriates were also evaluated with the luminescent bacteria, *Vibrio fisheri.* Amphipod exposures to inter-tidal sediments receiving oil-control treatments resulted in higher mortality than sediments receiving oil-plus-dispersant treatments. Only sediment elutriates prepared with oil-control treatments produced a measurable toxic response with the bacterial assay. Conversely, sub-tidal sediment samples receiving oil-plus-dispersant treatments showed elevated amphipod mortality compared to oil-control treatments. When lethal-plus-sub-lethal amphipod effects were evaluated, there was no difference between the oil-control and oil plus dispersant treatments. Total Petroleum Hydrocarbon (TPH) analysis showed that inter-tidal sediments receiving oil-control treatments had significantly higher TPH concentrations than both oil-plus-dispersant and no-oil control treatments. There was no correlation between sub-tidal

amphipod responses and TPH concentrations.

Introduction

Chemical dispersant use as an oil-spill chemical counter measure in U.S. waters is currently regulated by regionally specific pre-approval zones that generally restrict dispersant use to deeper offshore areas (i.e. where water depths exceed 33 to 60 ft and distances from shore exceed 0.5-3 nautical miles) due to ecological concerns of both the dispersants and chemically dispersed oil (RRT-6 2005). Dispersant exposures have been reported to result in non-reversible respiratory damage and reversible nervous system damage (Scarlett et al. 2005). Both bio- and synthetic- surfactants have been shown to result in elevated aromatic petroleum solubility and toxicity (Kanga et al. 1997). Other studies showed that dispersants resulted in elevated crude oil concentrations, bioavailability, and larval fish mortality compared to no dispersant use (Couillard et al. 2005; Ramachandran et al. 2004). Gill damage has been reported in finfish exposed to dispersant and dispersed oil (Khan and Payne 2005).

While toxic effects are associated with dispersant exposures, currently used dispersants are less toxic than the dispersed oil (Fuller et al. 2004; NRC 2005). Others have shown chemically dispersed oil exposures to display similar or reduced toxicity compared to oil only exposures. Cohen et al. (2003) showed that fish exposed to both oil only and chemically dispersed oil had similar biliary (bile duct) PAH concentrations. Liu et al. (2006) found no significant toxicity difference between Alaska North Slope Crude (ANSC) oil and ANSC + Corexit™ as indicated by the median lethal

concentrations determined with gulf killifish, eastern oyster, and white shrimp. Dispersants caused elevated crude oil exposure concentrations while the toxicity of the chemically dispersed oil, as indicated by the toxicity endpoint, was equal to or less than the oil only exposures (Long and Holdway 2002; Fuller et al. 2004).

Dispersants are generally composed of surfactants in a solvent carrier and are designed to enhance the formation of oil droplets and their entrainment into the water column. Once entrained, the droplet concentration may be reduced by biodegradation and physico-chemical processes. Harris et al. (2001) showed that chemically dispersed oil readily biodegraded under aerobic conditions. More recently, a submerged dispersed oil plume resulting from the British Petroleum Deepwater Horizon blowout was found to have stimulated indigenous petroleum-degraders (Hazen et al. 2010). Sterling et al. (2004a, 2004b, 2004c, 2005) showed oil-oil and oil-particle aggregations and subsequent Stokes settling to be important dispersed oil transport mechanisms in marine environments. A mesocosm study showed that dispersant treatments increased water column PAHs, accelerated dissolution and biodegradation of PAHs, and settling of PAHs in sediment traps (Yamada et al. 2003). The environmental benefit of these processes has been demonstrated as reduced oil accumulations in both wetland and simulated sandy beaches compared to no-dispersant treatments (Page et al. 2002a, 2000a).

Before the regulatory community will consider dispersants for near shore use, more data are needed to demonstrate the efficacy and safety of these chemicals compared to other methods. Current near shore counter measures are often restricted to

physical containment and removal methods (i.e. booming and skimming) which are not effective with all spills. Thus, when a spill occurs near shore, the response options are limited. The incentives to develop and approve effective response technologies for near shore applications include both the need to prevent or reduce ecological harm, and secondly to reduce the expense of remediation. If dispersants can be shown to be ecologically safe in near shore applications, then their use as a chemical countermeasure may be extended to these areas.

Most dispersant and dispersant plus oil toxicity studies have been restricted to laboratory settings where chemical oil dispersions were tested and compared against physical oil dispersions (Bragin et al. 1994; Bragin and Clark 1995; Fuller et al. 2004). Additionally, previous studies have focused on water column toxicity, not inter-tidal or sub-tidal substrate toxicity. While it is possible to conduct sediment toxicity studies in the laboratory, there is a lack of data describing the shoreline accumulation of constituents associated with chemically treated oil-spills. Thus, it is difficult to prescribe shoreline dosages that realistically simulate shoreline exposures associated with an actual spill event. These concerns were addressed in a comprehensive meso-scale physical fate and ecological impact study conducted at the Shoreline Environmental Research Facility (formerly Coastal Oil Spill Simulation System) in Corpus Christi, Texas (Page et al. 1999, 2000a; Fuller et al. 1999). A mass balance approach was used to evaluate the oil's physical fate by determining the fraction of total oil added, residing in each of three relevant environmental compartments (Page et al. 2000a). A series of *ex-situ* bioassays were used to evaluate sediment toxicity with samples collected from

both the inter- and sub-tidal zones impacted with oil-control and oil-plus-dispersant treatments. Two separate protocols were used for this study including sediment dwelling amphipod and the Microtox® sediment-elutriate bioassays.

Materials and Methods

Mesocosm experiment

Modeling standard sediment toxicity protocols for marine amphipods (ASTM 1997), a ten-day meso-scale oil and dispersant fate and effects study was conducted in eight wave tanks measuring 33.5 m (length) by 2.1 m (width) by 2.4 m (height). Each tank was equipped with a computer-controlled wave board that can produce variable wave patterns and feedback circuits to automatically control the tidal range and cycles. Tidal cycles were simulated with a continuous seawater supply taken from the Laguna Madre, Texas. Sea water intake and effluent ports were located between the wave board and the beach substrate (Fig. 2.1). Additional details of the facility are provided in Kitchen et al. (1997).

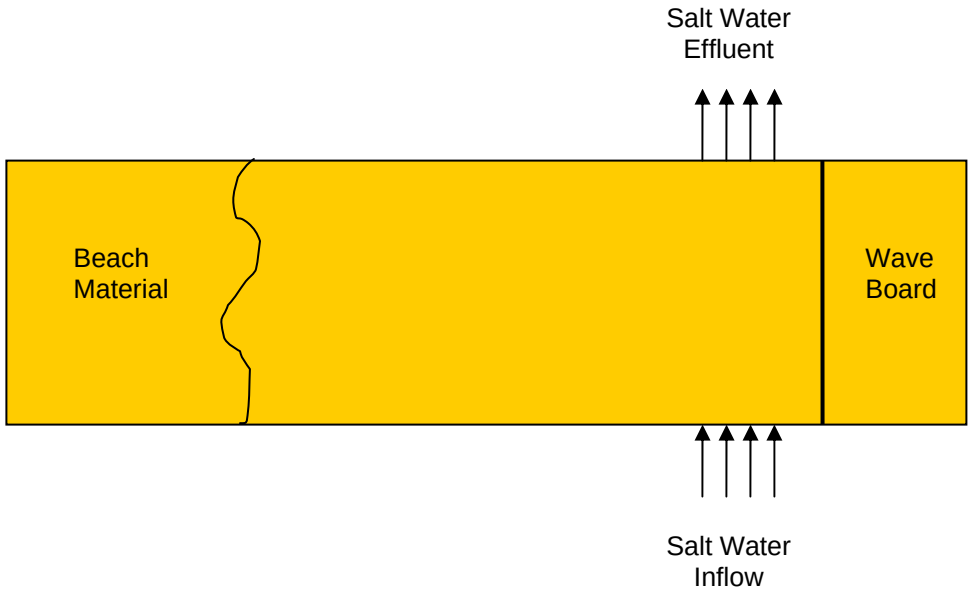

Fig. 2.1 Plan view wave tank schematic showing position of salt water inflow, effluent, beach and wave board (not to scale).

Wave and tidal regimes, beach profile, and ecological zones

Simulated beaches were constructed in the wave tanks with fine mortar sand with the closest available grain size to local beaches. The sand was initially placed in the tanks at an approximate slope of 10 degrees with a flat 3-m stretch extending from just above the high tide mark to back tank wall. This zone allowed the surf swash to extend to the back tank wall at high tide. Once the initial beach profiles were established in each tank, the semi-diurnal tide and wave cycles were initiated to set and stabilize the beach face.

Natural sea-water (Laguna Madre, Texas) was continuously circulated through the wave tanks throughout the experiment to simulate tides with a 12-hour period and a

stage variance of 61 cm. The tidal simulations were generated by maintaining a constant effluent flow rate at 200 l/min and varying the influent flows. Wave patterns followed a repeating 20-minute cycle that included 12 minutes of 3-inch (7.6cm) waves, followed by 1 minute quiescent period, 6 minutes of 5-in (12.7cm) waves, followed by another 1 minute quiescent period. Wave and tidal cycles were maintained for the 10 day experiment duration.

The inter-tidal zone was defined as the beach area between the high and low tide water levels which extended between the 3.5 and 8.5 m transect (measured from the beach wall). The sub-tidal zone was defined as the area below the low tide water level and extended from the 8.5 m transect (measured from the beach wall) to the wave board (Fig. 2.2). Sub-tidal beach sands extended approximately to the 20 m transect.

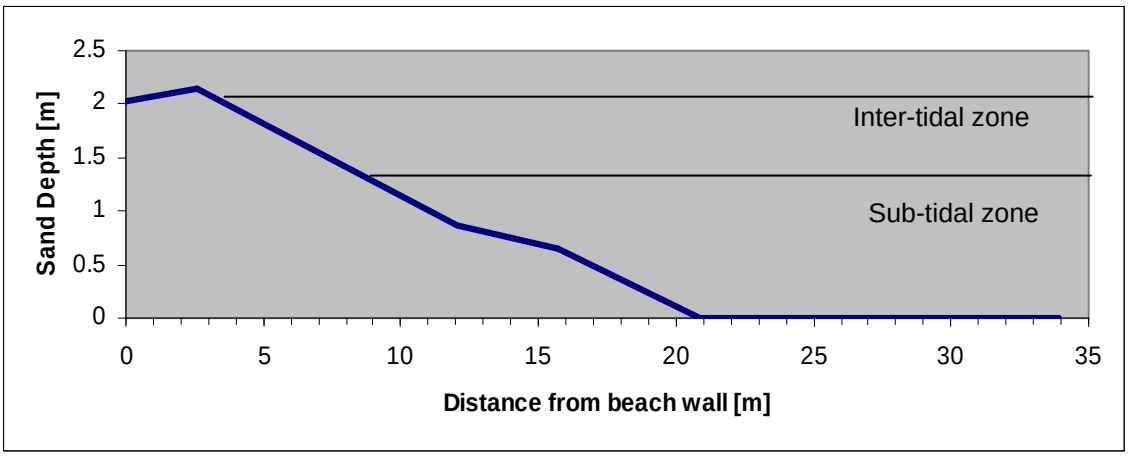

Fig. 2.2 Beach slope profile with inter- and sub-tidal zones for biological sampling shown (not to scale).

Experimental treatments

Eight tanks were randomly assigned one of three treatments: oil-control (3 tanks), oil-plus-dispersant (3 tanks), or no-oil control (2 tanks). To address sampling logistics and to meet environmental permit restrictions, experimental tank start up was staggered over a three day period. Each tank was covered at startup by a portable shelter and four blowers were placed near the wave board to simulate an onshore wind of approximately 5 km per hour. After 24 hours, the shelter and blowers were removed. Each tank was monitored for 10 days.

Crude oil application

Saudi Arabian medium crude oil was used in all oil-control and oil-plus-dispersant exposures. Prior to experimental applications, the oil was artificially weathered by air stripping in an enclosed-but-vented tank, until volume loss 30-35 % stabilized. This process simulated the oil characteristics expected following an actual spill at sea and reduced oil variability between replicate treatment applications. The weathered oil had a specific gravity of 0.9129, kinematic viscosity of 102.4 centistokes and 20° C, and a Reid vapor pressure of 2.1 kPa at 37.8°C (Page et al. 2000a). Each oil-control treatment tank received 6 liters of oil that was gently poured onto the water surface near the wave board. Care was taken to minimize oil penetration into the water column.

Oil plus dispersant treatments were prepared with the oil spill dispersant Corexit® 9500 (Nalco, Sugarland, Texas). The exact dispersant formulation is proprietary,

however the hazardous components and percentages include hydrotreated light petroleum distillates (10-30%), propylene glycol (1-5%), and proprietary organic sulfonic acid salts (10-30%) (Nalco 2005). Nalco (2010) recently provided more detailed ingredient information (Table 2.1) to the U.S. EPA. Prior to application into respective mesocosm tanks, 6 liters of the weathered oil (neat) was premixed with 600 ml of Corexit® 9500 (neat). The neat mixture was then mixed with seawater in a 500-gallon (1,893 liters) mixing vessel. The sea water-oil-dispersant mixture was then pumped into the respective wave tanks as normal tidal inflow. The tidal effluent was re-circulated between the wave tank and the mixing vessel to ensure that all the oil and dispersant had been introduced and well mixed throughout the wave tank. This application technique simulated a well-mixed dispersed oil plume approaching a beach area. After one hour, the re-circulation was terminated and normal wave tank tidal influent and effluent processes were restored.

Table 2.1 Corexit® 9500 ingredients. Adapted from Nalco (2010). * Contains 2 Propanediol.

CAS #	Name	Common Use Examples
1338-43-8	Sorbitan, mono-(9Z)-9-octadecenoate	Skin cream, body shampoo, emulsifier
9005-65-6	Sorbitan, mono-(9Z)-9-octadecenoate, poly(oxy-1,2-ethanediyl) derivatives	Baby bath, mouth wash, face lotion, emulsifier
9005-70-3	Sorbitan, tri-(9Z)-9-octadecenoate, poly(oxy-1,2-ethanediyl) derivatives	Body/Face lotion, tanning lotions
577-11-7	*Butanedioic acid, 2-sulfo-, 1,4-bis(2-ethylhexyl) ester, sodium salt (1:1)	Wetting agent in cosmetic products, gelatin, beverages
29911-28-2	Propanol, 1-(2-butoxy-1-methylethoxy)	Household cleaning products
64742-47-8	Distillates (petroleum), hydrotreated light	Air freshener, cleaner

Sediment sampling

Sediments used in the *ex-situ* toxicity tests (i.e. amphipod and Microtox assays) were collected from fiddler crab and polychaete exposure cages used during the *in-situ* biological monitoring portions of the experiment. The fiddler crab cages were filled with a 2:1 mixture of non-nutrient enriched soil and sand to mimic the desired fiddler crab substrate and partially buried in the upper-inter-tidal zone of each wave tank prior to introduction of fiddler crabs and initiating test treatments (Fig. 2.3). Polychaete chambers were made from 5-gal plastic buckets (38 x 29 cm diam.) and filled with beach sand to a depth of 18 -20 cm. To prevent polychaetes from escaping while allowing water exchange in the chambers, the tops were closed with 2-mm Nitex® screen. The chambers were positioned at the bottom of the wave tanks at the 20 m transect from the beach wall. Cages/chambers were sacrificially sampled at predetermined sampling times following oil applications. When sampled, a 5-cm diameter core from the top 5-cm was collected from the respective cage/chamber for petroleum chemistry analysis. The remaining top 5-cm of sediment was sampled and stored at 4° C until used in toxicity tests.

A)

B)

Fig. 2.3 A) Inter-tidal crab cage at low tide, B) inter-tidal crab cages in oil-control treatment tank showing heterogeneous oil distribution.

Toxicity assays

Amphipod and Microtox® toxicity assays were conducted with sediment samples collected at 24- and 96- hours from the inter-tidal zone (fiddler crab cages). Sub-tidal sediment samples collected at 96-hours from the polychaete chambers were evaluated only with the amphipod bioassay by Exxon Biomedical Sciences, Inc., East Millstone, NJ (EBSI). For inter-laboratory comparison and quality control, 96 hour, $CdCl_2$ water only reference toxicant tests were performed at both laboratories. Additionally, reference sediments provided by Chesapeake Cultures were used as negative controls.

Amphipod bioassay

The amphipod assay was conducted according to ASTM (1997) guidelines. Briefly, a 2-cm sediment layer was placed into a 1-liter glass beaker (exposure chamber). Each sediment sample was split between 3 replicate chambers. Additionally, a 4 oz. aliquot of each homogenized sample was collected and stored at 4º C for total petroleum hydrocarbon (TPH) analysis. The sediment in each test chamber was temporarily covered with a foil disk to reduce sediment suspension while seawater (30 psu) was added to each chamber to a nominal 8 cm depth above the sediment. The test chambers were gently aerated (≥ 2 cm above sediment) for the experiment duration. Following a 24-hour stabilization period, 20 organisms were randomly added to their respective exposure chambers. The test chambers were housed in a climate controlled room maintained at 21±1°C.

Adult amphipods *(L. plumulosus)* were purchased from Chesapeake Cultures and

shipped in water with a salinity of 25 psu. Once received, the organisms were acclimated in sand (<500-micron grain size) and test water (30 psu) for 3-5 days. The organisms were fed *ad libitum* during the acclimation period. Prior to loading the organisms into their exposure chambers, they were sieved from the acclimation sand, carefully pipetted into 70-ml beakers, and then transferred to their respective exposure chambers. Each exposure chamber received 20 organisms. The exposure period was 10 days under continuous illumination, at which time the amphipods were evaluated for survival.

To ensure the reliability of the amphipod test results, both negative control and Cadmium reference toxicant assays were performed concurrently with the inter-tidal and sub-tidal sediment assays. Negative controls used reference sediments (i.e. substrate that was used to ship amphipods) provided by the organism supplier. For both laboratories, negative control sediments resulted in cumulative 90% and 92% survival and is acceptable to the published guidelines (ASTM 1997). The 96-hr Cadmium reference toxicant test LC50 = 3.3 mg/L with 95% confidence intervals of 2.5-5.1 mg/L. EBSI's 96-hr reference toxicant test LC50 = 1.6 mg/L with 95% confidence interval of 0.6-6.6 mg/L. LC50 values were calculated using the Probit procedure (Finney 1971) or SAS/STAT (1989). Additional quality control was ensured by monitoring water quality parameters including; dissolved oxygen, temperature, and pH. These parameters remained within acceptable ranges for the test duration.

Microtox bioassay

Toxic responses with the Microtox® system are characterized by the fluorescence inhibition of the bacterium *Vibrio fisheri.* This system used the 100% protocol where serial dilutions (dilution factor = 2) of a neat liquid sample were inoculated with the bacterium (Microbics 1992). Following a 5-minute exposure duration, the fluorescence activity of each serial dilution was measured and evaluated against the fluorescence activity of a diluent-control receiving the same bacterium inoculation. Typically, toxicity values are expressed as a median effective concentration (EC50) and are determined by the dilution concentration that results in a 50% reduction in luminescence activity compared to the diluent control. In this assay, neat liquid samples were replaced with sediment elutriates prepared by adding a 7 gm sediment sample to 35 ml Microtox® SPT diluent and vigorously mixing with a magnetic stir bar for 10 minutes in a 4-ounce wide mouth I-Chem sample jar (Mearns et al., 1995). Next, the entire contents in the jar were transferred to a 50-ml centrifuge tube and centrifuged for 5 minutes at 3,400 x g. The resultant supernatant was the 100% elutriate.

Sediment petroleum chemistry

The sediments were extracted according to EPA Method 3545 for TPH analysis. To summarize, the sediment samples were frozen at -20ºC then freeze dried, ground, and homogenized. The dried samples were extracted with a pressurized fluid extraction system (Accelerated Solvent Extractor, Dionex Corporation, Sunnyvale, CA) with the DCM (dichloromethane) using conditions developed previously (Bauguss 1997). The

DCM extracts were then re-constituted to a final 5-ml volume.

A 1-ul aliquot of the DCM extract was injected into a Hewlett-Packard (HP) 5890 Series II gas chromatograph (GC) interfaced to a HP 5972 mass selective detector (MS) and operated using HP MS Chemstation software (Hewlett-Packard Corporation, Palo Alto, CA). TPH concentrations were acquired through GC-MS analysis. A TPH value is defined as the sum of the total resolved and unresolved component mixture concentrations. Surrogate standards were added prior to extraction. The GC-MS was initially calibrated with a seven-point curve and checked every 12 hours. GC-MS operating conditions and other analytical details can be found in Mills et al. (1999).

Results and Discussion

Inter-tidal sediment petroleum chemistry

As originally designed, toxicity evaluations were to be based on petroleum chemistry results obtained from the single core samples collected from crab cages following crab mortality observations. Consistent with observations made during the meso-scale experiment (Page et al. 1999, 2000a), large standard deviations in the intertidal sediment TPH concentrations within experimental treatments indicated that oil distribution in the crab cages was heterogeneous. Considering these results, the decision was made to extend TPH analysis to samples collected from the homogenized substrates (0-5 cm) used for the amphipod and Microtox assays to better represent toxicity exposures. The average TPH values from the 5-cm core and homogenized samples are used to provide representative exposure concentration for the inter-tidal toxicity

evaluations (Table 2.2). Petroleum chemistry evaluations indicated that there was no significant difference (α=0.05) between the no-oil-control and oil-plus-dispersant inter-tidal sediment TPH concentrations (Table 2.2). Further comparisons indicated that the TPH concentrations in the no-oil control and the oil-plus-dispersant treatments were significantly (α=0.05) less than the oil-control treatments with mean concentrations of 32, 35, and 1370 μg/g respectively.

Table 2.2 Average inter-tidal sediment TPH concentrations (μg/g).

Tank # (treatment)	24 Hour	96 Hour
1 (oil-control)	572	1870
3 (oil-control)	1630	2650
5 (oil-control)	1050	437
2 (oil-plus-dispersant)	14.5	14.5
4(oil-plus-dispersant)	48.7	38.0
6 (oil-plus-dispersant)	66.4	30.0
7 (no-oil-control)	40.3	43.7
8 (no-oil-control)	17.2	26.1

Inter-tidal sediment toxicity

Amphipod exposures to oil-control treatment sediments collected at both 24 and 96 hours following oil application resulted in 100% mortality (Fig. 2.4). In contrast, sediment samples collected at 24 hours following oil-plus-dispersant application resulted in 31% mortality while the samples collected at 96 hours resulted in 77% mortality (Fig. 2.4) . Percent mortality in sediments collected from experimental control tanks at 24 and 96 hours were 41% and 31% respectively (Fig. 2.4). Comparison of these results showed that observed mortality in sediments receiving oil-control treatments collected at 24 hours were significantly (α=0.05) higher than both the no-oil-control and oil-plus-

dispersant treatments. Observed mortalities in the oil-control and oil-plus-dispersant treatment sediments collected at 96 hours were not significantly different, but were both significantly higher than the observed response to the 96 hour no-oil-control sediments. These results are confounding considering the petroleum chemistry data that showed similar no-oil-control and oil-plus-dispersant sediment TPH concentrations that were both significantly (α=0.05) lower than the 96 hour oil-control treatment sediments.

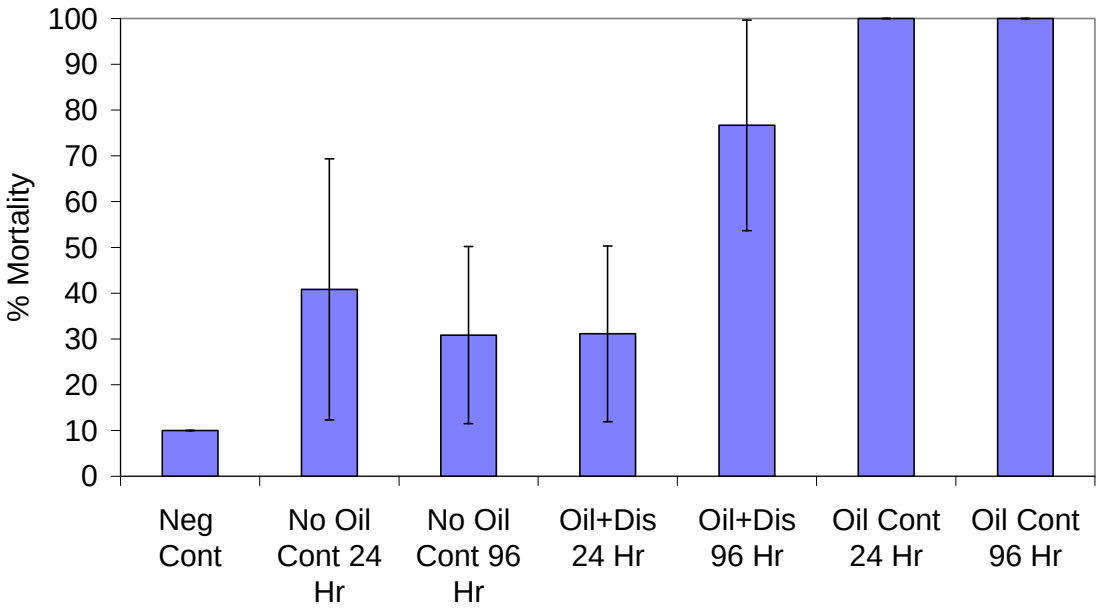

Fig. 2.4 Mean amphipod responses to inter-tidal sediment exposures (error bars represent standard deviation of the mean).

To evaluate the degree of correlation between observed toxicity and TPH, each mortality observation was plotted against the respective mean TPH value (Fig. 2.5). Evaluation of the combined 24 and 96 hour mortality observations (linear trend line not

shown) demonstrated a positive correlation (α=0.05) with TPH as indicated with a Pearson correlation coefficient (r)=0.5945 ($r_{critical}$=0.426) (Johnson 1984). Closer examination of the data suggest that the 100% mortality observed in the 2 oil-plus-dispersant replicates at 96 hours may not be due to TPH, especially considering that their TPH values of 30 and 15 μg/g, were less than the average TPH of the remaining control and oil-plus-dispersant exposures of 41 μg/g. Similar analysis of data collected at 24 and 96 hours (Fig. 2.5) resulted in r= 0.8112 and 0.4073, respectively ($r_{critical}$=0.662). Therefore, a linear correlation (α=0.05) between mortality and TPH was exhibited for samples collected at 24 hours and not 96 hours. This lack of agreement between linear correlation coefficients indicates that the increased mortality observed in the 96 hour oil-plus-dispersant sediment is not explained by TPH, yet may be related to oil-plus-dispersant treatment. The experimental design did not include petroleum chemistry of amphipod sediment pore water or over lying water. Therefore, no additional data was available to evaluate possible petroleum exposures. Overall, the intertidal amphipod mortality response to oil-plus-dispersant treatments remained below the 100% response observed in sediments receiving oil-control treatments.

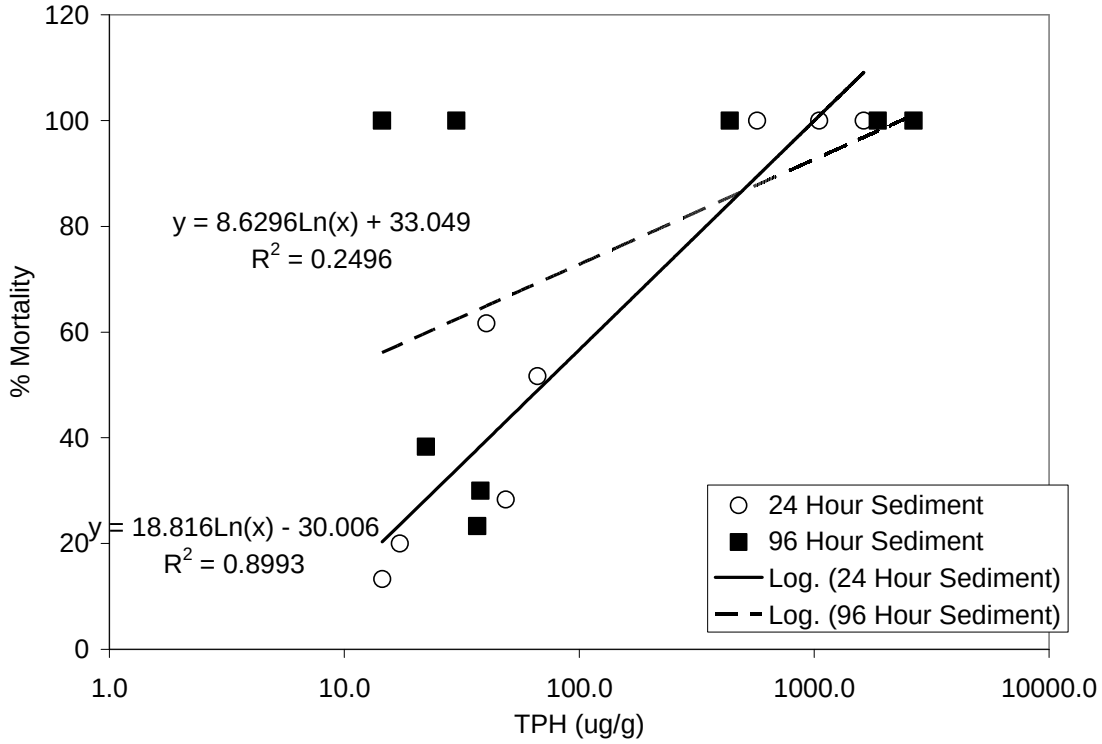

Fig. 2.5 Amphipod response to inter-tidal sediment TPH.

Microtox bioassay

Measurable Microtox® responses occurred only in the neat elutriates (100% solution) thereby eliminating the possibility of calculating EC50 values (concentration resulting in a 50% response). Therefore, only neat elutriate responses are presented as a percentage of luminescence change compared to blank SPS diluent luminescence (Fig. 2.6). Fluorescence inhibition (i.e. toxic response) is indicated by negative values. Comparisons between no-oil-controls and both oil-control and oil-plus-dispersant within each sampling interval (i.e. 24 or 96 hours) were evaluated using a single tailed ANOVA. These comparisons showed that only sediment elutriates prepared with samples collected from the oil-control at 96 hours demonstrated a significant (α=0.05, *df*

= 4) response relative to no-oil controls. Luminescence responses to all other sediments were comparable to the responses observed in the control sediments. It is unclear if the reduced luminescence in the 96 hour oil-control sediment elutriates resulted from sediment TPH, especially considering that the oil-control TPH concentrations collected at 24 and 96 hours were similar. Mueller et al. (1999) suggested that lack of correlation between observed toxicity and sediment TPH may be due to differences in elutriate and petroleum chemistry sample preparations. Microtox elutriates were prepared with saline solution thus restricting toxicity detection to the relatively water soluble TPH compounds. GC-MS samples are solvent extracted and include many TPH compounds that would otherwise remain adsorbed onto the sediments. This implies that GC-MS analysis is characterizing TPH fractions that are not available to bacteria exposed to sediment elutriates.

The lack of response observed in the Microtox elutriate assay suggest that this protocol lacked the sensitivity required for a more in-depth toxicity evaluation. More recently, an alternative solid phase Microtox assay was found to be more sensitive to oil toxicity in wetland sediments than the 100% elutriate protocol. However, it showed greater variability in observed toxicity (Mueller et al. 2003). The increased sensitivity of the solid phase protocol results from the direct contact between the bacteria and sediment-adsorbed TPH fractions. Increased variability has been attributed to factors including the bacteria loss via adhesion to particles and luminescence attenuation resulting from turbidity (Mueller et al. 2003). Despite the variability observed with the solid phase Microtox assay, its increased sensitivity should make this protocol a viable

alternative for future studies.

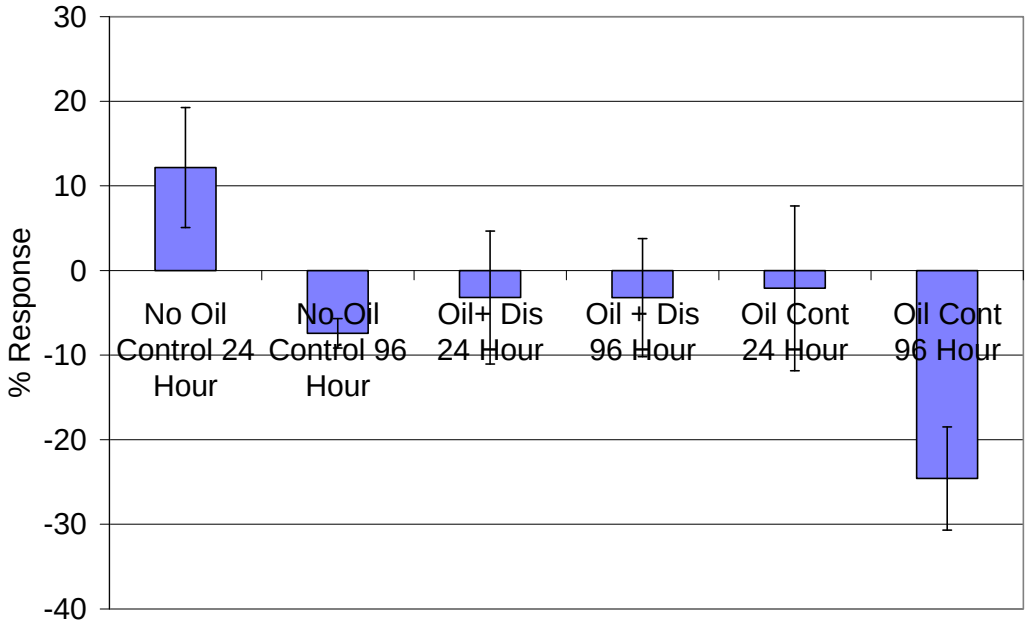

Fig. 2.6 Microtox® response to inter-tidal sediment exposures (error bars represent standard deviation of the mean).

Sub-tidal sediment petroleum chemistry

Sub-tidal sediment TPH concentrations measured in samples taken directly from the polychaete chambers (top 5 cm) were variable and inconsistent within treatments. TPH values in one oil-control and two oil-plus-dispersant treatments were equivalent to control treatment levels at the 96 hour sampling interval. TPH in the remaining two oil-control treatment chambers were both ~809 µg/g. TPH concentrations measured in the two remaining oil-plus-dispersant treatments at the 96 hour sampling were suspect. Samples for both tanks at 24 hr started at ~280 µg/g TPH. By 96 hour, the reported

concentration in one of these tanks (oil-plus-disp-2) increased by 400%, then, by day 10, dropped to about 200% the 24 hour sample level. For the remaining tank (oil-plus-dispersant-3), the sample concentration dropped below background by 96 hours, but on day 10 was essentially the same as the 24 hr measurement. The variable sub-tidal sediment TPH values indicate heterogeneous oil deposition, which when combined with the relatively small sample size (~5 cm diameter), adds to the observed variability of the amphipod exposure concentrations.

Sub-tidal sediment toxicity

Sub-tidal sediment exposures, no-oil-control, oil-control, and oil-plus-dispersant, were analyzed using Tukey's method of multiple comparisons (US EPA 1994). These are shown as "exposure" in Table 2.3. Each exposure was replicated in the meso-scale test tank treatments, referred as "Treatment" in Table 2.3. Sub-tidal sediment samples were then split 3 ways, for replicate amphipod toxicity analysis, referred as "Test replicate" in Table 2.3. In addition, individual experimental data were analyzed by a logistic regression model (Christensen 1990) with survivorship as the dependent variable and the experimental tank and replicate as the independent variables. These are shown as "treat" in Table 2.3. The A, B, C, and D designations are used to define treatments and exposures that are significantly different. (Table 2.3) For example, under the % Mortality column, treatments No-oil-control-1 and No-oil-control-2 both have a "treat" designation of A indicating the replicate meso-scale no-oil-control treatments resulted in statistically similar amphipod mortality (Table 2.3). Evaluating % Mortality exposures,

shows No-oil-control and Oil-control exposures resulted in significantly different amphipod mortality with designations of A and B, respectively (Table 2.3).

Table 2.3 Observations and statistical analyses (sub-tidal sediment samples). Treat or exposure with same letter are not significantly different from each other.

	% Mortality					% Sub-lethal + mortality				
	Test replicate					Test replicate				
Treatment	1	2	3	treat	exposure	1	2	3	treat	exposure
No-oil-control-1	0	0	10	A		15	5	30	A	
No-oil-control-2	0	0	20	A	A	5	5	25	A	A
Oil-control-1	30	45	45	B		100	100	95	B	
Oil-control-2	45	55	60	C	B	75	100	100	B	B
Oil-control-3	70	75	60	C		100	100	100	B	
Oil-plus-dispersant-1	100	100	100	D		100	100	100	B	
Oil-plus-dispersant-2	95	100	95	D	C	100	100	100	B	B
Oil-plus-dispersant-3	100	95	90	D		100	100	100	B	

Exposure treatment comparisons provide a metric to evaluate experimental quality control. Good experimental replication between experimental replicates was indicated by common treatment designations between treatments within specific exposures and observational endpoint (i.e. % Mortality or % Sub-lethal + mortality) (Table 2.3). The only exception occurred with Oil-control exposures evaluated as % Mortality where Oil-control-1 treatment with a B designation differed from Oil-control-2 and -3, both of which had a C treatment designation (Table 2.3).

Comparison of %Mortality exposure designations shows that No-oil-control,

Oil-control, and oil-plus-dispersant resulted in significantly different mortality responses as indicated by exposure designations of A, B, and C, respectively (Table 2.3). Evaluating %Mortality response magnitudes shows exposure toxicity in descending order with Oil-plus-dispersant > Oil-control > No-oil-control, as indicated by average %Mortality of 97, 54, and 5 %, respectively (Fig. 2.7). Evaluation the %Sub-lethal + mortality observations demonstrated that Oil-control and Oil-plus-dispersant exposures produced similar toxic responses as both had exposure designation B (Table 2.3). Further, both Oil-control and Oil-plus-dispersant exposures, with mean % Sub-lethal + mortality responses of 97 and 100%, respectively were significantly more toxic than mean No-oil-control response of 14% with an exposure designation of A (Table 2.3, Fig. 2.7). Toxicity correlation to sediment TPH concentration was not demonstrated as TPH values measured at or below concentrations resulted in up to 100% response. However, exposure evaluations clearly show elevated toxicity associated with both Oil-control and Oil-plus-dispersant exposures compared to no-oil-controls.

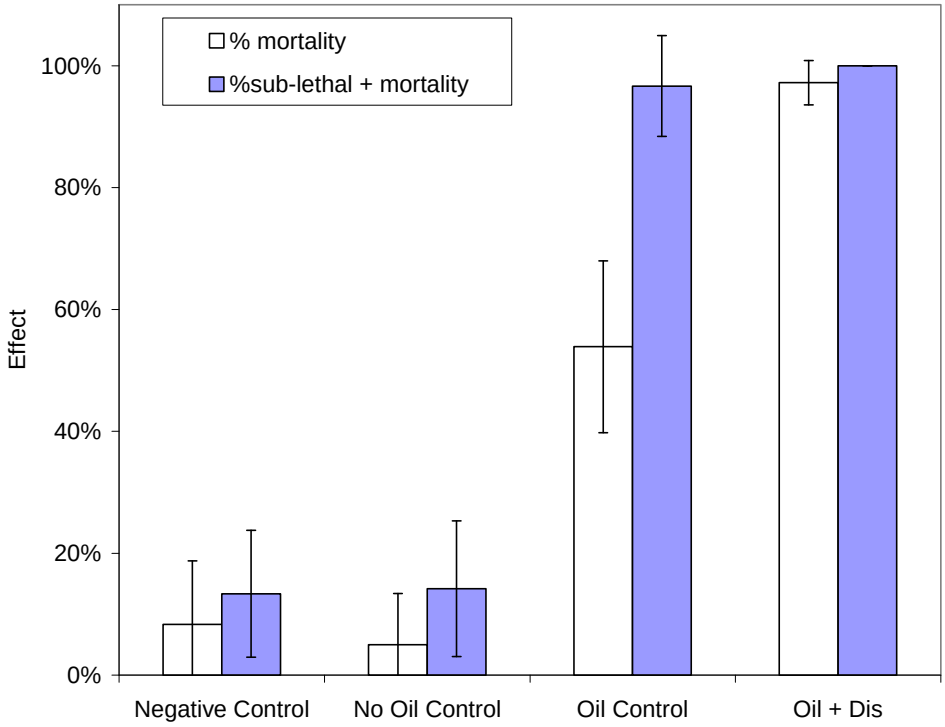

Fig. 2.7 Mean amphipod response to sub-tidal sediment exposures (error bars represent standard deviation of the mean).

Sub-tidal sediment chemistry showed that oil deposition in both the oil-control and oil-plus-dispersant treatment tanks was heterogeneously distributed. It is important to recognize that both the oil-control and oil-plus-dispersant treatments resulted in elevated sub-tidal sediment TPH concentrations. Considering the relative densities of oil droplets and water suggest that the oil droplets should accumulate on the surface of the water due to gravitational settling, thus suggesting that another transport mechanism is responsible for the benthic oil deposition. Researchers have long been aware that hydrocarbons will adsorb to particulate matter. Gearing et al. (1980) reported that oil adsorption to particulate matter resulted in the sedimentation of insoluble hydrocarbons. Following the Amoco Cadiz oil spill, oil was shown to exhibit patchy accumulation in

fine sediments while accumulation was discouraged in areas with characteristically coarse sediments (Cabioch et al. 1978). Sterling et al. (2004b) modeled oil droplet-sediment aggregation and found that clay-oil and silica-clay interaction readily formed aggregates with similar efficiency to cohesive clay particles. Further, it was shown that both the clay-oil and silica-clay aggregate settling time scale to aggregation time scale ratios, or Damkohler number (*Da*), ranged from 0.1 to 1 over a mean shear (G_m) typical of estuarine settings (Sterling et al. 2004b). At $Da \ll 1$, settling will occur faster than aggregation and implies that aggregate settling is a significant process (Sterling et al. 2004b).

This study was designed to evaluate the ecological effect and ultimate contaminant fate of the crude oil. As such the data is insufficient to evaluate with the oil-droplet-sediment aggregation model presented by Sterling et al. (2004b) which requires time series data on the particle size distribution, sediment and oil density, $G_{m,}$ suspended sediment, and oil concentrations. However, meso-scale water column TPH values ranged from < 1 to 68 mg/l in the oil-plus-dispersant tanks and < 1 to 45 mg/L in the oil-control treatment tanks (Page et al. 2000a). While no total suspended solids (TSS) data was collected during the meso-scale tidal simulations, mean TSS concentration of 6.5 mg/L in Laguna Madre, the water source for tidal simulations, was reported to be 6.5 mg/L in 2002 by Nicolau and Nunez (2005) and is a reasonable concentration to expect during the meso-scale simulations. These values are comparable within an order of magnitude of the sediment and oil loads evaluated by Sterling et al. (2004a).

Mean shear (G_m) is defined by Camp and Stein (1943) as

$$G_m = (Po/V\mu)^{0.5} \quad (2.1)$$

where, G_m = mean shear rate [s^{-1}], Po = power input to system (i.e. impeller and or wave power etc.) [kg*m^2/ s^3], V = system volume [m^3], μ=dynamic viscosity [kg/sec*m] = 1.0826 x 10^{-3} Pa*s [kg/m*s] (Sterling et al. 2004a). Wave power input (Po) to the system can be calculated using linear wave equations provided in the Shore Protection Manual (USACE, 1984) as

$$Po = EC_g \quad (2.2)$$

$$E = \rho g H^2 / 8 \quad (2.3)$$

$$C_g = L / T \quad (2.4)$$

$$L = gT^2 / 2\pi \quad (2.5)$$

where E, is the wave energy per unit surface area, C_g is the wave velocity, g is the acceleration due to gravity 9.8 ms^{-2}, L is the wavelength in meters, T is the wave period in seconds. Substituting Equation 2.2 into Equation 2.1 yields

$$G_m = (EC_g/V\mu)^{0.5} \quad (2.6)$$

System volume (V) is calculated as the tank volume occupied in one wavelength at the mid-tide. This derivation yielded estimated G_m values of 19 and 32s^{-1}, for wave heights of 0.076 and 0.13m waves, respectively. These values are comparable to mean shear rates evaluated by Sterling et al. (2004a, 2004b, 2004c, 2005).

Using the estimated values for suspended solids concentration, available crude oil concentration, the estimated G_m value shows that the conditions experienced in the meso-scale wave tanks were comparable to the experimental conditions used to evaluate

the *Da* in Sterling et al. (2004b). This analysis is based on many assumptions and is not definitive. However it suggests that reasonable conditions existed in the meso-scale wave tanks for oil-sediment aggregation and subsequent deposition of toxic petroleum fractions on sub-tidal substrates. Furthermore, the elevated sub-tidal toxicity observed both in Oil-control and Oil-plus-dispersant exposures relative to No-oil-control suggest this potential transport mechanism is mportant for oil-droplets formed with and without chemical dispersants.

Conclusions

Analytical chemistry data showed that inter-tidal sediment TPH concentrations were elevated in tanks receiving oil-control treatments, while tanks receiving oil-plus-dispersant treatments had TPH values comparable to no-oil controls. Inter-tidal sediment amphipod mortality generally correlated with the TPH. Similarly, the Microtox assay only demonstrated elevated toxic response in elutriates prepared from inter-tidal sediments receiving oil-control treatments. These observations suggest that dispersant treatments resulted in reduced oil accumulation in the inter-tidal zone with a subsequent reduction in observed toxicity.

The Microtox® elutriate test demonstrated an elevated toxic response with samples collected from oil-control treatment sediments compared to no-oil-controls, however there was no clear toxicity correlation to sediment TPH. Microtox® responses to elutriates prepared with oil-plus-dispersant treated sediments and no-oil controls were similar. The lack of correlation between TPH and toxicity with this assay suggests the

observed toxic response may be due to an un-characterized variable. Additionally, the limited luminescence response obtained with the elutriate preparations indicates that poorly soluble hydrocarbons bound to sediments are relatively unavailable for uptake by water column organisms.

No correlation between TPH and sub-tidal sediment toxicity was demonstrated. However, both oil-control and oil-plus dispersant treatments demonstrated elevated sub-tidal toxicity and heterogeneous oil distribution compared sediments receiving no-oil controls. These observations suggest oil-particle aggregation and settling as a possible mechanism responsible for the sub-tidal deposition of both untreated oil and chemically dispersed oil. Future studies should incorporate the use of sediment traps combined with petroleum chemistry analysis to quantify petroleum deposition resulting from ambient particle-droplet aggregation. Additionally, experimental tank characterizations should include suspended solids mass concentration, particle size distribution, water column TPH, and mean shear rate to characterize the fundamental parameters affecting oil-particle aggregation.

CHAPTER III

COMPARATIVE TOXICITY OF OIL, DISPERSANT, AND OIL PLUS DISPERSANT TO SEVERAL MARINE SPECIES*

Overview

Dispersants are a pre-approved chemical response agent for oil spills off portions of the U.S. coastline, including the Texas-Louisiana coast. However, questions persist regarding potential environmental risks from dispersant applications in nearshore regions (within three nautical miles of the shoreline) that support dense populations of marine organisms and are prone to spills resulting from human activities. To address these questions, a study was conducted to evaluate the relative toxicity of test media prepared with dispersant, weathered crude oil, and weathered crude oil plus dispersant. Two fish species, *Cyprinodon variegatus* and *Menidia beryllina*, and one shrimp species, *Americamysis bahia* (formerly *Mysidopsis bahia*), were used to evaluate the relative toxicity of the test media under declining and continuous exposure regimes. Microbial toxicity was evaluated using the luminescent bacteria *Vibrio fisheri.* The oil media prepared with a chemical dispersant was equal to or less toxic than the oil-only test medium. Continuous exposures to the test media were generally more toxic than

---

declining exposures. The toxicity of unweathered crude oil with and without dispersant was also evaluated using *Menidia beryllina* under declining exposure conditions. Unweathered oil-only media were dominated by soluble hydrocarbon fractions and found to be more toxic that weathered oil-only media in which colloidal oil fractions dominated. Total concentrations of petroleum hydrocarbons in oil-plus-dispersant media prepared with weathered and unweathered crude oil were both dominated by colloidal oil and showed no significant difference in toxicity. Analysis of the toxicity data suggests that the observed toxicity was a function of the soluble crude oil components and not the colloidal oil.

Introduction

An estimated input of 1.3 million metric tons of petroleum pollutants from both natural and anthropogenic sources may be discharged into the world's oceans annually (NRC 2003). Left untreated, the physical properties of crude oil and transport mechanisms such as ocean and wind currents can result in the accumulation of oil in sensitive environments including shorelines and estuarine wetlands. When oil accumulates in these areas, shoreline dwelling organisms may be subjected to toxic contaminant exposures (Mueller et al. 1999, 2003; Fuller et al. 1999). Page et al. (2000a) shows that oil treated with a chemical dispersant can reduce the amount of oil accumulation on sandy substrates. Subsequently, reduced toxicity to sediment dwelling organism was observed in sandy substrates impacted with chemically dispersed oil compared to untreated oil (Fuller et al. 1999). These studies demonstrate the potential

ecological benefits of oil spill dispersant use.

Currently, dispersants are pre-approved for use along the Texas and Louisiana (USA) coasts in waters greater than 10 meters deep and 3 nautical miles off shore (RRT-6 2001). However, the risk of spills is greatest in shallow nearshore waters where petroleum transportation traffic is highest. These shallow areas can receive greater oil loading per unit volume of seawater than deeper offshore waters (US EPA 1993a). Thus, concerns that harmful conditions may occur if dispersants are used in these shallow habitats prevents the preapproval of a potentially viable response option.

Past oil spill toxicity research has shown that the crude oil fractions responsible for the observed toxicity in aquatic organisms are the two- and three-ringed polycyclic aromatic hydrocarbons (PAHs) (Anderson et al. 1974). Conversely, Mueller et al. (1999) showed that total petroleum hydrocarbons (TPH), determined by U.S. Environmental Protection Agency (U.S. EPA) Method 418.1, in estuarine sediments correlated well with toxicity measured with Microtox® (Azur Environmental, Carlsbad, CA, USA), while correlation with target saturated and aromatic analytes were weak. A subsequent wetland study by Mueller et al. (2003) showed that the toxicity, also measured with Microtox, of sediment elutriates and sediment suspensions correlated well with both saturated alkanes and aromatic hydrocarbons. The laboratory studies demonstrate the potential for ecological harm to aquatic organisms from a broad range of petroleum fractions.

Dispersant toxicity to marine and aquatic species has been well documented since they were first developed as spill response technology (Marchetti 1965; Hall et al.

1989; Skidmore 1970; Swedmark et al. 1971; Abel 1974; Edwards et al. 2003). Etkin (1999) summarized a large collection of toxicological studies involving dispersants and/or chemically dispersed oil. Dispersants are intended to enhance oil mobilization into the water column, thus potentially resulting in increased biological stresses in affected areas because of elevated oil concentrations (US EPA 1993a). Supporting laboratory studies show that surfactants can increase crude oil PAH concentrations in the water column, thereby increasing the observed toxicity compared to no-surfactant controls (Kanga et al. 1997). Thus legitimate concern exists regarding the use of dispersants as a viable response option.

It is recognized that toxic exposures to oil spills in the open ocean can be limited by dilution and other mechanisms. A laboratory reactor study showed that chemically dispersed oil droplets were subject to coagulation and subsequent resurfacing (Sterling et al. 2002). Another related study reported similar dispersed oil behavior in mesoscale wave tanks (Page et al. 2002b). Biodegradation has also been shown to rapidly reduce the concentration of chemically dispersed oil in a laboratory study using estuarine waters (Harris et al. 2002a, 2002b). The combined effects of physical and biological mechanisms result in rapidly declining dispersed oil exposure concentrations. Investigations indicate that declining exposures require higher oil concentrations to achieve the same degree of toxicity (Singer et al. 1991). Such findings suggest that standard continuous exposure tests overestimate the toxic effects of real spill conditions (Pace et al. 1995).

The primary objective of this study was to determine the toxic effects of

dispersant only, weathered oil only, and weathered oil plus dispersant to several marine test organisms under continuous and declining exposure regimes. A secondary objective was to determine the toxic effects of declining exposures to unweathered oil only and oil plus dispersant with one marine species. Results from these tests were then evaluated to determine the dispersant contribution to oil-plus-dispersant toxicity, the relative toxicity of oil-plus-dispersant and oil-only, the relative toxicity of continuous and declining exposures, and the relative toxicity of weathered and unweathered oil. The toxicity effects of the different crude oil media were also analyzed to elucidate petroleum toxicity mechanisms of complex aqueous mixtures including soluble and colloidal petroleum hydrocarbon fractions.

Materials and Methods

Toxicity protocols

All aquatic toxicity tests utilized systems and methods for acute toxicity tests that are described in previous publications. Continuous flow, declining exposure assays used a flow-through system described by Singer et al. (1993). Static, continuous exposure assays followed protocols described by the US EPA (1993b). Bacterial toxicity tests used the Microtox system using the protocol for the 100% test (Microbics 1992).

Macro tests organisms

Americamysis bahia (mysid shrimp), formerly *Mysidopsis bahia* (Price et al. 1994) *and Menidia beryllina* (silverside minnow) (7 d old), were purchased from

Charles Rivers, formerly Aquatic Research Organisms (Hampton, NH, USA). The organisms were acclimated for 3 days in a 40-L glass aquarium with salinity adjusted sea-water to 20 psu. The organisms were fed *Artemia sp.* nauplii (24-48 h old) *ad libitum.* Both *A. bahia* and *M. beryllina* were 10 d old at the start of testing. Age specified in standard U.S. EPA effluent testing protocols is 1 to 5 d for *A. bahia* and 9 to 14 d for *M. beryllina* (US EPA 1993b). *Cyprinodon variegatus* (sheepshead minnow) (3 d old) larvae were purchased form Aquatic Biosystems (Fort Collins, CO, USA). The organisms were acclimated overnight in test water with a salinity of 20 psu. They were fed *Artemia* sp. nauplii *ad libitum*. *C. variegatus* exposures to test conditions at 4-d old were consistent with U.S. EPA Guidelines of 1 to 14 d old (US EPA 1993b).

All three macrospecies are listed as standard organisms for toxicity testing of effluents in marine and estuarine receiving waters (US EPA 1993b). Both *M. beryllina and C. variegatus* are widely distributed in North America along the coastal waters of the Atlantic and Gulf of Mexico (US EPA, 1993b). *Americamysis bahia*, a mysid is common to estuarine waters of the Gulf of Mexico from Florida to Mexico (Edwards et al. 2003).

Macro organism test protocols

Both oil-only and oil-plus-dispersant media were tested with static renewal and flow-through systems for continuous and declining exposure scenarios, respectively. The continuous exposure test protocol was adapted from standard U.S. EPA protocols used to test wastewater effluent (US EPA 1993b). Declining exposure tests were

conducted with flow-through system following methods previously described by Singer et al. (1993). Test durations for both test types were 96 h.

Declining exposure regimes were conducted using a continuous flow system consisting of 18 individual chambers, each with a 250-ml nominal volume and a continuous flow rate of 120 ml/h. All chambers were filled to approximately 95% capacity with respective test medium. Then five organisms were added to each randomly chosen chamber. This deviates from the U.S. EPA recommendation of 10 organisms per chamber for each of the macro test species to minimize depletion of dissolved oxygen (D.O.) concentrations due to the combined effect of organism overcrowding and elevated biological oxygen demand (B.O.D.) associated with test media in the small exposure chamber volume (US EPA 1993b). Following organism loading, the chambers were filled to capacity with the appropriate test medium, then a continuous flow of clean seawater to each chamber was initiated. Water quality was periodically monitored in collection flasks that combined the effluent of the three replicate treatment chambers. Toxicity results were based on the initial petroleum hydrocarbon concentrations.

Assuming that the flow-through chamber behaves as a continuous flow stirred tank reactor (CFSTR), the theoretical hydraulic residence time (t_r) of 2 h was calculated by

$$(t_r)=V/Q \tag{3.1}$$

where Q = volumetric flow rate and V = chamber volume. To evaluate the performance of the flow-through chamber, a dye study was conducted using and Ocean Optics®

(Denedin, FL, USA) fiber-optic ultraviolet spectrophotometer to measure RhodamineWT dye concentration *in-situ* as a function of time. Normalized results (C/C_0) from the dye study are shown in Fig. 3.1, where C = concentration at time = t and C_0 = concentration at t = 0. Also shown in Fig. 3.1 is the concentration as a function of time in an ideal CFSTR modeled by

$$C/C_0 = e^{-(\theta t)} \tag{3.2}$$

where $\theta = Q/V = 1/t_r = 0.48$/h and t = time (h). Excel® (Microsoft, Redmond, WA, USA) solver was then used to solve for θ by minimizing the sum of squares error to fit the model (Eqn. 3.2) to the dye study concentration data. The resultant model fit θ = 0.37/h (t_r = 2.8 h) was 40% longer than predicted for an ideal CFSTR. This deviation indicates the exposure chamber exhibits non-ideal behavior and justifies actual measurement of the system hydraulics to characterize the exposure environment.

The continuous exposure protocol was adapted from U.S. EPA effluent testing methods to meet the demands of toxicity testing with insoluble and volatile contaminants (US EPA 1993b). Static renewal exposures were conducted in 500-ml amber glass jars with Teflon®-lined lids. Use of amber glass jars is a deviation from the U.S. EPA methods, which specify light intensity and duration (US EPA 1993b). The degree of light attenuation caused by the amber jars was not determined for this study. Each jar was filled with respective test solution to within a few millimeters of the rim before organisms were loaded to the chamber. Once organisms were added, the chambers were sealed with Teflon-lined lids to prevent loss of volatile toxicant components. Volatile hydrocarbons were suspected to be a primary toxic agent in this study, making aeration

an unacceptable method to maintain dissolved oxygen concentrations in the test media. However, US EPA (1993b) methods suggest that aeration can be used as a last resort. Each day, 75% of the solution in each chamber was removed by straining through Nitex® (Safar, Depew, NY, USA) (100 μ) mesh to prevent loss of test organisms, replaced with fresh test solution, and then resealed. Toxicity results (effective concentrations) were based on daily average petroleum hydrocarbon concentrations.

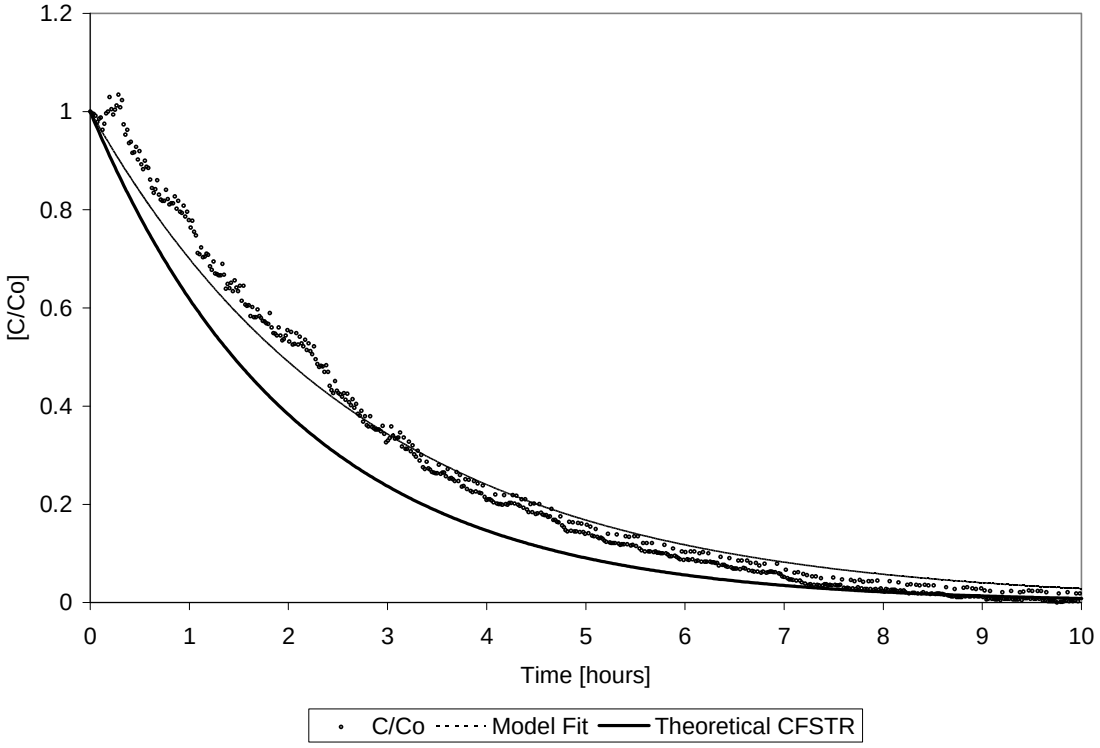

Fig. 3.1 Declining exposure chamber hydrodynamic characterization. The C/C_0 represents the experimental dye concentration at any time divided by the initial dye concentration. Model fit represents the C/C_0 predicted using the derived equation $C/C_0=e^{(-0.37t)}$. Theoretical CFSTR represents the C/C_0 predicted for an ideal continuous flow stirred tank reactor.

For all declining and continuous microorganism bioassays, each experimental treatment was tested in three replicate test chambers. Each bioassay was repeated at least twice. Definitive mortality observations were made after the 96-h exposure. Mortality was based on the number of live organisms recovered from the three replicate chambers at the end of each bioassay. Effective concentrations, reported as no-observed-effects concentration (NOEC) and median effective concentration (LC50), were calculated for each bioassay using ToxCalc 5.0® software package (Tidepool Scientific Software, McKinleyville, CA, USA). This package permits calculation/estimation of relevant effective concentrations using several appropriate methods, including Spearman-Karber, probit, logit, and so on. The method employed in LC50 determination was dependent on available mortality data (US EPA 1993b). For all tests, increased toxicity is indicated by lower effective concentration values. The average toxicity values reported in this text represent the arithmetic mean of the repeated bioassays. Significant variance between the experimental treatments (e.g. oil-only continuous exposure vs oil-plus-dispersant continuous exposure) was determined with a single-tailed analysis of variance at the 95% confidence interval using Microsoft Excel. Analysis of variance determinations were based on the LC50 values calculated for each bioassay.

Microtox® protocol

The Microbics Microtox system was used to evaluate the microbial toxicity of dispersant only, oil-only, and oil-plus-dispersant media. All test used the 100% protocol

outlined in the Microtox Manual (Microbics 1992). Filtered seawater (salinity = 20 psu) was used to prepare all media. Each assay was performed in duplicate with two controls and eight test concentrations. The highest test concentrations were 98% of the initial test media. The seven remaining concentrations were prepared by serial dilution (dilution factor = 1.5). Median effective concentrations (EC50 values) were determined for 15-min exposures.

Media preparations

Dispersant-only and oil-plus-dispersant media were prepared with the dispersant Corexit® 9500 (Nalco/Exxon Energy Chemicals, Sugar Land, TX, USA). Arabian medium crude oil was used to prepare all oil-only and oil-plus-dispersant media. The oil was weathered in a vented tank by air-stripping the volatile fractions. Following this treatment, the weathered crude oil volume was approximately 25% less than the initial unweathered crude oil volume (Page et al. 2002a).

Both oil-only and oil-plus-dispersant media were prepared were prepared in either 2- or 4-liter glass aspirator flasks. The sidearm of each flask was closed off with a short length of silicone tubing and a tubing clamp. Crude oil was added gravimetrically onto the premeasured dilution water with a gastight syringe, resulting in oil load units of oil mass/water volume. The flasks were immediately sealed with Teflon® stoppers. The sealed flasks were placed on magnetic stir plates and speeds were adjusted to obtain zero vortex for oil-only media and 25% vortex for oil-plus-dispersant media. A 25% vortex is defined as vortex that reaches a depth of 25% of the total water column depth. All stir

plates were equipped with digital tachometers to permit identical settings of all stir plates. For the oil-plus-dispersant media, the dispersant was applied to the center of the vortex at a dispersant mass: crude oil mass ratio of 1: 10. Oil-only media were mixed for 48 h (nominal) while oil-plus dispersant media were mixed for 24 h (nominal). All flasks were covered with aluminum foil during the mixing period to minimize photo-oxidation of the media. All solutions were prepared at ambient room temperature 25±2°C. Oil-only media were drawn from the aspirator flasks immediately after the stir plates were turned off at the end of the mixing period. Oil-plus-dispersant media were allowed to settle 3 to 6 h before collecting samples for toxicity testing and chemical analysis.

Chemical analysis

Corexit® 9500 solutions were quantitatively analyzed using ultraviolet spectroscopy. Briefly, Corexit® 9500 calibration standards were prepared with filtered salinity-adjusted seawater. The filtered seawater was used to set baseline absorbance for the standard curve at a wavelength of 240 nm. Standard concentrations of 20, 40, 50, and 100 mg/L provided linear standard curves (R^2=0.99) that were used calculate the concentrations of the dispersant only test solutions. Solutions with nominal dispersant concentrations above those used to prepare the standard curve were diluted accordingly to maintain absorbance readings within the linear range of the standard curve. Final dispersant concentrations were then corrected for any required dilutions. All dispersant only solutions were analyzed the day of preparation.

Analysis of nonvolatile hydrocarbons included both saturated hydrocarbons and aromatics. The saturated group included *n*-alkanes (decane [C_{10}] – pentatriacontane [C_{35}]) as well as branched compounds pristine and phytane. The aromatic group included naphthalene, fluorine, phenanthrene, anthracene, debenzothiothene, pyrene, chrysene, and the alkylated homologues. The analysis was conducted using a gas chromatography-mass spectrometer method that was previously presented by Mills et al. (1999). This analysis included liquid-liquid extraction of the solutions with methylene chloride. The gas chromatography-mass spectrometer analysis was conducted on an HP 5890 II gas chromatograph coupled to and HP 5972A mass spectrometer integrated with HP MS Chemstation softwater (Hewlett-Packard, Palo Alto, CA, USA). The mass spectrometer was operated in the electron ionization mode and tuned with and internal standard according to the manufacturer's specifications. All analyses were completed using the scan mode from 50 to 550 *m/z* (method is based on U.S. EPA SW-846 8260). The target compounds were quantified using the extracted ion chromatograms for the appropriate quantifying ions.

Results and Discussion

Water quality parameters

In all macro-organism tests, the water quality was monitored for quality assurance of test results. The pH for all tests ranged from 7.0 to 7.9. Water temperatures for all tests were 25±2°C. At a test temperature of 25°C and salinity of 20 psu, the oxygen saturation limit in water is 7.3 mg/L (US EPA 1993b). For warm-water

species, dissolved oxygen (D.O.) concentrations must not fall below a minimum concentration of 4.0 mg/L (US EPA 1993b). For all microorganism tests, allowable dissolved oxygen concentrations were maintained above the minimum concentration.

Corexit® 9500 toxicity

Average toxicity results for Corexit® dispersant-only toxicity tests are shown in Table 3.1. Validity of laboratory test procedures is supported by similar Corexit® 9500 continuous exposure LC50s, reported in an independent study by Edwards et al. (2003) for *A. bahia* and *M. beryllina* of 21 and 79 mg/L, respectively. Of the three macoorganisms evaluated in the present study, *A. bahia* was the most sensitive macrospecies to Corexit® 9500 continuous exposures as indicated by the lowest mean LC50 of 32 mg/L compared to the mean LC50 values of 79 and 180 mg/L for *M. beryllina* and *C. variegatus,* respectively . Conversely, *A. bahia* was observed to be the least sensitive macrospecies to declining Corexit® 9500 exposures with the highest average LC50 of 900 mg/L compared to 670 and 76 mg/L for *C. variegatus* and *M. beryllina,* respectively. Closer inspection shows that the *M. beryllina* LC50 was nearly the same for both continuous and declining exposures, whereas the declining exposure LC50s for both *A. bahia* and *C. variagatus* were greater than the continuous exposure LC50s by factors of 28 and 3.7, respectively. This observation suggest that *M. beryllina* is possibly subject to a toxicity threshold, while the toxic effects of Corexit® 9500 are cumulative over time for both *A. bahia* and *C. variegatus.* Microtox (*V. fisheri*) data resulted in a mean LC50 of 170 mg/L (n = 4), which fell between the average

continuous and declining LC50 of the three macroorganisms and suggest that Microtox is a suitable method for determining the toxicity of Corexit® 9500 in estuarine and marine systems.

Table 3.1 Dispersant-only average (n = 2) toxicity results in mg/L Corexit® (Nalco/Exxon Energy Chemicals, Sugar Land, TX, USA). *n = 3; **n = 4; NA = not applicable; NOEC = no-observed-effects concentration; LC50 = median lethal concentration; EC50 = median effective concentration.

	Continuous NOEC	Continuous LC50	Declining NOEC	Declining LC50	15-min EC50
Americamysis bahia	18	32	103	900	NA
Menidia beryllina	50	79	42*	76*	NA
Cyprinodon variegatus	107	180	305	670	NA
Vibrio fisheri	NA	NA	NA	NA	170**

Oil-only toxicity determination

Mean effective toxicity results for weathered Arabian medium crude oil-only media are shown in Table 3.2. *Americamysis bahia* was the most sensitive organism tested to the weathered Arabian medium crude oil-only media with the lowest continuous exposure of 0.62 mg/L, compared to *M. beryllina* and *C. variegatus* LC50s which were both higher by an order of magnitude. Additionally, *A. bahia* was the only organism with a response sufficient to calculate a declining oil-only exposure LC50. The declining exposure LC50s for both *M. beryllina* and *C. variegatus* exceeded the highest the highest oil-only media concentrations. The data further indicates that the two fish species, *M. beryllina* and *C. variegatus,* had similar continuous exposure LC50s that were greater than then shrimp species (*A. bahia*) LC50 by an order of magnitude and

suggesting that fish species may be more tolerant to petroleum hydrocarbon exposures than shrimp. The 15-min *V. fisheri* EC50 was comparable to the macroorganism average oil-only continuous exposure LC50 of 3.3 mg/L.

Table 3.2 Oil-only average (n = 2) toxicity results in mg/L. > represents that toxicity endpoint was greater than highest test concentration shown. ** n = 4; NA = not applicable; NOEC = no-observed-effects concentration; LC50 = median lethal concentration; EC50 = median effective concentration.

	Continuous NOEC	Continuous LC50	Declining NOEC	Declining LC50	15-min EC50
Americamysis bahia	<0.32	0.62	13	55	NA
Menidia beryllina	1.2	5.2	23	>32	NA
Cyprinodon variegatus	2.5	4.1	5.5	>6.1	NA
Vibrio fisheri	NA	NA	NA	NA	1.1**

Oil-plus-dispersant toxicity determination

The mean weathered Arabian medium crude oil-plus-dispersant effective concentrations are shown in Table 3.3. *Americamysis bahia,* with the lowest continuous LC50, was the most sensitive microorganism to the continuous oil-plus-dispersant exposures followed by *M. beryllina* and *C. variegatus.* The average continuous exposure LC50 included the highest test concentration for *C. variegatus* to provide a conservative estimate of the median lethal concentration. Conversely, species sensitivity to declining oil-plus-dispersant exposure was reversed as indicated by the declining exposure LC50 values. No significant difference exists between the declining exposure fish LC50s. However, the average fish (*M. beryllina* and *C. variegatus*) declining exposure LC50 of 33 mg/L was significantly lower than the average mysid shrimp

declining exposure LC50 of 59 mg/L. This observation contradicts the oil-only observation and suggests that the two fish species are more sensitive to oil-plus-dispersant media than the shrimp. *Vibrio fisheri* sensitivity to oil-plus-dispersant was comparable to the macroorganism sensitivity as indicated by an EC50 that fell between the mean continuous and declining exposure macroorganism LC50 values.

Initial *C. variegatus* continuous exposures to oil-plus-dispersant resulted in no response at concentrations previously tested in *M. beryllina* and *A. bahia* bioassays. However, higher concentrations that resulted in lethal responses were accompanied with deficient oxygen concentrations within 24 h. Thus, concern arose that observed mortality was due to low oxygen concentrations and not oil-plus-dispersant toxicity. To address this concern, a media series was prepared and monitored for oxygen depletion over a 24-h period (the time span between required solution exchanges) in the absence of test organisms. The results showed that oxygen levels dropped below acceptable levels at oil-plus-dispersant loads of 0.40 g/L and above. Therefore, the highest oil loads for oil-plus-dispersant continuous exposure tests were limited to 0.25 g/L. No observed adverse effects resulted from exposures to media prepared with the low oil loads.

Table 3.3 Oil-plus-dispersant average (n = 2) toxicity results in mg/L. ** n = 4; NA = not applicable; NOEC = no-observed-effects concentration; LC50 = median lethal concentration; EC50 = median effective concentration.

	Continuous NOEC	Continuous LC50	Declining NOEC	Declining LC50	15-min EC50
Americamysis bahia	<0.97	0.65	46	59	NA
Menidia beryllina	<1.2	2.0	26	31	NA
Cyprinodon variegatus	10	>11	36	36	NA
Vibrio fisheri	NA	NA	NA	NA	18**

Unweathered oil-only and oil-plus-dispersant toxicity evaluation

The majority of the tests presented in this paper used weathered crude oil. The rationale behind this experimental design is that oil at sea loses most of its volatile hydrocarbons through weathering processes within 24 to 48 h following a spill (US EPA 1993a). Because of the logistics involved in mounting a full-scale dispersant response to a spill, it was assumed that ample time would pass for significant weathering to occur. For these reasons, dispersant toxicity testing with unweathered crude oil was deemed unrealistic. However, media prepared with unweathered crude oil were subjected to limited testing with *M. beryllina* under declining exposure conditions. Toxicity results (effective concentrations) of unweathered oil media were calculated only on the basis of the non-volatile hydrocarbons to allow direct comparison to effective concentrations obtained from the weathered crude oil tests. Average *M. beryllina* LC50s for both unweathered and weathered crude oil-only and oil-plus-dispersant media show that the unweathered crude oil-only LC50 is considerably lower than the oil-plus-dispersant LC50 (Fig. 3.2). A decrease in toxicity (elevated LC50) associated with the oil

weathering process was determined, implicating the volatile hydrocarbons as the responsible agents for the increased toxicity observed with the unweathered oil media.

Volatile organic hydrocarbons represented about 25% of the unweathered crude oil (Page et al. 2002a). Therefore, analysis of unweathered crude oil media was extended to include the volatile compounds, benzene, toluene, ethyl-benzene, and xylene and are referred to as volatile hydrocarbon in the remaining text. Fig. 3.3 shows that the unweathered oil-only hydrocarbon concentrations are dominated by the more soluble volatile hydrocarbon fractions compared to nonvolatile hydrocarbon fractions. Conversely, Fig. 3.4 indicates that the nonvolatile fractions dominate the unweathered oil-plus-dispersant media. Figs. 3.3 and 3.4 show similar volatile hydrocarbon in the two media types, while nonvolatile hydrocarbons are considerably higher in the oil-plus-dispersant media relative to the oil-only media. Evaluation of the toxicity data presented in Fig. 3.2 and media chemistry data presented in Figs. 3.3 and 3.4 suggest a possible relationship between lower toxicity and the presence of nonvolatile hydrocarbons.

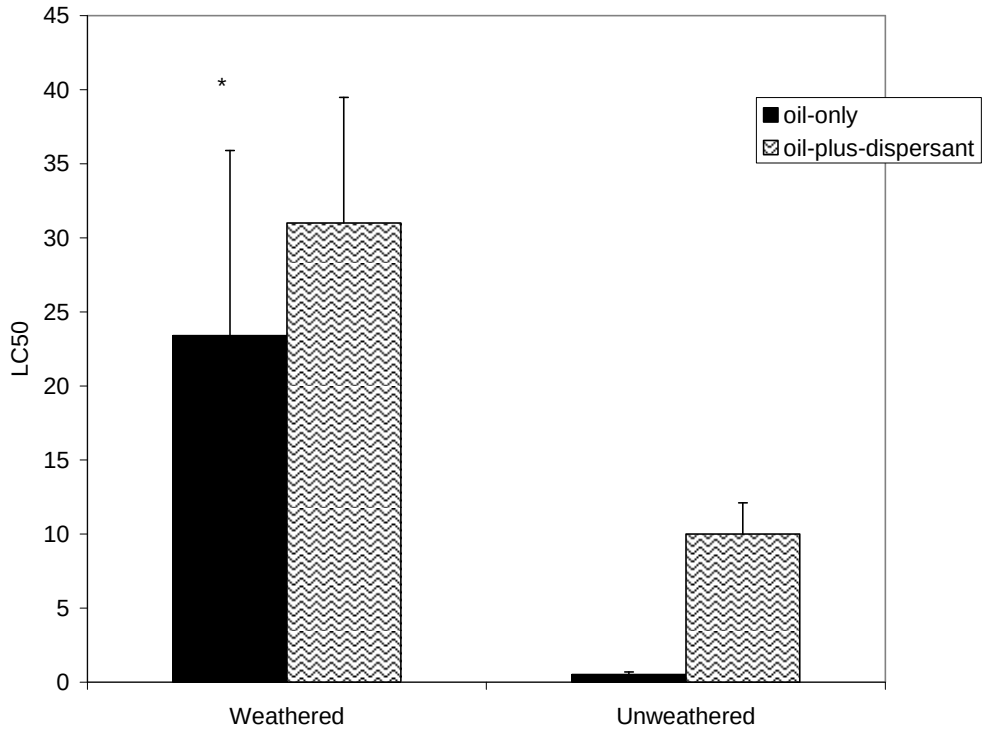

Fig. 3.2 *M. beryllina* declining exposure toxicity results for weathered and unweathered crude oil media. Median lethal concentration (LC50) represents the units of mg/L nonvolatile hydrocarbons. * = no-observed-adverse-effects concentration.

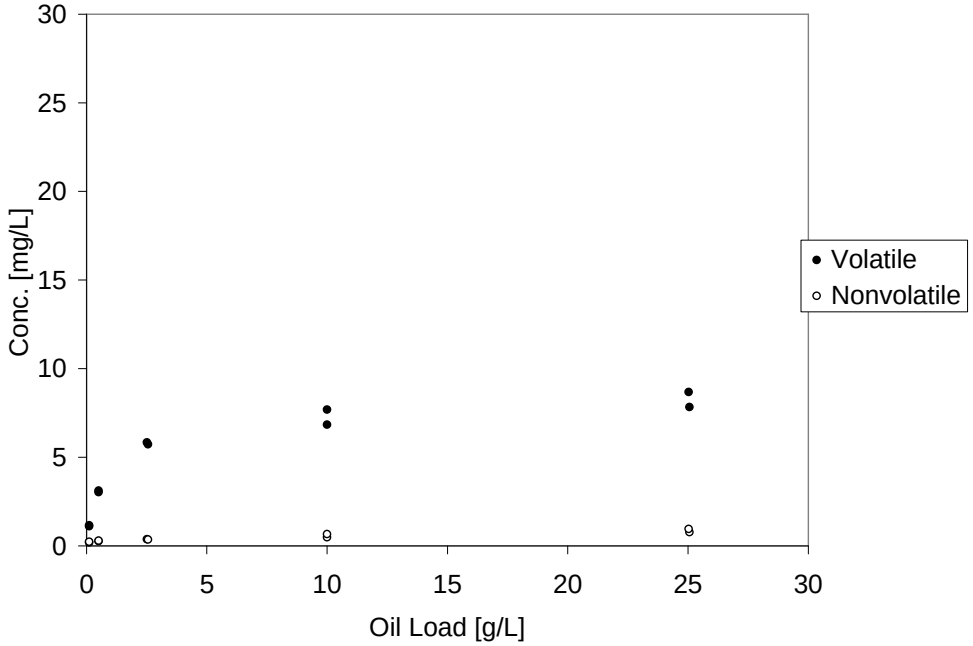

Fig. 3.3 Unweathered oil-only media component characterization. Each data point represents a single analytical result.

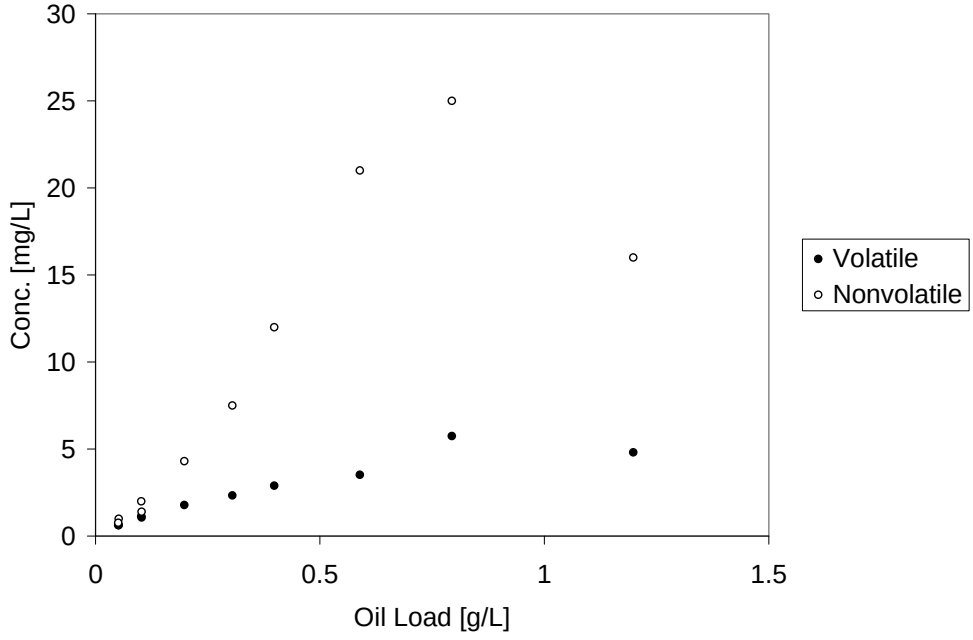

Fig. 3.4 Unweathered oil-plus-dispersant media component characterization. Each data point represents a single analytical result.

Dispersant contribution to oil-plus-dispersant toxicity

The cumulative mean dispersant-only LC50 of 320 mg/L for the three macroorganisms under both continuous and declining exposure regimes is one order of magnitude greater than the cumulative (all macroorganisms and exposures) average oil-plus-dispersant LC50 of 21 mg/L. Nominal oil loads on the order of 0.5 g/L are required to reach an oil-plus-dispersant nonvolatile hydrocarbon concentration of 25 mg/L (data not shown). Applying the manufacturer's prescribed dispersant dosages (one part dispersant to 10 parts oil) to these nominal oil loads translates to a maximum dispersant load of 50 mg/L in the oil-plus-dispersant media, a factor six below the cumulative average dispersant-only LC50. Actual dispersant concentrations in oil-plus-dispersant media may be substantially lower as some dispersant would be absorbed into the non-aqueous hydrocarbon phase. After mixing oil-plus-dispersant media, the preparations were allowed to settle for 3-6 hours, resulting in a distinct hydrocarbon phase on the media surface. All, media collected for the oil-plus-dispersant exposures were collected below the hydrocarbon layer where some of the initial dispersant load would be retained. However, no analytical chemistry was performed to quantify the dispersant concentration in the oil-plus-dispersant media. These observations indicate that the dispersant's contribution to the observed oil-pus-dispersant toxicity is minimal.

Oil-only versus oil-plus-dispersant toxicity evaluation

The mean continuous exposure oil-only LC50 of 3.3 mg/L (Table 3.2) was not significantly ($\alpha = 0.05$) different from the mean continuous exposure oil-plus-dispersant

LC50 of 4.6 mg/L (Table 3.3). Similarly, the *A. bahia* declining exposure oil-only LC50 of 55 mg/L (Table 3.2) was not significantly ($\alpha = 0.05$) different from the mean declining exposure oil-plus-dispersant LC50 of 59 mg/L (Table 3.3), although the oil-plus-dispersant toxicity is higher in both cases. Contrary to the macroorganism evaluation, the *V. fisheri* data indicated that the oil-only LC50 of 1.1 ($n = 4$) (Table 3.2) was significantly ($\alpha = 0.05$) lower than the oil-plus-dispersant LC50 of 18 ($n = 4$) (Table 3.3). This observed difference between the micro- and macro-organisms suggests that uptake of toxic components bound in a colloid are less available to bacteria than soluble toxins. As a generality, the results demonstrate that the oil-plus-dispersant media have toxicity that is either equal-to or less toxic than the oil-only media. This may be an important consideration from the perspective of dispersant use risk analysis.

Exposure regime evaluation

Comparisons between continuous and declining exposure toxicity data were made within media type groups (dispersant-only, oil-only, and oil-plus-dispersant) to determine the difference between the exposure regimes. For Corexit® 9500, the mean declining exposure LC50 was greater than the mean continuous exposure LC50 by a factor of five, but the difference was not significant ($\alpha = 0.05$) (Table 3.1). Evaluation of the mean oil-only LC50 values showed that the mean continuous exposure LC50 of 3.3 mg/L was significantly ($\alpha = 0.05$) less than the *A. bahia* declining exposure LC50 (Table 3.2). *Americamysis bahia* was the only organism with sufficient response to calculate and oil-only declining exposure LC50.

The observation that declining oil-only exposures resulted in higher LC50 values clearly demonstrates that declining exposures are less toxic than continuous exposures. Supporting evidence for this result was given by finding the mean continuous oil-only LC50 of 3.3 mg/L was not significantly different ($\alpha = 0.05$) from the mean declining exposure NOEC of 14 mg/L (i.e. concentrations that produced a 50% response during continuous exposures produced no response with the rapidly declining exposure) (Table 3.2). Similarly, the average oil-plus-dispersant (Table 3.3) data showed that the declining exposure LC50 was significantly ($\alpha = 0.05$) greater than the continuous LC50 by a factor of nine. In all media evaluated (dispersant-only, oil-only, and oil-plus-dispersant), the average declining exposures were greater that the continuous exposure effective concentrations, indicating that toxic threshold concentrations for declining exposure are elevated compared to continuous exposures, but the difference is statistically significant only for the oil-plus-dispersant media.

The previous test matrix toxicity evaluation indicated no toxicity difference between the oil-only and oil-plus-dispersant media when tested with the macrooganisms. Therefore, the combined average of both the oil-only and oil-plus-dispersant toxicity results from the continuous exposure tests was compared to the combined mean of the oil-only and oil-plus-dispersant toxicity results from the declining exposure tests. A single-tailed analysis of variance indicated that the cumulative average continuous exposure LC50 of 3.9 mg/L was significantly ($\alpha = 0.05$) lower that the cumulative average declining exposure LC50 of 37 mg/L and shows that the combined declining exposures are significantly less toxic than the combined continuous exposures.

Unweathered oil versus weathered oil toxicity evaluation

The unweathered oil-only LC50 of 0.52 mg/L was lower than the weathered crude oil-only NOEC of 23 mg/L by a factor of 44 (Fig. 3.2). This toxicity difference may be explained by compositional differences between the two oils and the subsequent compositions of the resultant toxicity media. Page et al. (2000b) showed that the nonvolatile hydrocarbon concentrations in dispersed oils prepared with weathered crude oil were composed of both colloidal and soluble fractions. To evaluate the extent that colloidal or solubility mechanisms contributed to the nonvolatile hydrocarbon concentration in the unweathered oil media, it was necessary to calculate the predicted solubility of the volatile and nonvolatile hydrocarbon fractions, respectively. Then the colloidal fraction was determined by the difference between the total component concentration and the soluble fraction (Page et al. 2000b).

Using a modification of Raoult's law, the solubility of the nonvolatile and volatile hydrocarbon components was estimated (Banerjee 1984). Banerjee (1984) developed a solubility analysis for organic complex mixtures (such as petroleum crude oil) where the aqueous-phase concentration of an organic compound in a two-phase water/complex mixture system is defined as

$$C_w = X^* S_L \tag{3.3}$$

where C_w is the compound concentration in the aqueous phase (mg/L), X is the mole fraction of the compound in the organic phase, and S_L is the aqueous solubility of the pure liquid compound (mg/L). For this demonstration, the nonvolatile hydrocarbon mole fraction in the unweathered parent oil was estimated to be 100% minus the volatile,

resin, and asphalt fractions. The weathering process resulted in a 25% reduction in the crude oil volume due to volatile losses of all fractions lighter than nonane (C9) (Page et al. 2002a). The mean weight percent of resins plus asphalts in crude oils is reported to be about 14% (Tissot and Welte 1978). Therefore, the nonvolatile hydrocarbon mole faction was estimated to be 100% - 25% -14% = 61%. Chromatogram analysis indicated that the volatile hydrocarbon mole fraction was on the order of 0.45%, based on area percentage. The solubility constant for the nonvolatile hydrocarbon fraction was estimated as the mean solubility of selected normal alkanes, including C10, C12, C14, C15, C17, C19, C21, C22, C25, C26, C28, C29, C31, C33, and C35 (Howard and Meylan 1997). Solubility constants and parent oil mole fractions of individual volatile hydrocarbon components are shown in Table 3.4 (Howard and Meylan 1997). Using the expression in Equation 3.3, the predicted aqueous phase concentration of volatile and nonvolatile hydrocarbon fractions would be 1.5 and 0.00081 mg/L, respectively (Table 3.4).

Observed volatile hydrocarbon concentrations in the unweathered oil-only media ranged from 1.1 to 8.7 mg/L (Fig. 3.3) and were within the same order of magnitude as the predicted aqueous volatile hydrocarbon concentration of 1.5 mg/L (Table 3.4). Conversely, the observed oil-only nonvolatile hydrocarbon concentrations ranged between 0.20 and 0.96 mg/L (Fig. 3.3) and were greater than the predicted aqueous concentration by three orders of magnitude, indicating that the nonvolatile hydrocarbon fractions are composed almost entirely of colloidal oil.

Table 3.4 Predicted aqueous concentrations based on modified Raoult's law (Equation 3.3). Mole fractions estimated from gas chromatography-mass spectrometry data; BTEX solubility data published in Howard and Meylan (1997); BTEX = benzene, toluene, ethylbenzene, xylene.

	Mole fraction	Solubility (mg/L)	Predicted Aqueous Conc. (mg/L)
Benzene	0.0003	1,800	0.54
Toluene	0.0006	526	0.32
Ethylebenzene	0.0009	169	0.15
mp-Xylene	0.0012	162	0.19
o-Xylene	0.0015	178	0.27
Total BTEX	0.0045		1.5
Total nonvolatile hydrocarbon	0.61	0.00132	0.00081

If the nonvolatile hydrocarbon fraction is assumed to be 100% colloidal, as an extreme case, the colloidal volatile hydrocarbon contribution can be estimated by

$$[\text{Volatile}_{\text{colloidal}}] = [\text{Parent Oil}]^* X_{\text{volatile}} \quad (3.4)$$

where [Parent Oil] = concentration of the parent oil test media and is estimated by

$$[\text{Parent Oil}] = [\text{Nonvolatile}]/X_{nonvolatile} \quad (3.5)$$

where X_{volatile} = mole fraction of volatile components in parent oil, $X_{nonvolatile}$ = mole fraction of nonvolatile components in parent oil, [Nonvolatile] = nonvolatile hydrocarbon concentration determined by gas chromatography – mass spectrometry. The calculation indicates that the colloidal volatile hydrocarbon contribution in the unweathered oil-only media is estimated at 10^{-3} mg/L and is four orders of magnitude less than the observed total volatile hydrocarbon concentrations (Fig. 3.5). These observations suggest that colloidal and solubility mechanisms drive the nonvolatile and volatile hydrocarbon concentrations, respectively. From an ecological risk assessment perspective, the propensity of petroleum hydrocarbons to exist as a colloidal suspension or soluble fraction can affects its bioavailability and subsequent toxicity in the marine

environment.

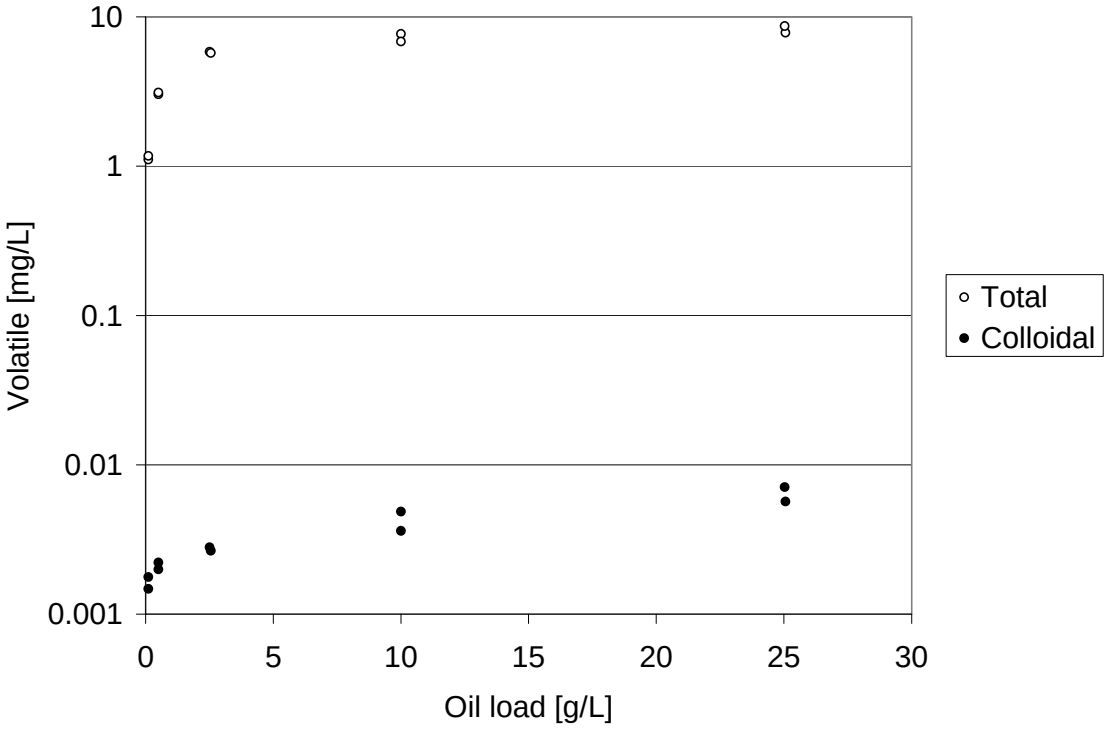

Fig. 3.5 Total and colloidal fractions of volatile hydrocarbons in unweathered oil-only media.

The volatile hydrocarbon fractions were lost during the oil weathering process, resulting in weathered oil volatile and nonvolatile hydrocarbon mole fractions of 0 and 100%, respectively. Based on the modified Raoult's law, the predicted aqueous-phase volatile and nonvolatile hydrocarbon concentrations at equilibrium would be 0 and 0.00132 mg/L, respectively. Observed non-volatile hydrocarbon concentrations in the weathered oil-only media ranged from 2.5 to 32.0 mg/L (data not presented) and were well above the predicted aqueous-phase concentrations, suggesting that a colloidal mechanism was the primary contributing factor to the non-volatile hydrocarbon

concentrations in the weathered oil-only media.

This analysis demonstrates that both physical and chemical differences existed between the two media types (unweathered and weathered oil-only media). Physically, the petroleum components in the unweathered oil-only media were primarily soluble compared to the weathered oil-only media that were predominantly colloidal. Chemically, the petroleum components in the unweathered oil-only media were dominated by the soluble aromatic fraction (volatile hydrocarbons) as shown in Fig. 3.3. The volatile components were removed during the weathering process and therefore not present in the weathered oil-only media. Combining this analysis with the toxicity data suggest that oil-only media with high soluble petroleum hydrocarbon concentrations were more toxic than media with high colloidal hydrocarbon concentrations. The findings are consistent with previous work suggesting that petroleum hydrocarbons absorbed in macromolecular dissolved organic structures (colloidal micelles) are relatively unavailable for uptake by clams (Boehm and Quinn 1976). Further, another study has shown that soluble aromatics are responsible for oil's toxic properties in the marine environment (Anderson et al. 1974).

The unweathered oil-plus-dispersant LC50 of 9.5 mg/L was not significantly (α = 0.05) different from the weathered oil-plus-dispersant LC50 of 31 mg/L (Fig. 3.2), although the weathered oil-plus-dispersant LC50 was higher than the unweathered oil-plus-dispersant LC50. Fig. 3.4 shows that the nonvolatile hydrocarbon fractions dominated the unweathered oil-plus-dispersant media, with nonvolatile hydrocarbon concentrations ranging between 0.77 and 25 mg/L compared to a volatile hydrocarbon

range of 0.62 to 5.7 mg/L. At the higher oil loadings, nonvolatile hydrocarbon concentrations exceeded the predicted aqueous concentration of 0.0032 mg/L by three to four orders of magnitude. This again suggests that the observed nonvolatile hydrocarbon fractions existed in a colloidal form. The volatile hydrocarbon concentrations of the unweathered oil-plus-dispersant media, at the higher loadings, exceeded the predicted solubility by a factor four. However, the oil-plus-dispersant volatile hydrocarbon concentrations (Fig. 3.4) were comparable to the oil-only volatile hydrocarbon concentrations (Fig. 3.3), indicating that solubility mechanisms were driving the observed volatile hydrocarbon concentrations in the oil-plus-dispersant media.

To evaluate solubility as the mechanism driving the volatile hydrocarbon concentration in the unweathered oil-plus-dispersant media, the colloidal volatile hydrocarbon contribution was calculated using Equation 3.4. Results from this simulation are shown in Fig. 3.6 and show that the mean colloidal volatile hydrocarbon contribution is about 1.9% of the total volatile hydrocarbon concentration. Thus, the unweathered oil-plus-dispersant media have a substantial soluble volatile hydrocarbon load compared to the weathered oil-plus-dispersant media where volatile hydrocarbons fractions are not present in colloidal or soluble form. This observation again shows that increased toxicity (lower LC50s) is associated with the presence of soluble hydrocarbon components. The lack of significant difference in the toxicity values of the unweathered and weathered oil-plus-dispersant media is likely due to high concentrations of colloidal nonvolatile hydrocarbon fractions in the oil-plus dispersant media prepared with both weathered and unweathered oil.

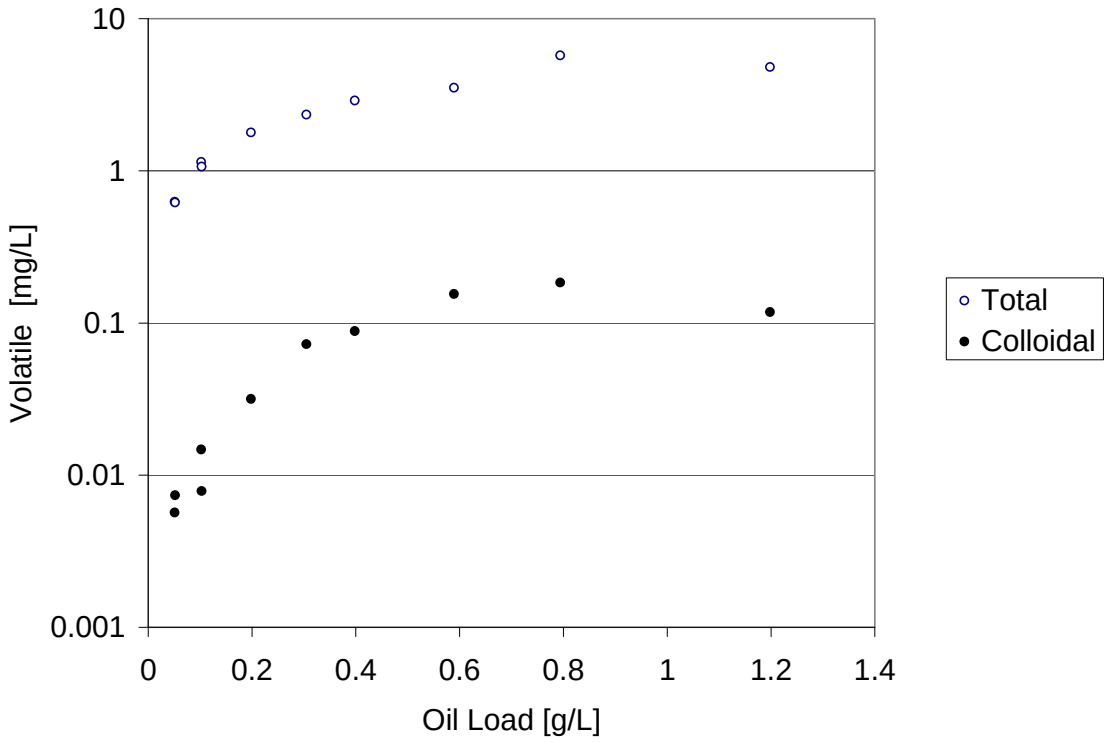

Fig. 3.6 Total and colloidal fractions of volatile hydrocarbons in unweathered oil-plus-dispersant media.

Unweathered oil-only and oil-plus-dispersant evaluation

Comparison of the *M. beryllina* data showed that the declining exposure unweathered oil-plus-dispersant LC50 of 9.5 mg/L was significantly ($\alpha = 0.05$) greater than the declining exposure oil-only LC50 of 0.52 mg/L by a factor of 18 (Fig. 3.2). This variance in toxicity may also be explained by the physical and chemical differenced of the two media. Figs. 3.3 and 3.4 indicate that the volatile hydrocarbon concentrations in both media are similar with oil-only media ranging from 1.1 to 8.9 mg/L and the oil-plus-dispersant media ranging from 0.62 to 5.7 mg/L. However, the mean oil-plus-

dispersant nonvolatile hydrocarbon concentration of 9.1 mg/L is greater than the mean oil-only nonvolatile hydrocarbon concentration of 0.46 mg/L by a factor of 20, which is comparable to observed difference in the LC50s. As discussed in the previous sections, the volatile fractions exist primarily as soluble components in both media, while the nonvolatile fractions exist primarily as a colloidal suspension because of its low solubility. Therefore, the median lethal effects are being manifested in media with similar soluble hydrocarbon concentrations, while the average LC50s of the two media differ proportionally to the nonvolatile hydrocarbon concentration. This observation agrees well with the mechanism presented by Boehm and Quinn (1976) where a hydrocarbon dissolved in a colloidal micelle will pass through the gills and therefore will not be taken up by the organism while the uptake of soluble hydrocarbons is an equilibrium process across the gill membrane. This mechanism also implies that the apparent toxicity differences are due to LC50 determinations based on differences in the relatively non-effective, with respect to observed toxicity, colloidal components.

Conclusions

The goal of the study was to evaluate the potential ecological effects of using dispersants in marine oil spills. The goal was accomplished with bioassays to determine the toxicity of the relevant dispersant only, oil-only, and oil-plus-dispersant media with three macro- and one bacterial indicator species. The study was also designed to determine the relative toxicity of two different exposure regimes, declining and continuous. Finally the effects of weathering of oil-only and oil-plus dispersant media

were evaluated, and this analysis included the determination of toxicity mechanisms as related to solubility and the contribution of colloidal particles composed of petroleum hydrocarbons.

Dispersant toxicity in field applications would be negligible compared to the oil toxicity. Weathered oil-plus-dispersant toxicity was less than or equal to the toxicity of the weathered oil-only on a nonvolatile hydrocarbon basis. Exposure regime evaluation indicated that continuous exposures to oil-only and oil-plus-dispersant media produced toxic responses more readily than declining concentrations, thus implying that dispersed oil toxicity would be significantly less in systems where dilutions produces rapidly declining exposures compared to relatively long, continuous exposures.

Limited testing with the unweathered oil-only and oil-plus-dispersant media demonstrated that solubility and colloidal mechanisms were responsible for mobilizing petroleum hydrocarbon fractions into the different media. In the unweathered oil-only media, solubility was the dominant mechanism with the primary petroleum hydrocarbon component being the volatile hydrocarbon fractions. In the unweathered oil-plus-dispersant media, a colloidal phenomenon was the dominant mechanism with the primary petroleum hydrocarbon component being the nonvolatile hydrocarbon fractions. Increased toxicity was associated with the presence of soluble (volatile) hydrocarbons. Conversely, lower toxicity was associated with media where colloidal oil fractions were shown to be the major nonvolatile hydrocarbon component.

CHAPTER IV

IN-SITU REAL TIME OPTICAL SENSORS TO DETECT AND MONITOR OIL SPILLS

Overview

The majority of significant environmental activity may be characterized as series of episodic (i.e. pulsed) events. In the aquatic or marine environments these episodes may occur naturally (example: storms, harmful algal bloom) or may originate from anthropogenic activity (example: oil spill, accelerated sedimentation). Characterizing these events with respect to intensity, duration, and spatial extent is critical to mitigate their deleterious effects. Recent advances in *in-situ* instrumentation are key to implementing continuous real-time and event based monitoring on static and mobile data collection platforms, respectively. This study evaluated five sensors (both *in-situ* and *ex-situ*) for rapid, quantitative detection of crude oil suspensions using a range of technologies including optical transmittance, small forward-angle scattering, and single wavelength spectrofluorometry. Each instrument tested showed linear responses to crude oil mass concentration. Additionally, measured crude oil volume concentrations were shown to be linear with nominal oil loads, indicating that crude oil plumes may be characterized and measured as a droplet suspension. The performance of each instrument is presented with a discussion of potential applications and interferences.

Introduction

Globally, the coastal zone is of major economic importance as demonstrated in the U.S. with more than half the population residing in coastal counties with an expected growth of an additional12 million between the 2003 and 2015 (Crosset et al. 2004). The coastal zone has been defined by the IGBP (International Geosphere Biosphere Programme) as the region between the 200 m elevation and depth contours. This zone accounts for approximately 90% of sea food production, while simultaneously serving as a sink for 90% of land based pollution (Cracknell 1999). These numbers illustrate the conflicting anthropogenic use of our coastal resources.

To better manage and or mitigate anthropogenic impacts requires that they be characterized with respect to intensity, frequency, and duration. Such tasks become overwhelming considering the spatial extent and episodic nature of environmental events. For example the British Petroleum Deepwater Horizon oil spill affected 37% the U.S. federal waters in the Gulf of Mexico as indicated by the areas closed to fishing (NOAA 2010b). In 1997, U.S. Coast Guard initiated the Special Monitoring of Applied Response Technology (SMART) program to evaluate the effectiveness of dispersant applications during spill response operations (U.S. Coast Guard 2006). The primary sensor implemented in the initial protocol was an *ex-situ* single wavelength fluorometer developed in the 1980s. Being *ex-situ* poses limitations and special requirements for deployment on board a response vessel at sea. On-scene response parties including the U.S. Coast Guard identified several deficiencies in protocols using *ex-situ* instrumentation including instrument set up and calibration during emergency responses

as well as the need to account for data lag between sample collection and analysis. Instruments relying on a continuously pumped sample stream through a flow cell are also affected by sample smearing (dispersion) caused by the combined effects of velocity gradients over the tubing cross-section and molecular diffusion in the radial direction (Taylor 1954). To address these concerns the Texas General Land Office (TGLO) directed our research group to design and build an integrated system (Fig. 4.1) including a *in-situ* fluorometer and Global Positioning System (GPS) to provide real time geo-referenced oil concentration data (Fuller et al. 2005). Expanding this concept led to the establishment of a vessel based monitoring program to be mobilized during and actual spill of opportunity (Ojo et al. 2007a). This vessel based system (Fig. 4.2) combined *in-situ* sensors, real-time telemetry, and direct numerical simulation to provide real time data visualization. Once an oil spill is detected, vessel based systems are ideally suited to track and define the spill boundaries. However, they are not well suited for continuous monitoring. To address this issue, a networked system including fixed monitoring stations (Fig. 4.3) were established in Corpus Christi Bay to provide real time measurements on water quality, water currents, and meteorological data (Bonner et al. 2003a). Established systems including continuous monitoring stations and mobile platforms enable stake holders (scientist, response personnel or regulatory agencies) to capture the episodic events and evaluate their intensity, spatial extent, and movement.

A)

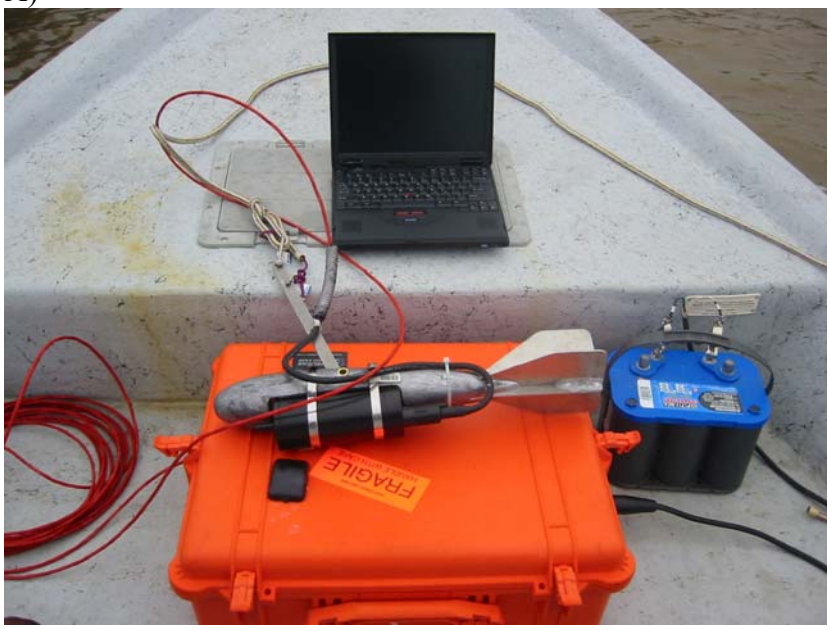

B)

Fig. 4.1 Integrated *in-situ* fluorometer with GPS for tracking dispersed oil plume. A) WETLabs WETSTAR Color Dissolved Organic Material (CDOM) fluorometer mounted to lead tow-fish, B) net work interface to combine GPS and WETSTAR data streams.

Fig. 4.2 Mobil monitoring platform. Instrument suite including particle analyzer, conductivity- temperature-depth (CTD) sensor, dissolved oxygen sensor, and fluorometer are mounted to the computer controlled undulating tow body, allowing sensor parameters to be mapped over horizontal and depth axis.

Fig. 4.3 Fixed platform in Corpus Christi Bay, WATERs test bed. Robotic profiler provides autonomous depth profiles of water quality parameters including salinity, dissolved oxygen, particle concentration and size distribution, and fluorescence.

Networked systems based on *in-situ* sensors are valuable tools to characterize and model environmental constituent transport processes (Ojo et al. 2006a, 2006b, 2007a, 2007b). Other significant environmental events including hypoxia, water column stratification, flooding, particle resuspension, etc., occur episodically. Characterizing the fundamental processes controlling these events is limited by the lack of data at the required spatial density and temporal frequency (Montgomery et al. 2007). To address these needs, the previously established sensor network including both mobile and stationary monitoring platforms in Corpus Christi Bay, Texas was selected as a National

Science Foundation (NSF), WATer and Environmental Research Systems (WATERS) test bed (WATERs Network 2005) and effectively extended the system applicability beyond oil spill monitoring. The initial research objective addressed with the Corpus Christi Bay test bed was an annually recurring hypoxic event (Montagna and Kalke 1992). Data collected from this system identified salinity stratification as a possible mechanism leading to hypoxia (Islam et al. 2011a). These examples demonstrate the wide applicability of *in-situ* instrumentation and sensor networks to characterize environmental disturbances and processes affecting overall system health.

Oil spills represent one anthropogenic episodic event that continues to be both politically and environmentally significant as demonstrated by the recent Deepwater Horizon explosion and oil spill in the Gulf of Mexico that occurred on April 20, 2010 and declared a Spill of National Significance (Gibbs 2010). Response actions at the Deepwater Horizon spill included *in-situ* burns and dispersant application, both of which are the primary response actions targeted by the SMART program (U.S. Coast Guard 2006). Such events accentuate the need for continued development of oil spill monitoring capabilities. This research attempts to partially address this need through the evaluation of five optical sensors with respect to their ability for quantitative detection of crude oil suspensions in artificial sea water.

Optical methods including fluorescence spectroscopy, transmittance, and laser *in-situ* transmissometry are ideally suited for implementation as *in-situ* instruments. Each method differs in their basic operating principles and may be characteristically better suited for a particular application than the other. For example, fluorescence

techniques are shown to be linear over wide concentration ranges (Guilbault 1990). Thus, fluorescence would be the technology of choice in a situation where expected concentration ranges would be outside the detection limit of alternative technology with a characteristically low detection range.

Fluorescence spectroscopy is based on the principle that molecules absorb light energy and are excited to an elevated energy state. The amount of light energy (photons) absorbed by the molecules is described by Beer's law as $dI = -k[J]Idx$ where dI is the reduction in light that passes through a control layer thickness dx containing an absorbing species J at a molar concentration $[J]$, k is the molar extinction coefficient (in $M^{-1}cm^{-1}$), with and incident light intensity I (Atkins 1990). As the excited molecule relaxes back to ground state it emits light photons at a lower energy (longer wavelength) in the fluorescence process. The amount of photons produced in the fluorescence step is a function of the overall quantum yield which is quotient of photons emitted over the photons absorbed (Lakowicz 1999).

The upper and lower linear detection limits of fluorescence techniques can span multiple orders of magnitude (Guibault 1990). This linear correlation will typically hold until the fluorophor concentration is great enough to absorb significant amounts of the excitation energy or light scattering restricts the uniform distribution of excitation energy (Guilbault 1990). Furthermore, the upper and lower detection limits may be adjusted by altering the excitation intensity (Guibault 1990). A benefit of this quality is the ability to accurately measure unknown concentrations over a broad range without the need to concentrate or dilute samples to achieve lower or higher detection limits, respectively.

Different chemical species have independent and identifying fluorescence spectra, which translates to analytical specificity (Guilbault 1990). There are many examples where fluorescence specificity has been used to characterize complex organic mixtures. Fluorescence spectroscopy has been used to characterize dissolved organic matter in seawater (Coble 1996). Aromatic hydrocarbon emission bands tend to increase with increasing molecular weight. With excitation wavelengths being 25 – 50 *nm* lower than the respective emission bands, single ring aromatics emit strongly at 280-290 *nm*, 2-ring PAHs tend to show a peak emission at 300-340 *nm*, followed by 3 and 5 ring emissions peaks at 360-390 and 420-480 *nm*, respectively (Patra and Mishra 2002; Wakeham 1977). This PAH emission specificity has been applied to characterize crude oils with respect to relative PAH concentrations of variable molecular weights (Von der Dick and Kalkreuth 1985). Synchronous fluorescence spectroscopy has been used to measure binary and ternary micellar PAH mixtures in sea water (Rodriguez et al. 1993). Similarly, excitation-emission matrix spectroscopy has been used to differentiate oil fluorescence emission finger prints dispersed in sea water and is able to track alterations resulting from weathering processes or dispersant treatments (Bugden et al. 2008).

The suitability of fluorescence spectroscopy has long been recognized for its capabilities to measure oil concentrations in natural waters and sediment, however early methods involved a solvent extraction process (Hargrave and Phillips 1975; Chen and Bada 1992; Law et al. 1987). By 1995, a flow-through-fluorometer was used to show that dispersant treatments enhanced natural oil dispersion (Lunel et al. 1995). Direct fluorescence has also been applied to monitor oil-mineral aggregate formation and to

evaluate the effect of chemical dispersant on oil spills (Kepkay et al. 2002, 2008).

Many environmental contaminants with low solubility constants, including dispersed oil, exist in aqueous environments as colloidal suspensions (Page et al. 2000b). Thus, suggesting the applicability of alternative detection methods such as optical transmittance, which is the inverse of the light removed (i.e. attenuation) from the original source via scattering by the suspended particles (droplets). Optical attenuation is proportional to twice the total particle area and can be represented as $\int_{a}^{a+da} n(a)a^2 da$, where a is the particle radius and $n(a)$ is the number of particles in the size range a and $a + da$ (Agrawal and Pottsmith 1994). Therefore, transmittance is a function of the particle size distribution, not the mass.

Total particle (droplet) volume concentration may also be inferred from the particle size distribution (PSD) as demonstrated with the LISST-100. Small-angle forward scattering is used to determine the particle size distribution over 32 ring detectors that correspond to log-normally distributed particle diameters (Agrawal and Pottsmith 1994). Each ring detector measures a scattering intensity that scales typically to the fourth power of the particle radius and is weighted by the number density. Scattering intensity from an ensemble of particles, assuming spherical geometry, can be expressed using the Mie equation as $I(\theta) = \int K(a,\theta)n(a)da$, where $K(a,\theta)$ is the scattering Kernel describing the intensity contribution from a particle of radius a at a scattering angle θ (Agrawal and Pottsmith 1994). While changes to the particle size distribution are accounted for with this technique, it does not account for variable

geometry. This may be especially relevant during flocculation where mass is conserved but volume concentration is not. The LISST has also demonstrated its applicability for dispersed oil detection through the characterization of oil-oil and oil-sediment aggregation processes (Sterling et al. 2004a, 2004b, 2005).

While the variety of instruments has increased, the effectiveness of each instrument for quantitative oil spill monitoring remains unclear. Additionally, each instrument has inherent limitations directly related to their respective operating principles. This work compares the responses from several commercially available fluorometers and a particle-sizing instrument to a range of dispersed oil loadings. Additionally, potential advantages and limitations of each instrument for oil spill monitoring are discussed.

Materials and Methods

Experimental design

This study evaluated the response curves of 5 *in-situ* optical instruments to standard oil suspensions of know concentration. Standard crude oil suspensions were prepared with artificial sea water (Instant Ocean, Aquarium System, Mentor, OH) at a salinity of 30 psu. Salinity was verified using a DataSonde (HydroLab, Loveland, CO). The suspensions were prepared in one of two specially designed mixing vessels to provide continuous mixing via a stainless steel impeller while allowing simultaneous data collection with multiple instruments (Fig. 4.4). Both vessels were fitted with a water tight flange that allowed the LISST 100 to be operated in a horizontal orientation,

A)

B)

Fig. 4.4 Cylindrical 40 liter reactor vessel. A) Side view showing LISST with horizontal orientation and mixer mounted above, B) top down view showing LISST sensor head in reactor vessel with mixing impeller. Small black cylinder in ring stand is WETLabs FL3 fluorosensor.

thereby allowing the optical windows to have a vertical orientation to minimize particle accumulation resulting from gravitational settling. Other custom features included hose barb bulkhead fittings to facilitate installation of a pump to continuously circulate the suspension through the SAFire, Turner 10-AU, and the mixing vessel.

Artificially-weathered Arabian medium crude oil was used to prepare all crude oil suspensions in this study. The natural weathering of the crude oil was simulated by air stripping the volatile fractions which reduced the oil volume by 30-35%. The weathered oil has a specific gravity of 0.9129, kinematic viscosity of 102.4 centistokes a at 20° C, and a Reid vapor pressure of 2.1 kPa at 37.8 C. This oil was premixed with the dispersant Corexit 9500A (Nalco, Sugar Land Texas) at a 10:1 oil mass to dispersant mass ratio.

Oil-dispersant fluorescence characterization

Crude oil is a complex organic mixture that can show marked variability in its relative concentrations of various hydrocarbon components with corresponding fluorescence spectra variability. For comparison to the field deployable instruments a three-dimensional excitation-emission spectra of the oil-dispersant mixture was generated with a bench top spectrofluorometer (Perkin Elmer LS50B). The LS50B was controlled with FL Winlab (version 4.00.02) interfaced to desktop computer with a Windows-7 operating system. Both excitation and emission slit widths were set to 3.5 *nm* with and emission scan speed of 300 *nm/min.* The emission spectra ranging from 230-800 *nm* were collected for at excitation wavelengths ranging from 220-620 *nm*

(Δλ=20nm). Discrete samples were analyzed using silica cuvette for ultra-violet fluorescence. To eliminate scattering effects, the oil-dispersant was dissolved in cyclohexane and diluted until no shift in the emission spectra at a constant excitation wavelength of 220 *nm* was detected. The 3-dimensional spectra showed a peak fluorescence emission at approximately 220/337*nm* (excitation/emission) with the total fluorescence region approximately bounded by emission wavelengths of 280 to 500 *nm* and excitation wavelengths of 220 to 460 *nm* (Fig. 4.5). This emission spectra is consistent with the fluorescence spectra of single ring aromatics and PAHs (Patra and Mishra 2002; Wakeham 1977). No apparent fluorescence emissions resulting from the oil-dispersant mixture were observed outside this region.

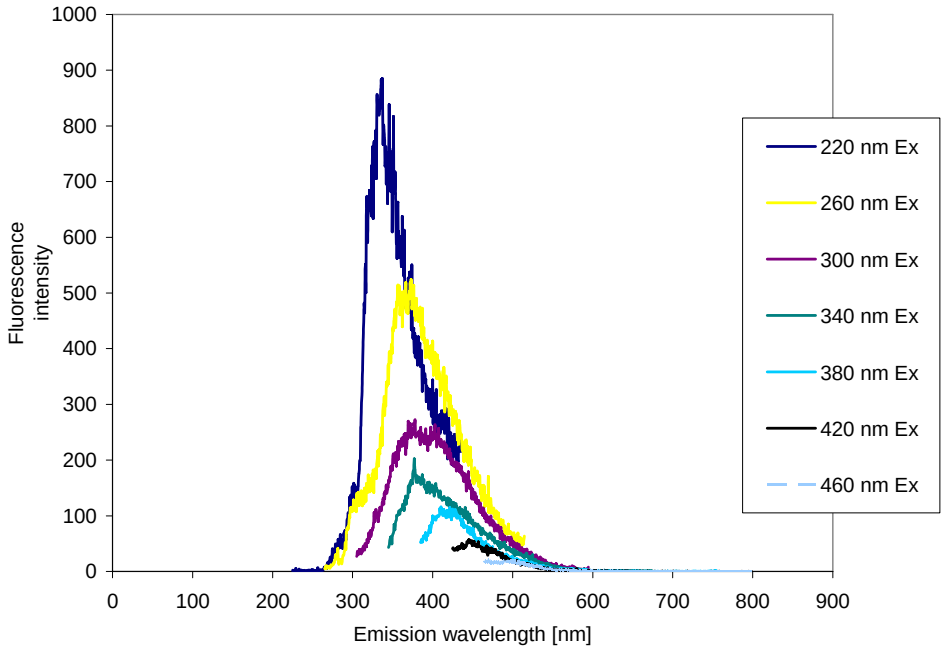

Fig. 4.5 Fluorescence spectra of crude oil-dispersant mixture dissolved in cyclohexane. Spectra shown for Δλ=40 nm for clarity. Spectra shows fluorescence only for emission wavelengths greater than excitation wavelengths to alleviate peaks resulting from 1st and 2nd order diffraction by the monochromator as described by Lakowicz (1999).

Volume concentration and transmittance

The LISST-100, Type-B (Sequoia Scientific, Bellevue, WA) utilizes a specially constructed detector consisting of 32 log-spaced rings, for detecting light scatter from particles with diameters log-normally distributed between 1.3 – 230 μm. The detector also has a center hole allowing direct beam passage for transmissometry measurements. Since the LISST measures the concentration based on the volume concentration (i.e. particle size and count) there are no target analyte specific calibrations. Volume concentration calibrations may be performed by comparing the measured volume concentration against a standard particle volume concentration. Adjustments are then made to the volume concentration coefficient (VCC) until the measured and standard concentrations agree within acceptable limits. Particle sizing calibrations are performed at the factory but may be verified by comparison of measured mean particle diameter against particle size standard. Data was collected with factory supplied software, LISST.exe, Version 1.0.0.1. Reported values are the mean of 30 samples.

Standard oil suspension preparation for LISST 100

Standard oil suspensions for the LISST 100 were prepared in a round 40 L cylindrical mixing vessel. Uniform mixing was provided by a stainless steel impeller composed of four cylindrical rods evenly staggered in the reactor volume (Fig. 4.4) (Sterling et al., 2004a). Mixing shear, G_m, for this reactor-impeller system was determined as a function of impeller angular velocity (ω=rpm) using the digital wattage display on the laboratory mixer (Lightnin®, Model L1U08). As described by Sterling et

al. (2004a) mixing power values were converted to mean shear rates, G_m, using the equation (Camp and Stein 1943)

$$G_m = \left(\frac{Po}{\mu V} \right)^{1/2} \quad (4.1)$$

where, G_m= s^{-1}, Po=watts, μ=1.002E-3 kg-m^{-1}-s^{-1}, V=reactor volume=0.04 m^3. For $70 \leq \omega \leq 200$, the following empirical calibration resulted for this mixing system:

$$G_m = 2.34\omega - 118.7, \; R^2 = 0.998 \quad (4.2)$$

To maintain a stable oil suspension, the reactor volume was mixed continuously at a shear rate, G_m = 233 s^{-1}.

The standard oil suspensions generated for the LISST 100 were prepared by injecting the appropriate neat oil-dispersant volumes into the reactor, using a Gastight® syringe, to achieve dispersed oil volume concentrations of 1000, 5000, 10000, 15000, 20000, 25000, and 30000 ppb (volume/volume). Each oil-dispersant addition was injected adjacent to the mixing impeller shaft just below the surface of the salt water media. The reactor was allowed to mix for 5 minutes following each oil-dispersant addition before measurements were collected with the LISST. A total of 30 measurements were taken for each dispersed oil standard.

Fluorescence detectors

The Wetlabs Flashlamp is an open path fluorescence detector configured with an excitation wave length of 230 *nm*. An emission filter in front of the photodetector allows emission at 350 *nm* to be measured at the photo-detector. Benzene has been

shown to have a strong fluorescence at an excitation/emission of 240/300 *nm* (OMLC 2007). Therefore these wavelengths are often used to detect refined fuels that include benzene, toluene, ethyl-benzene, and xylene (Turner Designs 2010). Communication with the Flashlamp is via serial connection (RS-232, 9600 Baud) using Hyper Terminal. All fluorescence values are raw counts requiring post processing using calibration curves prepared by the user.

The Turner Designs (Sunnyvale, CA) 10-AU field fluorometer was configured with a 25 mm one-piece flow cell. Fresh sample was supplied to the flow cell via a pump to recirculate the sample stream between the 10-AU and the mixing vessel. Turner Designs provides two filter kits for monitoring oils. For consistency with the Special Monitoring of Advanced Response Technologies (SMART) protocol (U.S Coast Guard 2006) the filter kit for long wavelength oils was used. This filter kit allows excitation at 300-400 *nm* while an emission filter in front of the photodetector allows emissions at 500 *nm* +/- 100 *nm* to be measured register. A broad range of oils, including motor, fuel, and crude oil have been shown to demonstrate strong fluorescence in the visible wavelength range of 400-600 *nm* when excited at near ultra-violet wavelengths 300-400 *nm* (Turner Designs 2007). An alternative filter kit is available for short wavelength oils that allows for excitation at *254* nm with an emission at 350 +/- 50 *nm* to be measured and is consistent to the fluorescence spectra for benzene (OMLC 2007). Prior to use, a three-point calibration of the instrument was performed using fluorescein dye. Measurements were made with the Auto Ranging feature enabled. The fluorescence responses recorded were raw fluorescence counts (i.e. no units).

The WETLabs (Philomath, OR) ECO-FL3 is an open path, *in-situ*, multiple wavelength fluorometer designed to measure the fluorescence of chlorophyll-*a*, colored dissolved organic matter (CDOM), and, uranine. Data collection with the ECO-FL3 was via a serial interface (RS-232) at 19200 baud using HyperTerminal. Standard oil suspension response curves were collected with both the chlorophyll-a and CDOM channels. Excitation and emission wavelengths for the chlorophyll-*a* channel were 470 *nm* and 695 *nm*, respectively. Excitation and emission wavelengths for the CDOM channel were 390 *nm* and 460 *nm*, respectively. All fluorescence values obtained with the ECO-FL3 are raw counts. Quantitative measurements require post processing with user generated calibration curves.

The WETLabs (Philomath, OR) SAFire is a multi-spectral closed cell fluorometer. Sample was carried to the flow cell via a pump that circulated the oil suspension between the SAFire and the mixing vessel. Excitation wavelengths are 228, 265, 313, 340, 430, and 437 *nm* while emission wavelengths are 228, 265, 313, 340, 375, 400, 430, 460, 490, 540, 565, 590, 620, 650, 685, and 810 *nm*. This results in 96 measured excitation/emission fluorescence pairs. For this study oil suspension response curves, were collected at 228 *nm* excitation-340 *nm* emission and 340 *nm* excitation-460 *nm*. These excitation-emission pairs generally correspond to the spectra for refined (Turner Designs 2010) and crude oils (Turner Designs 2007), respectively. As with the other *in-situ* instruments no provisions are made for end user calibration. Communication with the SAFire was made using vendor supplied software package (SAFView).

Standard oil suspension preparation for fluorescence detectors

Dispersed oil suspensions for the fluorescence detectors were generated by first preparing a dispersed-oil stock suspension. Using a volumetric flack, the stock suspension was prepared by adding 10 ml of oil-dispersant mixture into 1 Liter artificial seawater. Using a wide tipped pipette, the appropriate stock volumes were injected into the 50 L reactor vessel adjacent to the rotating impeller shaft. The standard oil concentrations were 10, 100, 250, 500, 750, 1000, 5000, and 10000 parts per billion (ppb), nominally.

All fluorescence sensors were used to collect data during a five-minute sampling interval following each standard oil addition. The fluorescence values reported in this research are the average value collected during this period. No data logging capabilities were available on the Turner 10-AU evaluated in this study. Therefore, the values listed were manually recorded.

Results and Discussion

LISST-100

Preliminary trials using the LISST 100 to measure dispersed oil suspensions showed that standard deviations exceeded measured volume concentration measurements at oil concentrations equal to or less than 100 ppb. Therefore, LISST-100 response curves were generated for oil concentration range of 1000 to 30000 ppb. Linear responses resulted for both volume concentration and transmittance with $R^2>0.99$ for both parameters and replicates over the measured range (Fig. 4.6). Slopes showed

virtually no difference between replicate transmittance measurements and only a 2% difference in volume concentration measurements. Thus, the LISST provided reproducible slopes with respect to dispersed oil measurements. Evaluation of the transmittance slopes (Fig. 4.6) indicates that the maximum oil detection limit by the LISST to be approximately 51,000 ppb. At higher concentrations, light transmittance through the media would be zero. An important observation is that the volume concentration responses from both replicates had slopes that were approximately 1 with y-intercepts being less than 2% the volume concentration range (Fig. 4.6A). This demonstrates the particulate (i.e. droplet) nature of the crude oil suspensions as shown in previous studies (Page et al. 2000b; Sterling et al. 2004a). The LISST-100 infers the particle/droplet concentration from the particle size distribution assuming a spherical geometry (Agrawal and Pottsmith, 1994). Considering that the total volume concentration measured with the LISST-100 agreed well with the nominal oil loads as indicated with slopes of unity and R^2 values greater than 0.99 suggest the oil droplets exist as spheres (Fig. 4.6).

A)

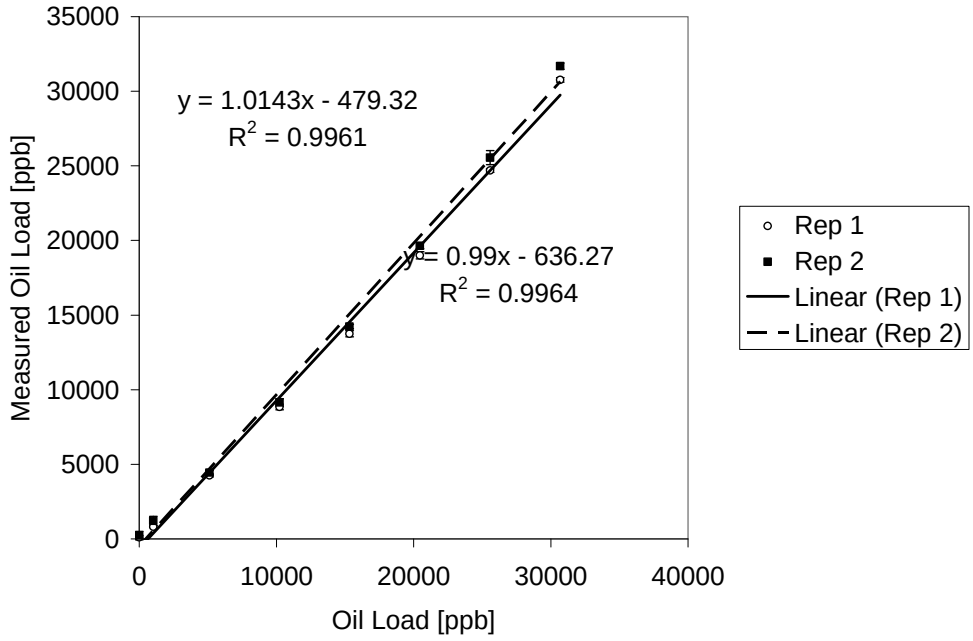

B)

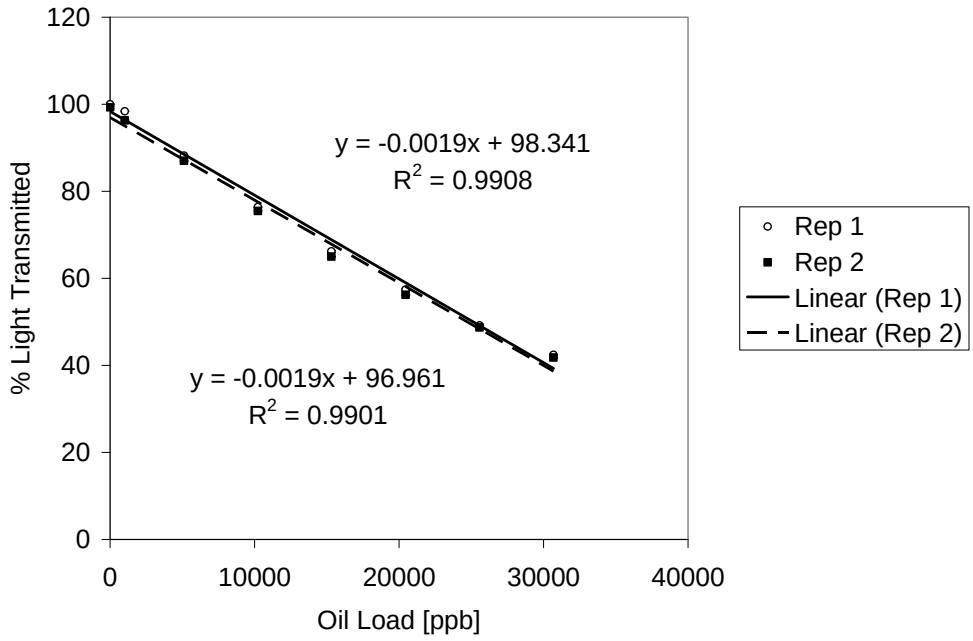

Fig. 4.6 LISST 100 response curves to standard oil droplet suspensions, A) volume concentration B) transmission.

Agrawal et al. (2008) showed that laser diffraction can overestimate the size of natural particles by 20-40% due to bias resulting from a departure from spherical geometry. An overestimation in the particle size would translate to a proportional overestimation of the inferred volume concentration (i.e. slope of measured volume concentration to nominal concentration would be greater than unity). A departure from a slope of unity may indicate the occurrence of oil-oil and/or oil-particle aggregates which have been shown to have characteristically fractal geometry where porosity is proportional to floc size (Sterling et al., 2005). This implies that total floc volume is greater the sum of the discrete oil droplets and/or particles contained within a floc. Therefore, total oil volume concentration inferred with the LISST-100 from oil-oil and/or oil-particle aggregates would be greater than the nominal oil volume load.

In addition to volume concentration data, the LISST 100 provides valuable information in the form of the particle size distribution (PSD) (Fig. 4.7). Oil droplet size distribution was bimodal with two peaks at 1.4 and 8.4 microns (Fig. 4.7). The PSD was conserved between successive standard oil additions and replicates. PSD data can provide valuable insight pertaining to the physico-chemical processes affecting oil and oil particle aggregation and subsequent settling (Sterling et al. 2004a, 2004b, 2004c, 2005). Further, it may be possible to differentiate oil-droplets from ambient particles based on characteristic particle size distribution of the respective, suspensions.

The LISST can effectively measure crude oil suspensions with detection limits spanning 2 orders of magnitude. Higher detection limits may be possible by shortening the optical path length with accessories available from the manufacturer (Sequoia

Scientific), but lower detection limits would likely increase proportionally. Evaluation of the transmittance (Fig 4.6B) shows that nearly 100% of the light was transmitted through control media (i.e. prior to any oil addition) volume, indicating that few particles existed in the media to interfere with measurement. In addition to solid and liquid particles (i.e. oil) the LISST will detect bubbles. Therefore, discretion must be used when evaluating volume concentration and transmittance data collected from characteristically turbulent and/or turbid waters. Interference from ambient particles or droplets may be discernable via evaluation of PSD.

A)

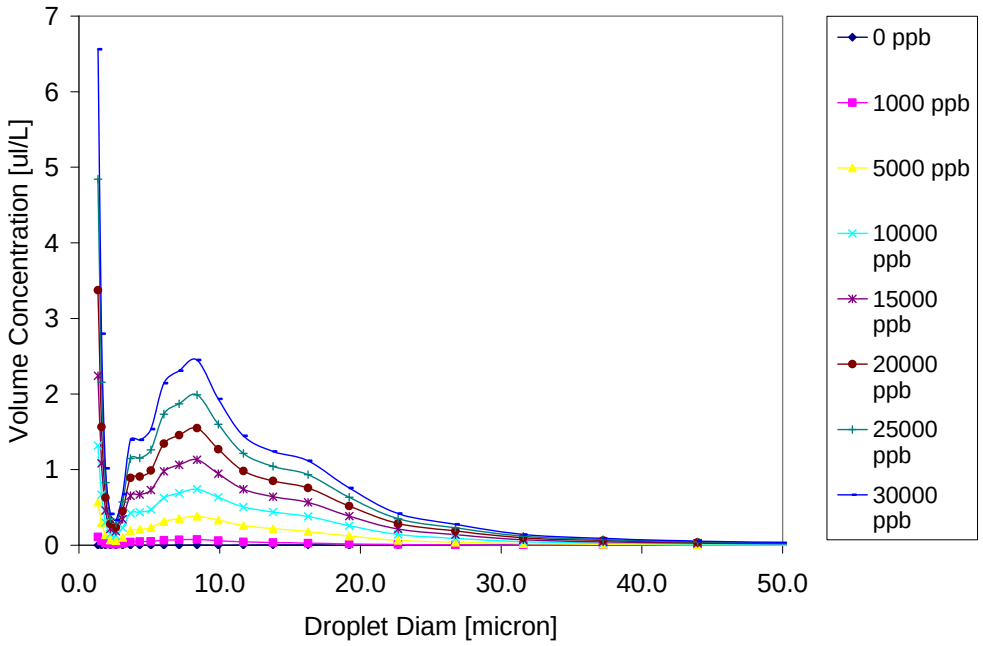

Fig. 4.7 LISST 100 oil droplet size distribution, A) Replicate 1 B) Replicate 2. x-axis truncated to 50 micron to show detail.

B)

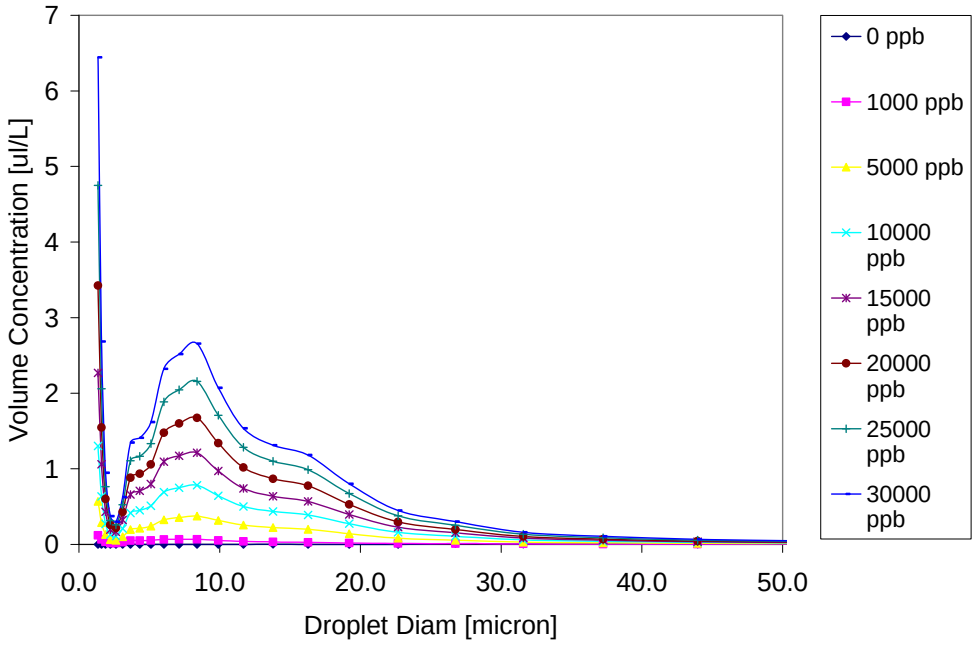

Fig. 4.7 continued

WETLabs Flash Lamp

The Flashlamp responses to the standard crude oil suspensions showed good linearity with $R^2 > 0.98$ for both replicates (Fig. 4.8). Good reproducibility was indicated with replicate slopes agreeing within 10%. Additionally, the response was greater than the noise throughout the measured oil range spanning 4 orders of magnitude, clearly showing that fluorescence responses can retain linearity over wide concentration ranges as suggested in Guilbault (1990). The strong response observed with the Flashlamp at 230/350*nm* (excitation/emission) is consistent with the 3-dimensional scan showing peak emission at the excitation/emission at similar wavelengths (Fig. 4.5). This observation demonstrates that despite the loss of volatile

fractions, ultraviolet excitation and emission wavelengths may be useful for quantitative weathered crude oil measurements.

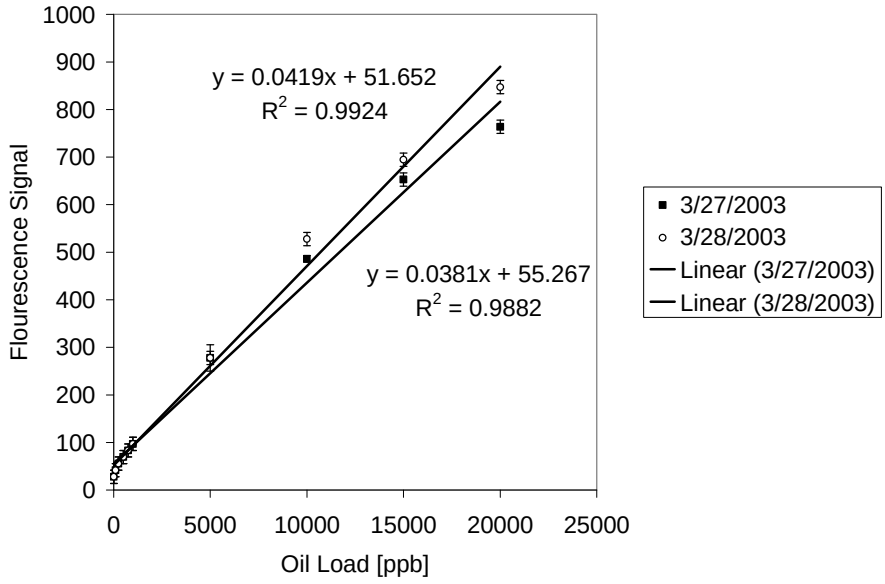

Fig. 4.8 WETLabs Flashlamp fluorescence response for crude oil suspensions.

Turner Designs 10-AU field fluorometer

The Turner, 10-AU field fluorometer, demonstrated linear responses to the standard crude oil suspensions with R^2>0.99 on both replicates (Fig. 4.9). This indicates the appropriateness of the filter kit for long wavelength oils used in this study. However, the slopes varied about 15% which is less consistent than observed in with the WETLabs Flashlamp. Oil concentrations of 15,000 and 20,000 ppb were above the measurement range of the instrument indicating an upper detection limit of 10,000 ppb (vol/vol). Despite the comparatively lower upper detection limit, the 10-AU still showed a linear response over a concentration range spanning 4 orders of magnitude with a single calibration. One advantage of the Turner is the ability to perform field calibrations that

allow the user to adjust the span (i.e. fluorescence range) so that the detection limits could be adjusted to the required operating range. No data logging options were available for the 10-AU evaluated, therefore a single fluorescence reading was manually recorded for each standard oil suspension. As such fluorescence signal standard deviations were not shown in Fig. 4.9.

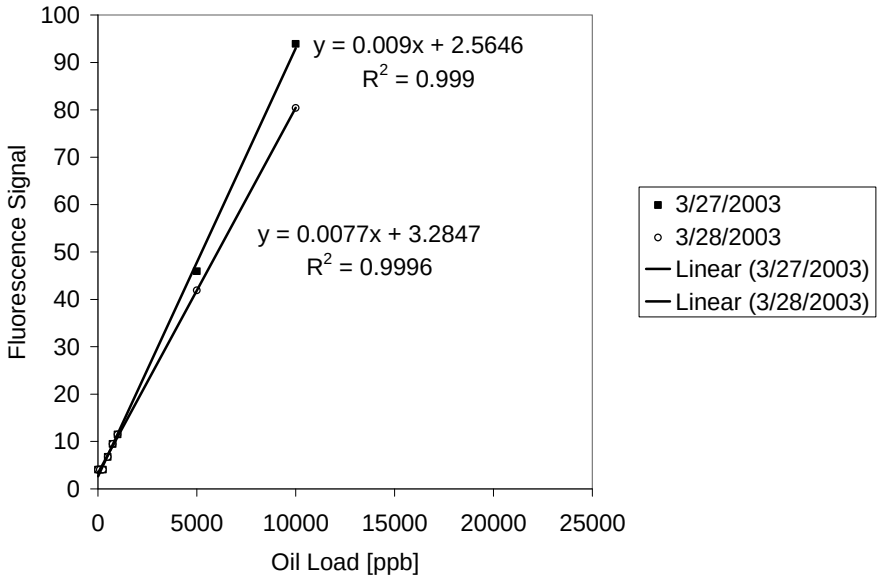

Fig. 4.9 Turner Designs 10-AU field fluorometer response for crude oil suspensions.

WETLabs ECO-FL3

The WetLabs ECO-FL3 produced linear responses to crude oil suspensions with both the chlorophyll-*a* and CDOM as indicated with R^2 >0.97 (Fig. 4.10). The strongest response was observed at the chlorophyll-*a* wavelengths (EX 470 *nm/* EM 695 *nm*), while only minimal responses were observed on the CDOM (EX 390 *nm/* EM 460 *nm*) wavelengths. This is an unexpected observation considering that the 3-dimensional fluorescence spectrum shows no fluorescence at the chlorophyll-*a* wavelengths (Fig.

4.5). Furthermore, evaluation of fluorescence spectra of several oil samples including crude, fuel, and lubricating oils show that the when excited with a 300 *nm* source, the fluorescence of the oils evaluated dropped sharply after 500 *nm* (Turner Designs 2007). At this time, the cause of the anomalous crude oil response at the chlorophyll-*a* wavelength is unknown. Similarly, WETLabs technical support could not explain the elevated fluorescence responses to crude oil at chlorophyll-*a* emission wavelengths during field deployments during the DeepWater Horizon oil spill response (personal communication, Julie Rodriguez, WETLabs, October 26, 2010). Despite this unexpected response, the chlorophyll-*a* response curve reproducibility was similar to that of the Turner 10-AU with slopes agreeing within 15%. A minimum detection limit of 1000 ppb was indicated by standard deviations greater than the mean response values at lower concentrations. The CDOM wavelengths were expected to show a strong response to the weathered crude oil as the emission wavelength of 460*nm* is comparable to the characteristic emission wavelengths for 5 ring PAHs (Wakeman 1977). However, the fluorescence spectrum (Fig. 4.5) shows only a minimal fluorescence response at the 390 *nm*/460 *nm* (excitation/emission) wavelengths. Similarly, the ECO FL3 CDOM channel demonstrated only a minimal fluorescence response of only 70 counts (about 2% of the instrument response range) over the complete concentration range (10 – 20000 ppb) (Fig. 4.10B). This limited fluorescence response suggests that the CDOM wavelengths are not well suited for measuring weathered Arabian medium crude oil suspensions. However, dispersed oils composed of petroleum fractions high in heavy molecular weight PAHs should produce noticeable responses on the CDOM channel.

A)

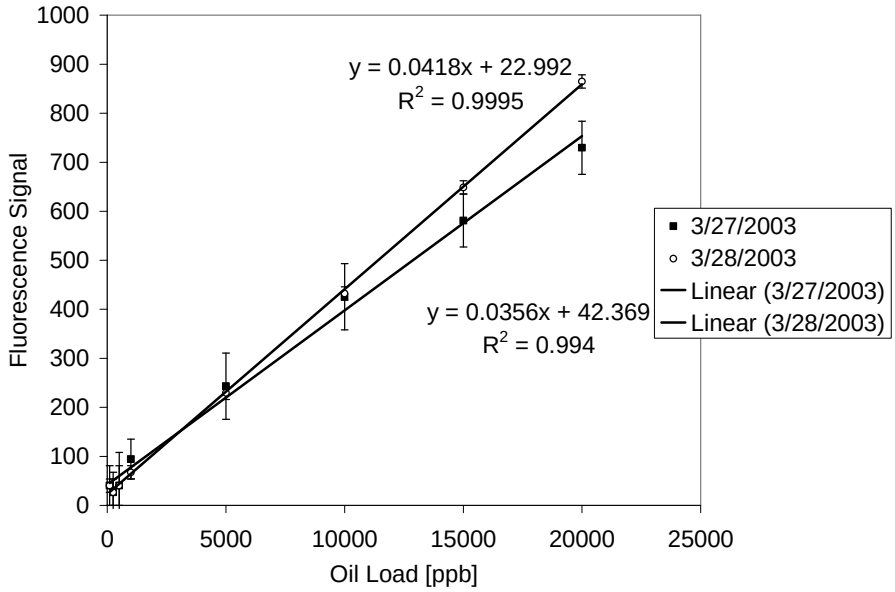

B)

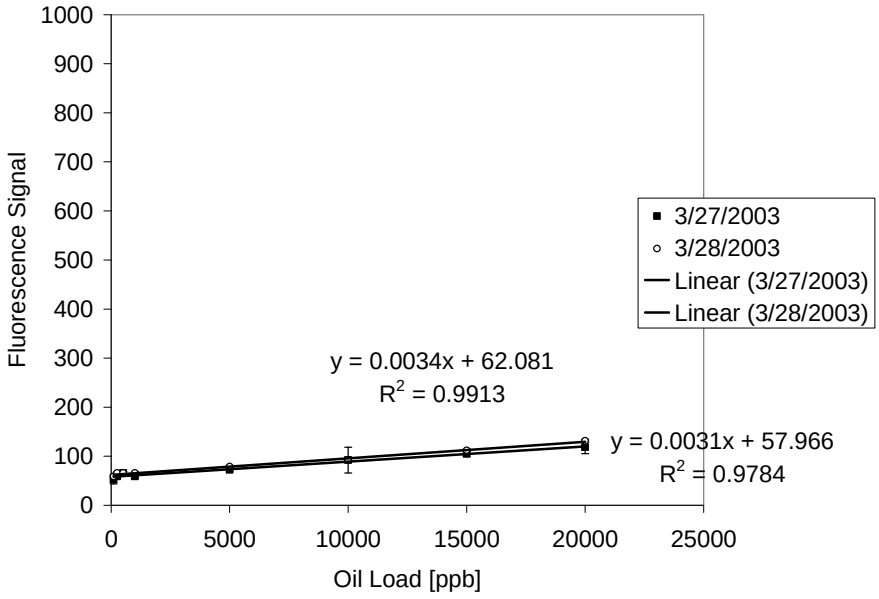

Fig. 4.10 WETLabs ECO-FL3 fluorescence response data for crude oil suspensions, A) chlorophyll-*a* 390 *nm*/460 *nm* B)CDOM 470 *nm*/695 *nm*.

WETLabs SAFire

The SAFire response measured with the 228 *nm* excitation/340*nm* emission pair was linear (R^2>0.98) for both replicates (Fig. 4.11A). The response curve slopes agreed within 10% for replicate treatments, demonstrating reproducibility required for quantitative field analysis. For the entire measured range, the mean response was greater than the measurement noise. For the 340 *nm* excitation/460 *nm* emission pair (Fig. 4.11B), the responses were less linear (R^2 > 0.92) and less consistent with slopes varying 30%. The responses from both excitation/emission pairs were consistent with the 3-dimensional emission spectra generated with the laboratory fluorescence spectra fluorometer (Fig. 4.5), (i.e. strong fluorescence emissions were observed with the 228 *nm* excitation/340*nm* emission pair with a comparatively weak fluorescence emission observed with the 340 *nm* excitation/460 *nm* emission pair) and suggest that ultraviolet wavelengths are appropriate to measure weathered crude oil dispersion generated with light to medium weight crude oils.

In addition to the being useful for measuring the concentration of dispersed oil, the two spectra obtained with the Saffire allow some qualitative inferences to be made with respect to dispersed oil's composition. The relatively strong response (i.e. greater response slope) observed with the 228 *nm* excitation/340 *nm* emission compared to the 340 *nm* excitation/460 *nm* emission pair suggests the dispersed oil contains relatively high concentration of 1-2 ring aromatics compared to 3-5 ring aromatic hydrocarbons. Making similar inferences from the other *in-situ* fluorometers is not possible as they do not contain corresponding spectra for direct comparison.

A)

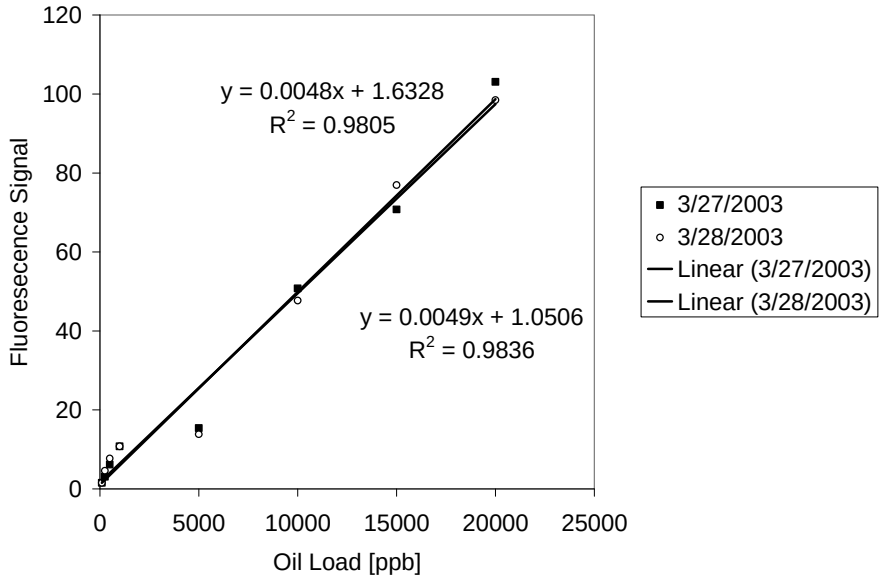

B)

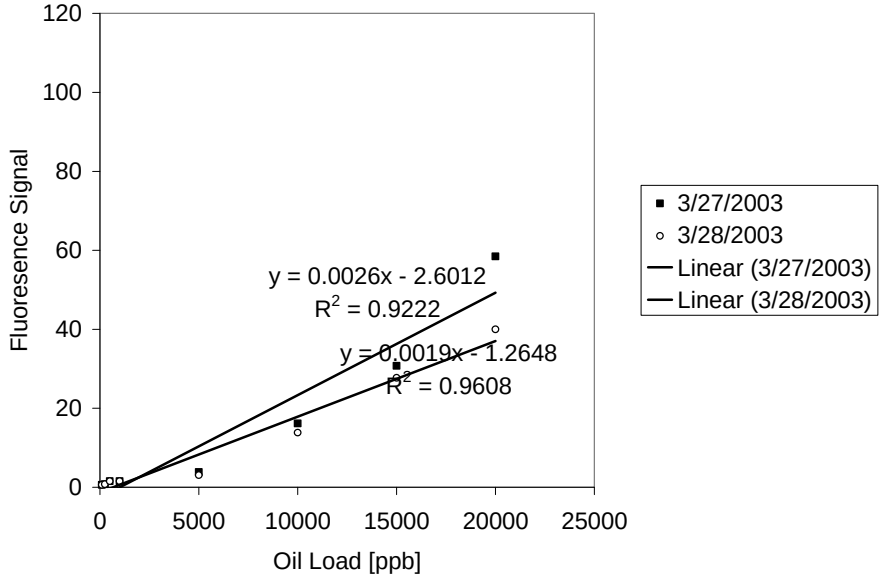

Fig. 4.11 WETLabs SAFire fluorescence response data for crude oil suspensions, A) 228 *nm/*340 *nm,* B) 340 *nm/460 nm.*

Of all the fluorometers evaluated in this study, those with ultraviolet excitation/emission pair, the Flashlamp and SAFire (228/340), showed the best

responses to the crude oil tested with respect to the upper and lower detection limits, linearity, and reproducibility. This excitation/emission pair is typically used for fluorescence detection of refined oils containing high BTEX concentrations. This observation is some what confounded by the strong response provided by the ECO-FL3 on the chlorophyll-*a* channel which uses and excitation and emission pair with higher wavelength than typically used for crude oil detection. These observations indicate that choice of fluorometers for a specific oil should not rely solely on the manufacture's suggested wavelengths. Another implication of this observation is that the fluorescence responses cover a broad spectrum with and there is often overlap in the spectra of different analytes and presence of the interfering species can not be detected using single wavelength spectroscopic techniques (Booksh et al. 1996). Thus, the potential exists for positive or negative fluorescence interference from many compounds prevalent in the environment.

Conclusions

This study showed that all the instruments tested responded linearly to oil suspensions ranging from 10 – 20000 ppb under ideal laboratory conditions. This implies that all the instruments can be used to quantify oil suspensions in an aqueous media, provided instrument specific calibrations are performed. This was further illustrated by the fact that the same oil resulted in widely varying responses in instruments using the same principles (fluorescence spectroscopy) at comparable excitation and emission wavelengths. For example, the ECO-FL3 with

excitation/emission wavelengths of 390*nm* /460*nm* showed little response while a relatively strong response was observed using the Turner 10-AU using comparable excitation and emission wavelengths. Further, it was demonstrated that oil suspensions may be measured as a particle suspension, not an aqueous solution and suggests that oil plumes may be detectable using surrogate technologies (i.e. acoustic backscatter).

As with all analytical methods, care must be exercised when interpreting results. The results presented in this study were conducted under controlled laboratory conditions. However, all of the instruments evaluated are intended for use in the field and with the exception of the Turner 10-AU are *in-situ* instruments. As such, all are subject to variable operating conditions that may adversely affect performance. Therefore, it is critical to understand the operational principles and limitations of each instrument so that potential interference can be identified. This knowledge is also critical to choosing the correct instrument and/or configuration for the target analyte.

This study showed that with careful consideration of target analyte, environmental conditions, and instrument capabilities, real-time *in-situ* sensors are viable tools for real-time environmental monitoring including oil spill response. Potential benefits from this type of real-time monitoring include 1) better understanding of the cyclical nature of near-shore ecological and physical parameters, 2) building a foundation for quantitative modeling and for oil spill response and designing long-term, cost-effective monitoring strategies; 3) formulating operational tools for environmental managers; and 4) disseminating results in “user-friendly” formats for the general public, educators, and policy makers.

CHAPTER V

ESTIMATION OF COLLOIDAL CONCENTRATION USING ECHO INTENSITY FROM AN ACOUSTIC DOPPLER CURRENT PROFILER

Overview

Interest has grown for using Acoustic Doppler Current Profilers (ADCPs) to measure suspended solids concentrations (SSC) in aqueous environments because simultaneous multipoint measurements with high spatial and temporal resolutions are possible. The acoustic backscatter intensity (ABS) measured by ADCPs is a function of the particle size distribution, concentration, and incident acoustic signal strength and thus provides the theoretical basis for measuring suspended solids concentrations (SSC). A controlled laboratory study providing minimal acoustic interference with reproducible SSC and particle size distributions was used to evaluate the applicability of using ABS from a 2400 kHz ADCP to estimate SSC, both in units of mass and volume concentration (measured with a Laser *In-situ* Transmissometer (LISST)), over variable particle size distributions with particle diameters ranging from 1 to 250 μm. Results from this study showed log linear relationships to both mass and volume concentrations over variable particle size distributions. However, the ABS responses to volume concentration produced higher linear correlation coefficients and better agreement between measured and predicted concentrations. Further, the ABS response was shown to be linear with the theoretical Rayleigh scattering target strength, calculated from the empirical particle size distribution, and thus explains the observed linearity over a

variable particle size distribution. These results indicate that ABS can be used to provide meaningful volume concentration estimates for colloidal suspensions.

Introduction

Many contaminant transport processes in aqueous systems may be described by particle transport mechanisms. It is documented that the most widespread pollutants affecting United States (U.S.) streams are silt and adsorbed contaminants (Gray and Gartner 2009; US EPA 2000). Additionally, non-aqueous phase hydrocarbons can exist as colloidal suspensions that are subject to aggregation and subsequent sedimentation processes (Page et al. 2000b; Sterling et al. 2004a, 2004b, 2005). Similarly, many hazardous materials including heavy metals, pesticides, and polychlorinated biphenyls will preferentially adsorb to suspended sediment particles in the water column (Garton et al. 1996; Kuwabara 1989). The particulate nature of these contaminants opens the possibility for indirect detection as a particle suspension.

Conventional suspended sediment data collection relies heavily on gravimetric analysis of water samples collected either manually or by automatic devices (Bent et al. 2003). Deficiencies in these conventional methods include high unit data cost, potential for significant risk to personnel when collecting samples in adverse conditions, and the need to interpolate data from a relatively small data set to estimate concentration values for periods lacking data (Gray 2002). Furthermore, the number of sites at which the U.S. Geological Survey (USGS) has collected daily sediment data has declined approximately 75% between 1981 and 2008 primarily due to budget limitations (Gray and Gartner

2009). These statements suggest the existing sediment monitoring network is inadequate to provide data necessary to accurately describe sediment conditions in U.S. waterways. However, the use of an appropriate surrogate technology for suspended sediment analysis may provide data of sufficient quality at a low unit data cost allowing implementation at the required spatial and temporal resolutions.

One surrogate suspended sediment technology that has gained recent attention is the use of acoustic backscatter (Wall et al. 2006; Reichel and Nachtnebel 1994; Gray and Gartner 2009; Gartner 2004). Wall et al. (2006) combined stream flow data with the suspended sediment concentration data inferred from an Acoustic Doppler Current Profiler (ADCP) acoustic backscatter to compute sediment flux. Thus, the Acoustic Doppler Current Profiler (ADCP) capability was extended to measure suspended sediment concentrations. Furthermore, ADCP deployments have been described as the most important development in stream flow measurements over the last decade (Simpson 2001). Rapid developments in ADCP technology have led to increased use by the USGS for stream flow measurements (Hirsch and Costa 2004). Combining the extended ADCP capabilities with their increased use for stream flow measurements represents a significant unit data cost reduction which is necessary for the development of comprehensive stream flow sediment monitoring network.

Previous studies have demonstrated the applicability of optical methods to measure aqueous particle suspensions. Optical backscatter (OBS) sensors were used to study fine-grained sediment suspensions (Bryce et al. 1998). Additionally, OBS has been used to evaluate the fractal-related parameters involved in sediment flocculation

and settling velocity (Nikora et al. 2004). Similarly, Laser *In-situ*-Scattering Transmissometry (LISST) has been used to measure dispersed oil concentrations and observe subsequent aggregation kinetics (Sterling et al. 2004a, 2004b).

The physical laws of attenuation and backscatter that apply to optical sensors also apply to acoustic measurement devices (Reichel and Nachtnebel 1994). With acoustic methods, suspended solids are measured as a function of the target strength echoed and scattered back to an acoustic receiver by the suspended particles. This target strength is a function of the particle concentration, size distribution, shape, density, compressibility, rigidity, and acoustic wavelength (Reichel and Nachtnebel 1994). The received echo intensity represents the integrated signal from all scattering particles in the volume, thus it is not possible to distinguish whether changes in echo intensity are the result of variations in particle concentration or size distribution when using a mono-frequency instrument (Reichel and Nachtnebel 1994). However, methods have been developed that combine both optical and acoustic backscattering methods to determine suspended sediment particle size information (Lynch et al. 1994). Additionally, the ability to determine mean suspended particle sizes has been demonstrated with multiple acoustic frequencies (Thorne et al. 2007).

Both acoustic and optical suspended solids determinations are limited in their respective abilities to characterize particle suspensions with respect to physical and chemical properties. However, both techniques share the characteristic of being well suited to *in-situ* detection which makes them desirable for suspended solids monitoring programs. Optical sensors are essentially point-source measurement devices and thus

restricted in spatial resolution (Hoitink and Hoekstra 2005). Conversely, acoustic technology can be deployed as an *in-situ* remote sensing device which is limited by the range of its acoustic signal. Additionally, acoustic methods are less affected by biological fouling and sedimentation than optical methods (Hamilton et al. 1998).

Perhaps the most convincing argument to develop this technology is that there are many acoustic instruments currently in use to measure river flows and ocean currents**.** Extending the capabilities of existing instrumentation represents a significant benefit in terms of economical suspended solids measurements. Considering sensor network viability is ultimately a function of available funding emphasizes the need to develop a cost effect sensor technology.

Theory

ADCPs are used extensively to measure ocean currents and river flow by measuring the Doppler shift in the signal echoed from scatterers in the water column (RD Instruments 1996). Using a technique called range-gating, where the received signal is broken into successive segments that are processed independently, it is possible to determine a velocity profile over the effective range of the acoustic signal. This is possible because echoes from more distant ranges lag behind echoes received from close ranges (RD Instruments 1996). The Doppler-shift required for velocity determinations is not required for suspended solids determinations. Rather, it is the echoed signal strength (echo intensity) that is required. Using the capability to measure echo intensity at prescribed distances from the acoustic source makes it possible to estimate the

suspended solids concentration profile at prescribed distances (depth bins) away from the acoustic transducer.

Echo intensity is a measure of the source acoustic signal that is reflected off small scatterers in the water column. These scatterers consist of small particles or plankton that exists in natural waters (RD Instruments 1996). Rayleigh scattering describes the echo intensity strength (TS_R) as a function of acoustic wavelength, particle size and concentration and is expressed mathematically as

$$TS_R = 10LogI_0\left(\frac{\pi^2}{\lambda^4}\left(1+\frac{3}{2}\mu\right)^2\sum_{p=1}^{n}\left(\frac{4}{3}\left(\frac{d_p}{2}\right)^3\pi\right)^2\right) \quad (5.1)$$

where I_0 = ADCP echo intensity at the source minus the transmission losses due to beam spreading and water absorption, , λ= acoustic wave length, μ is the cosine of the angle between the scatting direction and the reverse direction of the incident wave (1), n = number of particles, d_p= diameter of individual particle (Urick 1983; Reichel and Nachtnebel 1994). This relationship assumes that the particles are small rigid spheres whose ratio of circumference to wavelength is much less than unity. An important implication of Rayleigh scattering, with respect to this study, is that the signal strength is directly related to the particle size distribution.

Previous researchers have demonstrated that Acoustic Backscatter (ABS) intensity can reasonably estimate suspended solids mass concentrations using empirically derived ABS to mass concentration response factors when particle size distributions (PSD) remain relatively stable (Wall et al. 2006; Gartner 2004). However, suspended solids in natural systems are characteristically diverse with respect to particle

size distributions, particle geometry, density and rigidity. Also, characteristics can change both with respect to location and environmental conditions. To account for these differences, the authors typically developed site-specific ABS response factors for variable suspended solids concentrations as it was acknowledged that the mass concentration calibrations do not apply well when there are significant changes in the PSD. Applying these calibrations to distances away from the transducer (i.e. throughout the water column) requires that the measured ABS be corrected for signal attenuation resulting from beam spreading, water absorption, and suspended solids adsorption (Wall et al. 2006; Gartner 2004).

PSDs and volume concentration can be measured with a LISST-100 (Sequoia Scientific, Inc., Bellevue, Wa.). This instrument uses small-angle forward scattering to determine the particle size distribution over 32 ring detectors that correspond to log-normally-distributed particle diameters (Agrawal and Pottsmith 1994). Each ring detector measures a scattering intensity that scales typically to the fourth power of the particle radius and weighted by the number density. Scattering intensity from a particle ensemble can be expressed using the Mie solution $I(\theta) = \int K(a,\theta) n(a) da$, where $K(a,\theta)$ in the scattering Kernel describing the intensity contribution from a particle of radius a at a scattering angle θ (Agrawal and Pottsmith 1994). Comparison of Rayleigh scattering and the Mie solution shows that both may be calculated as the integral of the particle size distribution while their intensities differ proportionately by a factor of a^2. Additionally, the Mie scattering solution describes scattering by all particle sizes inclusive of Rayleigh scattering (i.e. when particle circumference is less than the wave

length). Thus illustrating the similarities between the acoustic backscatter and forward scattering inferred volume concentration and further suggests the basis for strong correlation between the two measurements.

The purpose of this study was to determine the relationships between depth-corrected ABS and suspended solids concentration measured in both units of mass and volume concentration. It is hypothesized that the ABS response to particle volume concentration responses can curves can be applied to particle suspensions with characteristically variable size distributions because ABS responses are defined by the Rayleigh scattering equation (i.e. ABS is a function of the particle size distribution). This hypothesis was tested by comparing the measured ABS response to the theoretical ABS calculated by integrating the Rayleigh scattering equation over the particle size distribution. The applicability of ABS-volume concentration response curves for estimating suspended solids concentrations was evaluated.

Materials and Methods

Experimental design

Echo intensity (EI) responses to standard clay particle suspensions were measured in a laboratory test tank using a 2400-kHz Teledyne RD Instruments StreamPro during three replicate tests on March 14, 23, and 26, 2010. Six EI depth profiles were collected for each replicate test including; one no-clay-control, four standard clay suspensions, and one following the addition of a flocculent aid to the maximum mass clay load (30 mg/L) in each replicate test. The StreamPro was selected

for this laboratory study due to its relatively short acoustic range, which alleviated tank wall interferences experienced with longer range units (i.e. 1200 kHz Workhorse Monitors, Teledyne RDI). The StreamPro was mounted in the Teledyne RDI Riverboat® with a down-looking orientation. Streampro transducers were positioned 5 cm below the water surface. Real time data collection was made with WinRiverII (Teledyne RDI) via a Bluetooth serial connection a to Dell Laptop computer with a Windows XP operating system. The StreamPro was configured in WinRiverII to collect echo intensity ensembles (profile samples) with the following parameters (6 pings/ensemble, ping rate = 2 Hz, depth bin size = 10 cm, number of depth bins = 15). All echo intensity values reported are the mean of all ensembles (minimum 50 ensembles) collected from each standard clay concentrations. To alleviate variations in incident signal strength resulting from variable power as described by Wall et al. (2006), the StreamPro was connected to laboratory power supply with an operating voltage set to 12.5 VDC. This modification was required because unlike the 600 kHz ADCP used by Wall et al. (2006), the StreamPro data output does not include the parameters transmit current and voltage which are required to make the appropriate echo intensity corrections.

Test tank configuration

All tests were conducted in a fiberglass tank (Inside Diameter 3.7m x Depth 1.7 m) and filled with potable fresh water. The tank bottom was lined with rubber mats (1.9 cm thick) to minimize acoustic signal reflection and subsequent interference with the ADCP. To mix the tank, a 1-Hp pool pump was plumbed to an octagonal PVC

distribution manifold installed on the tank bottom. The manifold contained 32 equally spaced distribution ports (diameter = 0.7 cm) oriented to direct the water toward the tank center and along the tank floor that created an upwelling current in the tank center that was replenished with a down-welling current around the tank circumference. (Fig. 5.1). Pump intake was through a 3.7 cm (I.D.) plumbing fixture in the tank wall located 15 cm above the tank bottom. The tank was completely drained, cleaned, and refilled with clean water between each experimental replicate.

A)

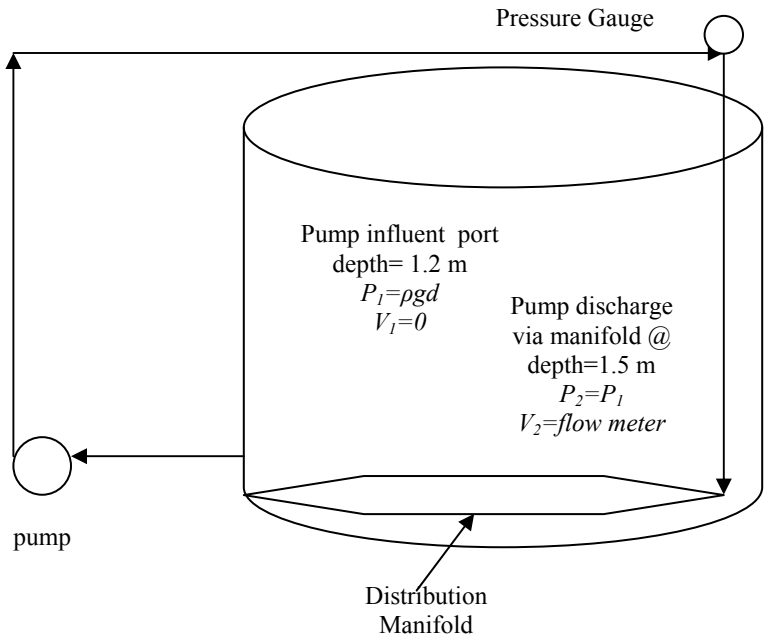

Fig. 5.1 Test tank flow schematic, A) side view B) plan view.

B)

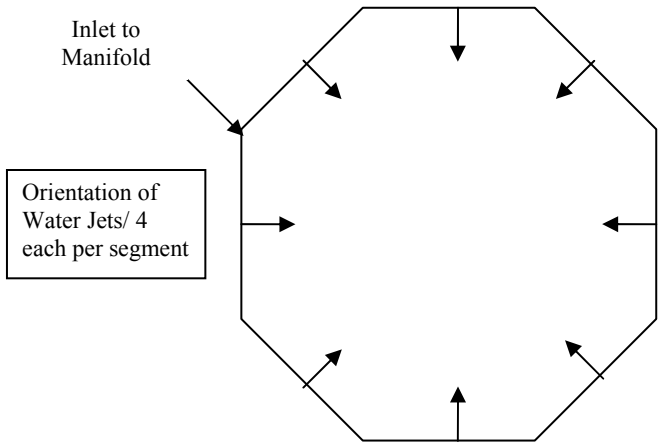

Fig. 5.1 continued

Clay standard preparation

Standard clay suspensions were prepared with bentonite clay (Volclay® 200, Univar U.S.A). This material (dry) will pass through a #200 sieve (74 micron) and has a dry density of 2.5 mg/µl. Before the clay was added to the tank, concentrated suspensions for each of the 4 standard clay additions, each addition representing an nominal mass concentration increase of 7.5 mg/L, were prepared to prevent the clay from clumping when added to the test tank. The concentrated suspensions were prepared by adding 118 g clay to 9.5 L tap water followed by mixing with an electric hand held mixer coupled to a multi-vane impeller at 850 RPM until well dispersed (i.e. until no clay clumps were visible). All suspensions were prepared at the beginning of the test. Between preparing the suspensions and adding to the test tank, visible clay flocs would form and begin to settle in the mixing vessel. Therefore, each standard clay

suspension was remixed with the electric mixer immediately prior to addition to the test tank. Each standard-addition was then poured in the center of the mixed test tank 10 minutes prior to sampling to allow the suspension to become well distributed throughout the tank.

To evaluate the effect of variable particle size distribution on the ABS responses to a clay-suspension-standard it was necessary to vary the PSD while holding the mass concentration constant. This was accomplished with the addition of a flocculent aid (Leslie Pool, Super Floc) following sampling of the final standard clay addition (30 mg/L nominal load). The optimal flocculent aid dosage was determined to be 50 ml/16,000L using standard jar testing procedures. This dosage was diluted in 1 L tap water prior to application. Following, flocculent aid addition, the tank was allowed to mix continuously for 30 minutes prior to sampling.

Determination of clay suspension concentrations

Suspended clay volume concentrations were measured *in-situ* with a LISST 100, Type B (Sequoia Scientific Inc., Bellevue, Wa. U.S.A.) that measures 32 log-normally-distributed particle size classes with diameters ranging from 1.2 to 250 microns. The LISST was configured to collect 1 sample/ensemble using the LISST MFC Application (Version 1.0.0.1). It was suspended on a chain in a horizontal orientation to reduce settling of suspended particles on the optical surfaces. All measurements were taken at 0.65 meters below the water surface. All volume concentrations and particles size distributions reported in this study are the mean of 30 ensembles.

The LISST-100 volume concentration calibration procedure (Doug Keir, personal communication December 17, 2010) used a single point response to a standard powder (ISO Coarse A.T.D. 12103-1, A4, Powder Technology Inc., Burnsville, MN) with a known density (2.6 g/cm^3). Briefly, the calibration was performed in a large volume acrylic test chamber (Sequoia Scientific, Inc., Bellevue, Washington) that was placed on a magnetic stir plate. After inserting the LISST-100 sensing head into the chamber, 3-liters degassed and deionized water at room temperature was added to the test chamber. A 5 cm magnetic stir bar was used to mix the chamber continuously for at least 1 hour to allow any bubbles that formed during the chamber filling process to escape. Additionally, any bubbles that formed on the LISST-100 or chamber surfaces were removed by agitation with a plastic transfer pipette. The ISO Coarse powder was then added to the mixed chamber (0.234 g) with a nominal volume concentration of 30 µl/L. Next, 30 volume concentration measurements were collected with the LISST-100. The volume concentration calibration was accomplished by adjusting the instrument specific Volume Concentration Coefficient (*VCC*) located in the InstrumentData.txt file. The *VCC* is determined from the nominal and measured mean volume concentrations by

$$VCC_{adjusted} = \left(VCC_{initial} \times \frac{C_{nom}}{C_{measured}} \right) \tag{5.2}$$

where C_{nom} is the nominal volume concentration and $C_{measured}$ measured volume concentration.

Total suspended solids (TSS) mass concentrations were determined by standard gravimetric analysis for total suspended solids (EPA Method 160.2). Briefly, one 1 L

grab samples for each test condition (i.e. no-clay control, each clay standard concentration, and following flocculent aid addition) was collected at the control depth (0.65 m) in amber Boston Bottles. The samples were then stored at 3-5° C until analyzed. A well-mixed sample was then passed through a GF/C filter (0.2 μm). The filter was then dried to a constant weight at 103-105° C. Suspended sediment concentrations were calculated as the difference between the filter final and tare weights divided by the filtrate volume.

All sampling was performed sequentially in the following order; LISST, TSS grab sample, and finally ADCP Stream Pro. Sequential sampling was required to alleviate possible acoustic interference with the StreamPro caused by acoustic signal reflection off LISST body. All samples were collected at a control depth of 0.65 meters.

Estimating Suspended-Sediment Concentration from EI

Estimating the suspended-sediment concentration (SSC_{est}) from EI uses a form of the sonar equation for sound scattering (Gartner 2004; Wall et al. 2006). The log form of this equation is

$$Log_{10} SSC_{measured} = A * ABS + B \tag{5.3}$$

where A and B are the empirically derived slope and intercept, respectively, of the semi-log regression of $SSC_{measured}$ versus the acoustic back scatter (ABS). Previously, researchers have successfully applied this relationship to estimate suspended sediment mass concentrations to ABS depth profiles by applying corrections to account for attenuation resulting from beam spreading, water absorption, and sediment attenuation

(Gartner 2004; Wall et al. 2006). These corrections allow a single response curve to be applied throughout the ensonified range of the ADCP. This correction requires that the *ABS* have units of decibels to allow direct application of calculated attenuation values to the measured *ABS*.

In the case of the 2400 kHz StreamPro, no factory determined Received Signal Strength Indicator (RSSI) scale factors to convert raw EI counts to decibel units are provided. This is a deviation from the previous research using 1200 and 600 kHz ADCPs where the RSSI factors were provided by the manufacturer (Gartner 2004; Wall et al. 2006). Therefore, it was necessary to determine RSSI using the empirically derived EI depth profiles and the theoretical depth-dependent attenuation values due to beam spreading and water absorption. Alternatively, depth-specific EI response curves must be determined. Another deviation from the previous researchers is that *SSC* is measured in units of volume concentration [µl/L], in addition to mass concentration, thus providing a means to evaluate the applicability of using the Rayleigh scattering equation to estimate suspended solids volume concentration over a variable particle size distribution.

Beam Normalization

The 2400 kHz StreamPro uses 4 acoustic beams that diverge 20° from a centerline axis from which four along beam velocity vectors are determined based on the Doppler shift in the returned signal. A minimum of 3 beams are required to resolve the 3 dimensional velocity magnitude and direction. The measured EI from the StreamPro

for a given depth bin can vary as much as 90 counts between beams on the same instrument (Dan Murphy, Teledyne RD Instruments, oral communication, Jan, 2010). To account for this variability, EI values were normalized as described by Wall et al. (2006) to a reference beam which was arbitrarily selected as beam #1. Briefly, the echo intensities from each beam were plotted against the echo intensities from the reference beam with respect to depth bin and ensemble (example: reference beam (#1) echo intensities from bin 6, ensemble 10 were plotted against beam 3, bin 6, ensemble 10) (Fig. 5.2). Linear regressions of each plot provided the slope and intercept that were applied to the echo intensity to normalize each beam. The beam specific regression statistics are shown in Table 5.1. Following beam normalization, the echo intensities from the four beams were averaged as

$$\overline{EI_{j,k}} = \frac{\sum EI_{i,j,k}}{4} \tag{5.4}$$

where i=beam number, j=ensemble, k=bin. Finally, the depth-bin-specific ensemble averages for each standard clay addition were calculated as

$$\overline{EI_k} = \frac{\sum_{n=1}^{n} EI_{j,k}}{n}. \tag{5.5}$$

where k=depth bin, and n=number of ensembles collected. The depth bin specific EI ensemble averages were then converted to decibel units as the product of $\overline{EI_k}$ and RSSI.

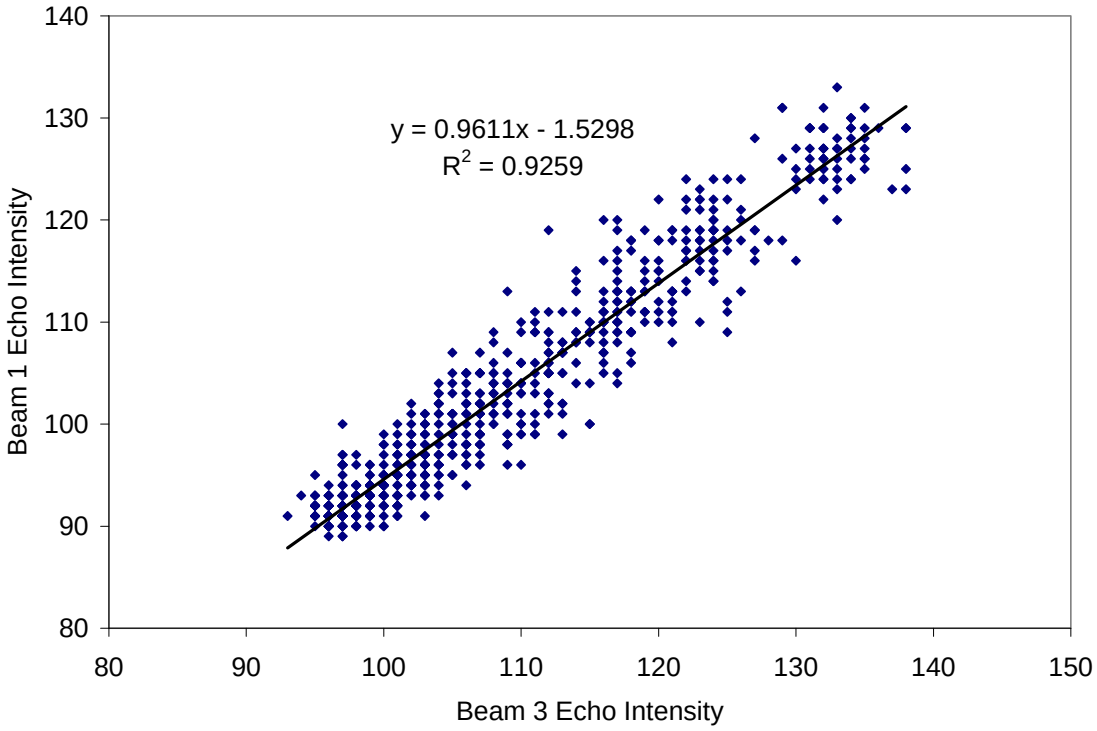

Fig. 5.2 Sample beam 3 normalization from March 14, 2010 profile.

Table 5.1 Regression statistics for beam normalization.

Beam	**Slope**	**y-intercept**	**R^2**
March 14, 2010			
2	0.9392	5.303	0.9240
3	0.9611	-1.5298	0.9259
4	1.0157	-32.286	0.9176
March 23, 2010			
2	0.8579	16.077	0.9087
3	0.8968	7.2077	0.9040
4	0.9423	-20.713	0.9247
March 26, 2010			
2	0.8798	12.217	0.8735
3	0.9348	1.6479	0.8722
4	0.9554	-23.718	0.8777

Acoustic Backscatter Corrections

The received acoustic backscatter attenuates with distance from the transducer due to beam spreading, water absorption, and sediment attenuation. These losses must be added back into the measured echo intensity prior to substitution into the sonar equation (Equation 5.3) used to estimate *SSC*. This corrected echo intensity or *ABS* is represented by

$$ABS_{k,corrected} = ABS_k + BS + WA + SA \tag{5.6}$$

where BS = beam spreading attenuation, WA = water absorption attenuation, SA = sediment attenuation, and k=depth bin (Wall et al. 2006).

Beam spreading attenuation

Acoustic beam spreading accounts for the geometric signal loss as a function of distance (RD Instruments 1996). Wall et al. (2006) presented acoustic beam spreading attenuation as

$$BS = 20 \times Log_{10}(R \times \psi) \tag{5.7}$$

R is the slant distance to the source of the return echo in meters (Deines 1999) and is calculated as

$$R=r+D/4 \tag{5.8}$$

where, $r = y/Cos20, y$=(ADCP Blank Distance + 0.5(D))+((D)x(k-1)), D=bin size [m], and k = bin #. The term D/4 accounts for the operational fact that the ADCP samples the ABS in the last quarter of the depth cell, not the center (Deines, 1999). ψ is the transducer near-field correction that accounts for the non-spherical spreading of acoustic

energy close to the transducer and is calculated as

$$\Psi = \frac{1+1.35z+(2.5z)^{3.2}}{1.35z+(2.5z)^{3.2}} \tag{5.9}$$

where, $z=R/R_{critical}$, $R_{critical}=\pi a_t^2/\lambda=0.17\ m$, a_t=*transducer radius* [m] = 0.00635, and λ = acoustic wave length [m] = (1484 m/s)/(2,400,000 Hz) = 6.2 x 10^{-4} m (Downing et al. 1995). *Cos20* accounts for the Janus angle (i.e. transducer angle from vertical axis).

Water absorption attenuation

Sound absorption in water is nearly proportional to frequency which results in an inverse relationship between frequency and range (RD Instruments 1996). Absorption attenuation is function of salinity, temperature, and pressure and is defined by Wall et al. (2006) and (Gartner 2004) as

$$WA = 2\alpha R \tag{5.10}$$

Schulkin and Marsh (1962) define α as

$$\alpha = \left(\frac{SAf_t f^2}{f_t^2 + f^2} + \frac{Bf^2}{f_t} \right)\left(1 - 6.54\times10^{-4} P\right)\times 8.69 = [\text{dB/m}] \tag{5.11a}$$

where, S=salinity (psu), A=constant (2.34x10^{-6}), $f_t = 21.9\times10^{[6-1520/(T+273)]}$,

T=temperature [°C], f=frequency [kcps], B=constant (3.38x10^{-6}), and P=pressure in atm. In fresh water ($S=0$) and in depths less than 50m, the salinity and pressure terms may be neglected thus reducing α to

$$\alpha = \left(\frac{Bf^2}{f_t} \right)\times 8.69 = [\text{dB/m}] \tag{5.11b}$$

Using Eqs. 5.6 -5.11b the beam spreading and water absorption attenuation

values relevant to the depth bins measured with the StreamPro ADCP were calculated and are shown in Table 5.2. The sum of both Beam Spreading and Water Absorption values were found to be negative at depth bins ranging from 0.15-0.85 meter. To remove the negative values, the total attenuation values (BS + WA) calculated for each depth bin were adjusted by subtracting the value of the first depth bin (0.15 m), so the attenuation value in depth bin 1 was equal to zero.

Table 5.2 Depth dependent acoustic backscatter attenuation due to beam spreading and water absorption.

Depth Bin, *k*	Bin Depth	BS [dB]	WA [dB]	BS + WA [dB]	Adjusted (BS+WA) [dB]
1	0.15	-14.3409	0.34957	-13.991334	0
2	0.25	-10.6391	0.55106	-0.0880064	3.903327924
3	0.35	-7.98351	0.75255	-7.2309561	6.760378224
4	0.45	-5.93907	0.95404	-4.9850277	9.00630664
5	0.55	-4.28135	1.15553	-3.1258193	10.86551502
6	0.65	-2.88838	1.35702	-1.5313639	12.45997038
7	0.75	-1.68759	1.55851	-0.1290787	13.86225557
8	0.85	-0.6325	1.76	1.12750485	15.11883921
9	0.95	0.308376	1.96149	2.26986658	16.26120095
10	1.05	1.157317	2.16298	3.32029771	17.31163208
11	1.15	1.930682	2.36447	4.29515251	18.28648687
12	1.25	2.640821	2.56596	5.20678153	19.19811589

Sediment attenuation

The acoustic backscatter attenuation resulting from suspended sediment is a function of both viscous and scattering losses (Flammer 1962). The characteristic scattering loss is a function of the acoustic wavelength (λ) to particle circumference ($2\pi a_p$) ratio, where a_p is the particle radius. When $2\pi a_p << \lambda$, viscous losses dominate. However, when $2\pi a_p >> \lambda$ scattering losses dominate (Gartner 2004). For a 2400 kHz acoustic signal $2\pi a_p = \lambda$ when particle diameter is 206 μm. Thus, for the particle sizes

evaluated in this study with the LISST 100 (particle size measurement range of 1-250μm) viscous losses will dominate. Acoustic attenuation due to suspended solids assumes rigid spherical particles is expressed in Gartner (2004) as

$$SA = 2\alpha_s[dB/m] = (8.68)(100cm/m)(\varsigma)(SSC) \tag{5.12a}$$

where, 8.68 is the conversion from nepers to decibels,

$\varsigma[cm^{-1}] = K(\gamma-1)^2\left\{ S \middle/ \left[S^2 + (\gamma+\tau)^2\right]\right\} + (K^4 a_p^3)/6$, K=2π/λ, λ is wave length in cm,

γ=(particle density/fluid density), τ=0.5+(9/(4βa_p), a_p is particle radius in cm, S=[9/(4βa_p)][1+1/(βa_p)], β = [ω/2v]$^{0.5}$, ω=2πf, f is frequency in Hz, and v is kinematic viscosity of water in stokes = 0.01 stokes [cm^2 sec^{-1}]. SSC is the suspended solids concentration expressed as the ratio of sediment volume to water volume, (µl/L)/1,000,000 (Flammer 1962). To account for variability in both SSC over distance and particle size distribution, sediment attenuation Eq. 5.12 may be integrated over the PSD for a given depth bin as

$$SA = \sum (8.68)(100cm/m)(\varsigma_i)(SSC_{i,k})\left(D \middle/ \cos 20\right) \tag{5.12b}$$

where i= the particle size bin, k is depth bin, and D is depth bin size in meters. To evaluate the level of sediment attenuation in this study, the PSD from the 4th standard clay addition prior to flocculent aid additions (i.e. 30 mg/L nominal mass load) was chosen as the representative particle suspension for the input $SSC_{i,}$. A representative clay density of 2.5 mg/µl was used to determine γ. Sediment attenuation calculated for this particle suspension over the ensonified range (1.25 meters) was less than the sum of beam spreading and water absorption attenuation by more than an order of magnitude

and was therefore omitted from Equation 5.6.

Calculation of Echo Intensity to Decibel Conversion Factor

No Received Signal Strength Indicator (RSSI) factors are provided for the StreamPro ADCP to convert echo intensity counts to decibel units. Therefore, the RSSI was determined as the slope of the normalized echo intensity depth profile when plotted against the respective ABS signal attenuation due to beam spreading and water absorption. The normalized echo intensity obtained from a standard clay suspension (15 mg/L nominal load) was calculated as

$$EI_{norm,k} = EI_{k=1} - EI_k \tag{5.13}$$

for k = 1 to 12, where k = 1 is the depth bin closest to the water surface at 0.15 m. ABS attenuation values, $(BS + WA)_k$, calculated for the respective depth bins (Table 5.2), were then plotted against $EI_{norm,k}$ (Fig. 5.3). Regression analysis showed a strong linear correlation (R^2=0.9979) between $EI_{norm,k}$ and the sum beam spreading and water absorption attenuation. An RSSI = 0.5605 was obtained from the slope of the linear regression. To evaluate the fit of the RSSI factor, it was applied to the echo intensity profile obtained from March 14 2010 trial, Standard Clay Addition 4, 30 mg/L nominal clay load using

$$ABS_k = EI_k \times RSSI \tag{5.14}$$

For comparison, a model profile was generated as

$$ABSm_k = ABS_{k=1} - (BS + WA)_k \tag{5.15}$$

where $ABSm_k$= model ABS at depth bin k. The results from this comparison show good

agreement between model and empirically derived acoustic backscatter (Fig. 5.4), demonstrating the appropriateness of the derived RSSI factor.

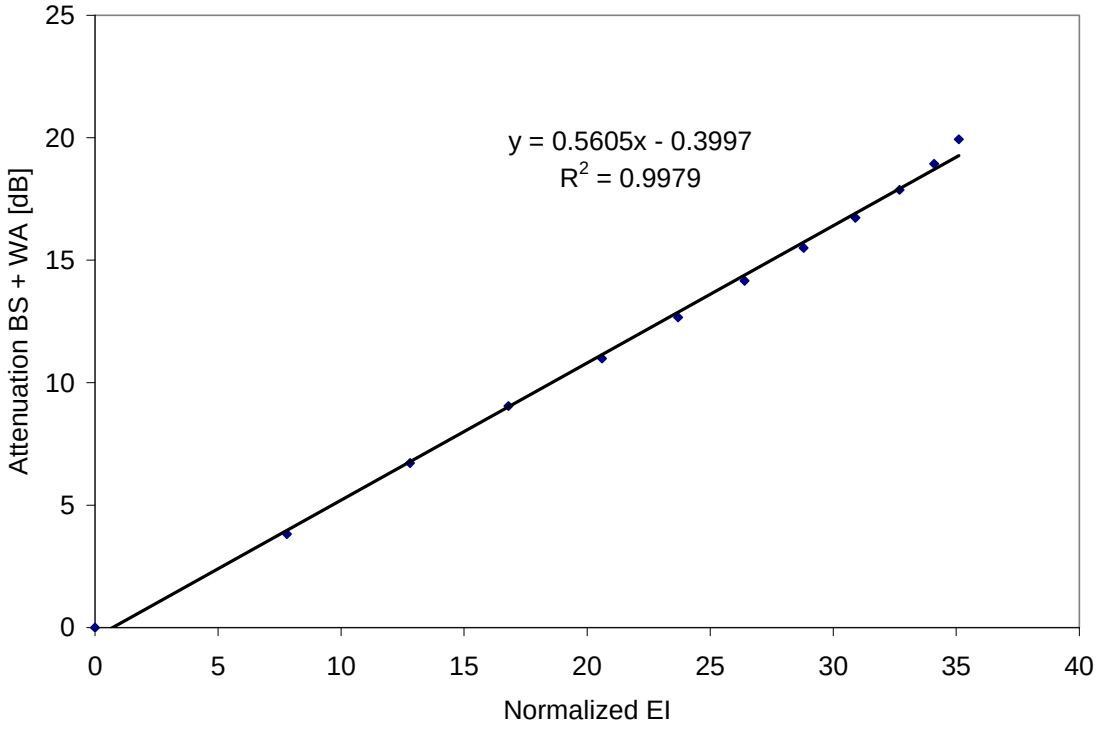

Fig. 5.3 Normalized EI vs derived depth dependant attenuation for RSSI determination from March 14, 2010, Standard 2 (15 mg/L mass load) EI depth profile.

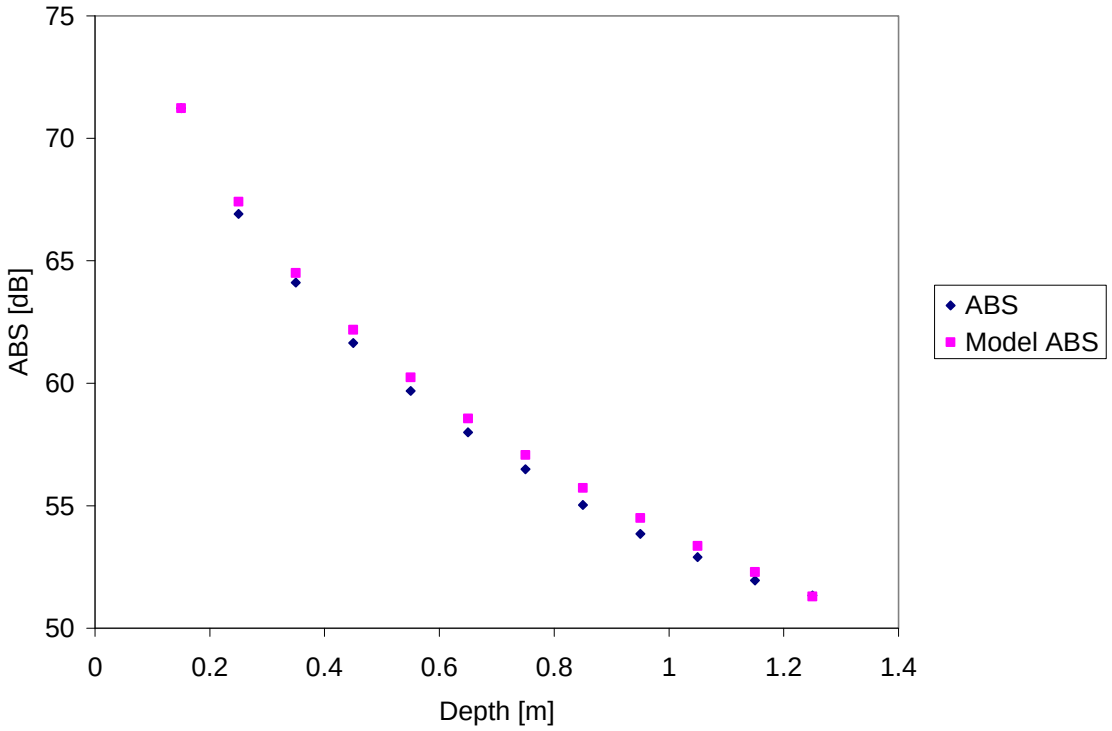

Fig. 5.4 March 14, 2010, acoustic backscatter depth profile for Standard Clay #4 (30 mg/L nominal load).

Computation of Theoretical Target Strength Echo Intensity

The LISST 100 measures the particle volume concentration as a function of 32 discrete logarithmically distributed particle sizes. This particle size distribution may then be used to calculate the theoretical target strength *ABS* in a given depth bin using the Rayleigh scattering equation (Equation 5.1). To apply the particle size distribution to Eq. 5.1, it was necessary to calculate the number of particles in each particle size category and depth bin by

$$N_p = \frac{C_p}{T_p} V_k \tag{5.16}$$

where N= ensonified particle count, C=particle volume concentration (m^3/L),

T=individual particle volume (m^3), p=particle size class, and k= depth bin. The bin volume, V_k, was calculated as the volume of a solid angle of a sphere

$$V_k = \frac{1}{4}\pi\phi^2 L\left[r^2 + \frac{L^2}{12}\right] \tag{5.17}$$

where L =vertical bin size/cos (Janus angle), φ= two way two sided beam width in radians (1° for 2400 kHz ADCP), and r= vertical distance to bin center/*cos* (Janus angle), and Janus angle = 20° (Gregory Rivalan, Teledyne RD Instruments personal communication, 2010). The summation term in Equation 5.1 is calculated as

$$\sum_{p=1}^{32}\left(\frac{4}{3}\left(\frac{d_p}{2}\right)^3\pi\right)^2 = \sum_{p=1}^{32} N_p \times \left(T_p\right)^2 \tag{5.18}$$

where p=particle size bins measured with the LISST 100. All length and volume terms have units of meters and meters cubed, respectively.

Results and Discussion

Suspended solids characterization

Suspended solids measurements were made both gravimetrically and optically with the LISST 100 to provided concentration data in units of mass and volume concentration, respectively. A plot of the measured mass concentration against the nominal mass loads showed good linearity (R^2=0.999) for all three replicates (Fig. 5.5) and indicates that the system (test tank) was well mixed. However, the slopes ranged from 0.87 to 0.93 suggesting that some mass was lost in the system or there were errors in the tank volume determination. A plot of the measured mass concentration against

total volume concentration shows a direct linear increase in volume concentration with respect to increasing mass loads, excluding the Floc+30 data points, with replicate R^2 ranging from 0.86 to 1.0 (Fig. 5.6). Following addition of the flocculent aid, the volume concentrations increased from 103, 96, and 93 to 189, 192, and 168 µl/L, for the March 14, 23, and 26, replicates respectively without an increase in the mass concentrations relative to final clay addition. This volume concentration increase with no coincident increase in mass concentration indicates the fractal nature of the clay flocs (Lee et al. 2000) which does not adhere to the strict Rayleigh scattering assumption of small rigid spheres.

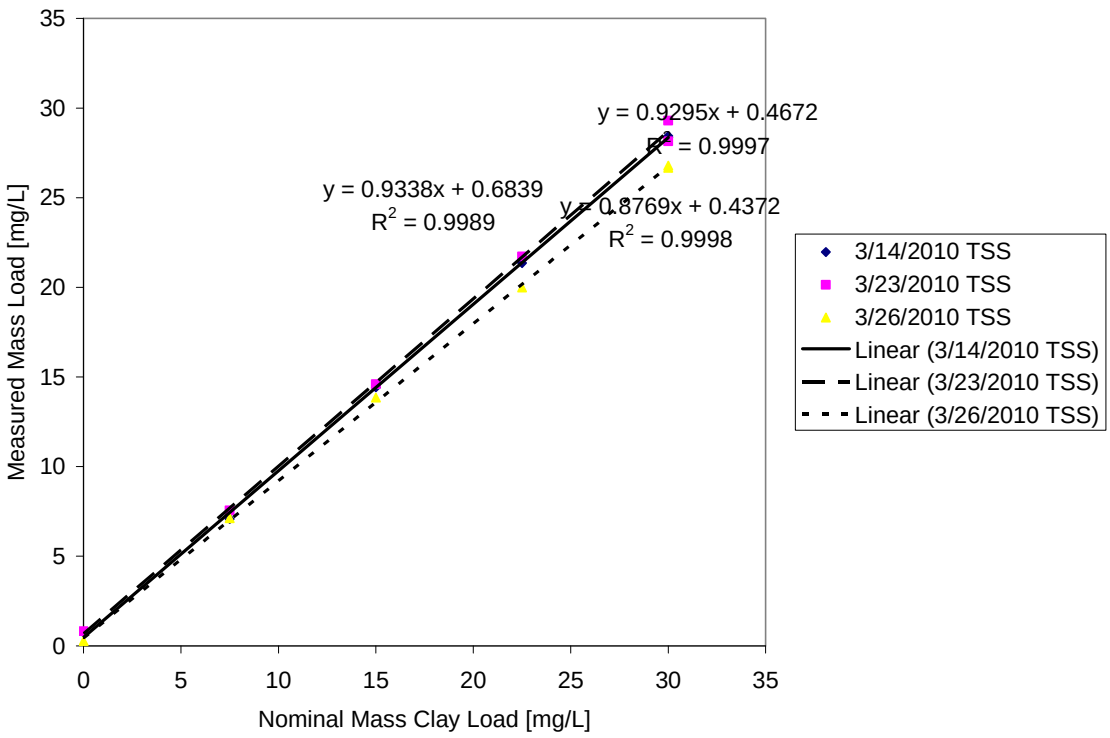

Fig. 5.5 Nomimal clay loads vs measured mass concentrations.

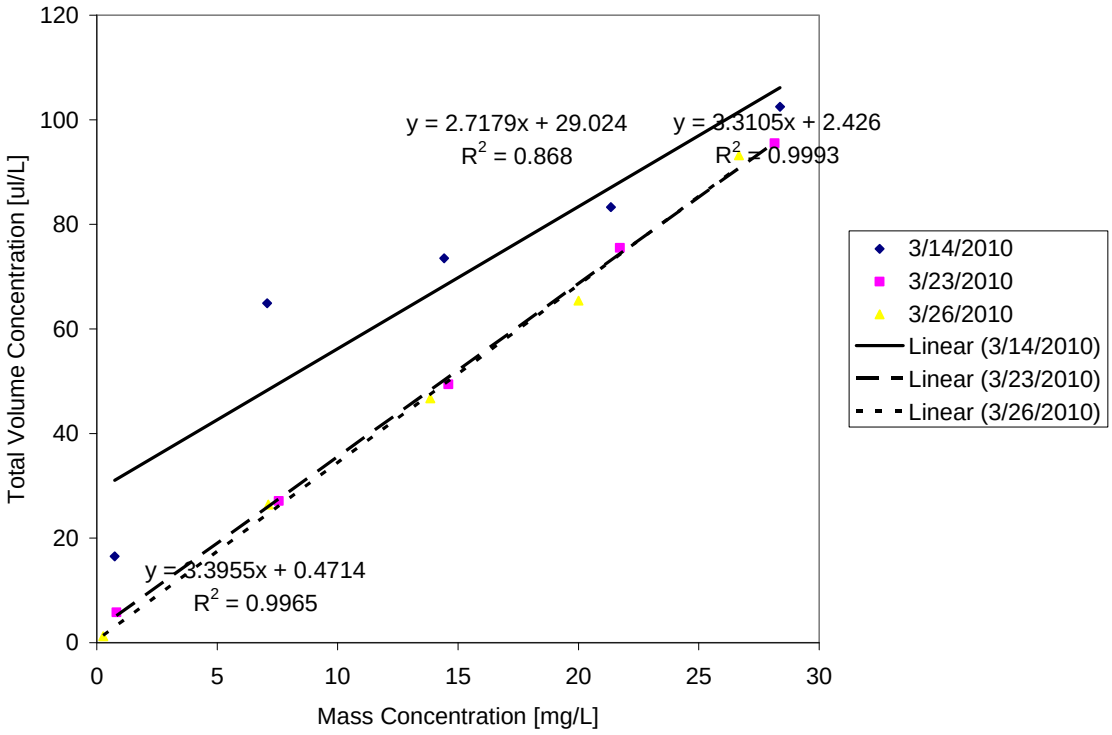

Fig. 5.6 Measured mass concentration vs total volume concentration (excluding volume concentrations resulting from flocculent aid addition).

PSDs were generally conserved between replicate tests and standard additions with exception of the Standards 1 and 2 on March 14 which showed elevated volume concentrations at the upper end of the distribution (Fig. 5.7A). This deviation in PSD resulted in a subsequent reduction in linearity of the March 14 TSS vs volume concentration plot (Fig. 5.6) compared to the linearity observed during replicate tests on March 23 and 26. Following addition of Standard 3 and 4, the PSDs of all three replicates were similar (Fig. 5.7A-C). Furthermore, the PSD's represented in Fig. 5.7 show the obvious shift toward larger particles following flocculent aid additions. Corresponding analysis of the mean particle diameters, obtained using the LISST Software, showed mean particle size = 55 microns (STDEV = 13) for the 4 clay

standards over all experimental replicates. A mean diameter=120 microns (STDEV = 1.4) was measured 30 minutes after the flocculent aid was added (Fig. 5.8). In the case of the standard clay additions the PSDs showed that clay particle diameters resided within the Rayleigh size limitation (i.e. <206 μm) as indicated by the right hand tail of the PSD (Fig. 5.7). Unfortunately, the LISST particle size limitation of 230 μm does not capture the upper PSD of the clay flocs resulting after flocculent aid addition (Fig. 5.7). Thus, it is suspected that the actual mean particle diameter of the Floc+30 clay suspensions exceeded the mean 120 μm diameter measured with the LISST 100. It is important to note that only the largest diameter (size bin 230 μm) measured by the LISST exceeds the Rayleigh limit. However, Agrawal et al. (2008) showed that laser diffraction can overestimate the size of natural particles by 20-40%, due to bias resulting from a departure from spherical geometry. Therefore, the total particle volume concentration inferred from the LISST 100 is comprised primarily from particles falling within the Rayleigh size limit.

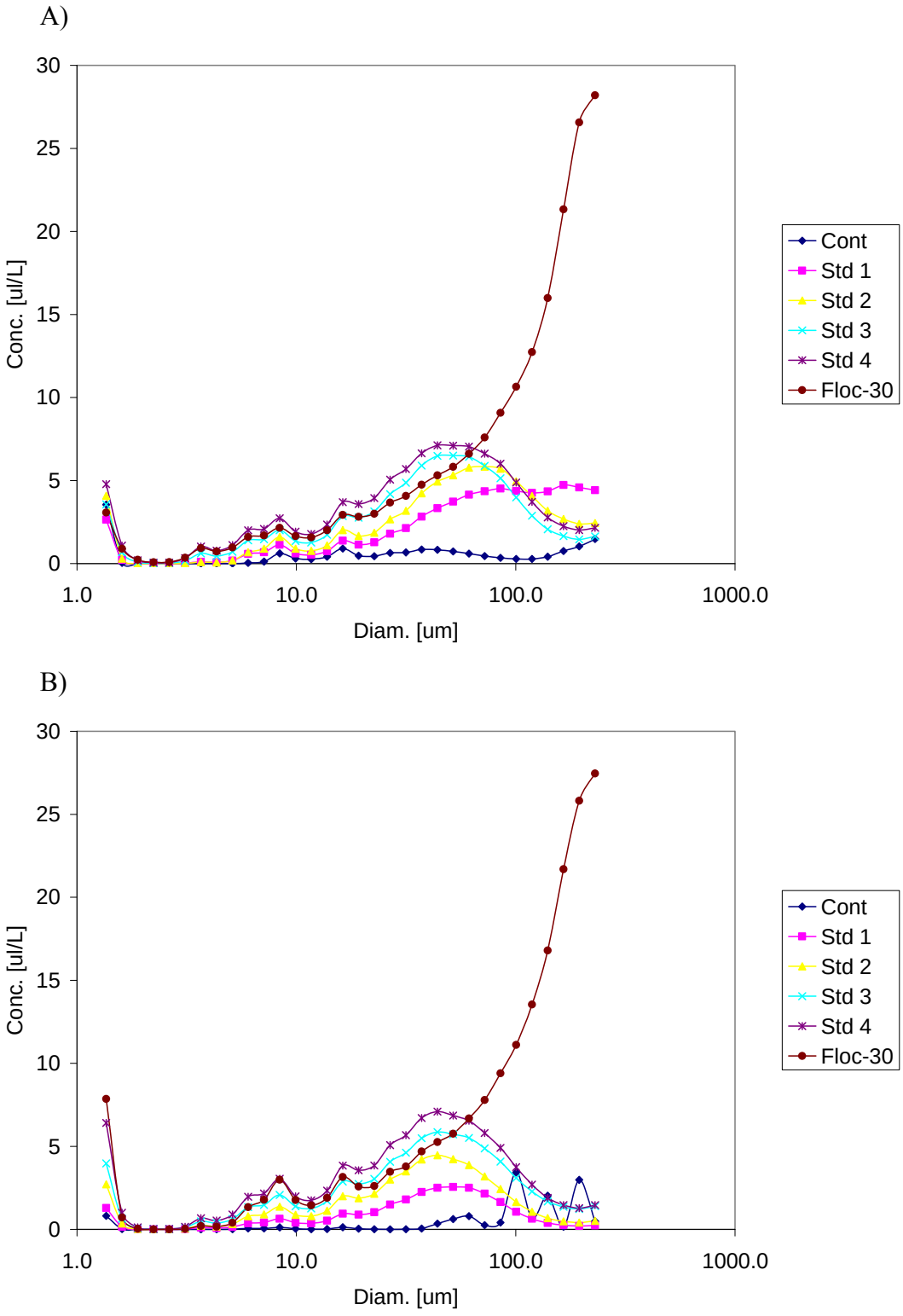

Fig. 5.7 PSD inferred from LISST 100, A) March 14, B) March 23, C) March 26.

C)

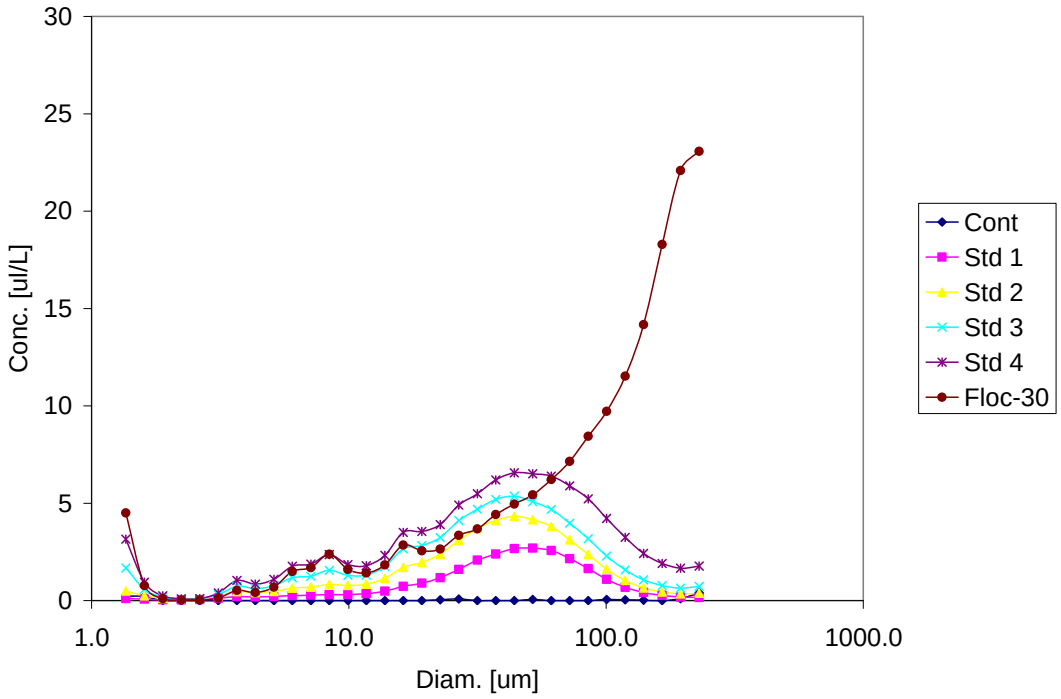

Fig. 5.7 continued

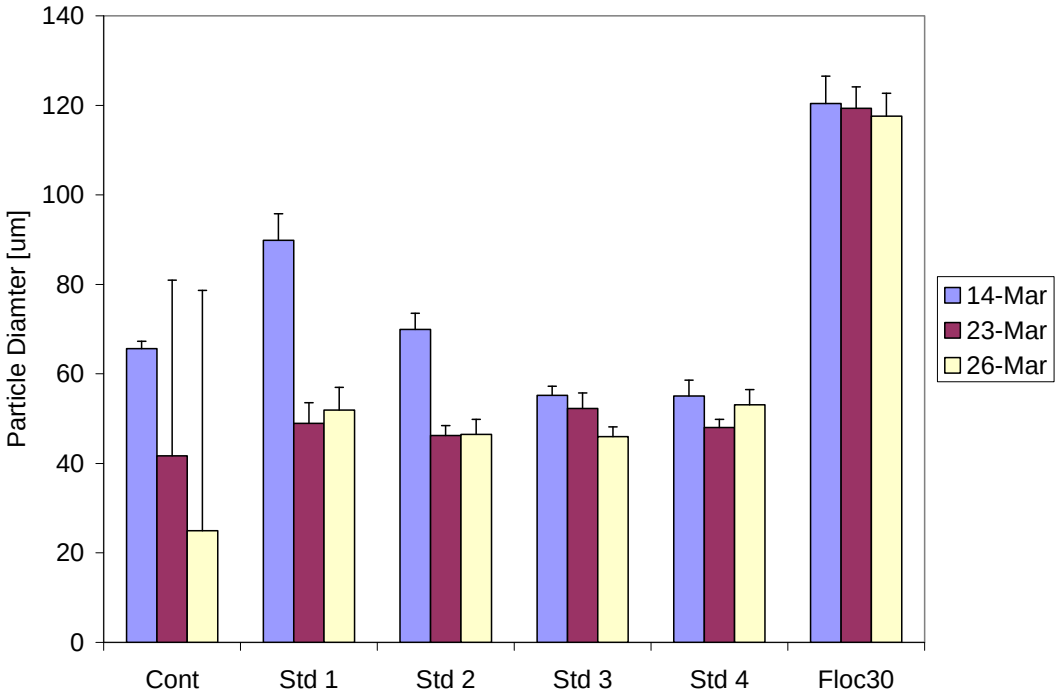

Fig. 5.8 Mean particle diameters (*n*=20 LISST ensembles). Error bars represent standard deviation of mean.

Acoustic backscatter depth profiles

The raw echo intensity depth profiles for each experimental condition were converted to acoustic backscatter (ABS) with decibel units by applying the RSSI factor (Equation 5.14). The resultant ABS values were then corrected for beam spreading and water absorption attenuation (Equation 5.6) and are plotted as depth profiles in Fig. 5.9 Visual inspection shows that the corrected ABS was nearly uniform across all depth bins within experimental conditions (i.e. individual clay standard concentrations) with the exception of the no sediment controls. Ideally, in homogeneous suspensions, the corrected ABS would be equal in all depth bins. Deviation from non-ideality is indicative of the error associated beam spreading and water absorption corrections.

Inspection shows that corrected ABS increased with depth, suggesting that the beam spreading and water absorption corrections may overestimate actual attenuation. The greatest depth variability was observed in the no-clay-control treatment during the March 26 trial which had the lowest control volume concentration = 1.2 µl/L compared to 13 and 28 µl/L for March 14 and 23 replicates, respectively. This suggests that a minimum scatterer concentration was required to obtain valid acoustic backscatter. Due to the variability observed in the no-clay-controls, they were omitted from the response curves used to determine the calibration coefficients A and B in Equation 5.3.

A)

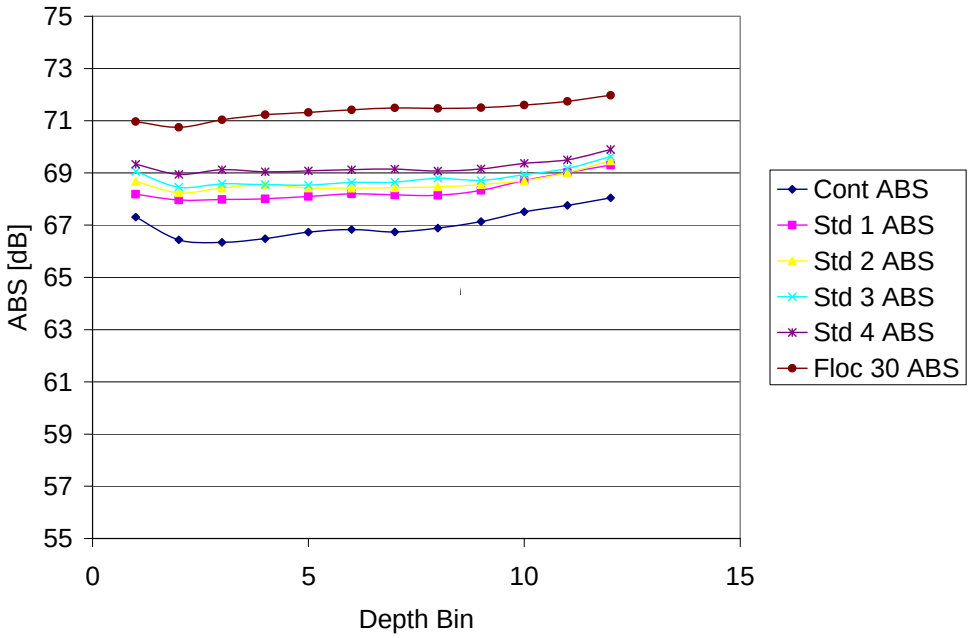

Fig. 5.9 ABS depth profiles, A) March 14, 2010, B) March 23, 2010, C) March 26, 2010.

B)

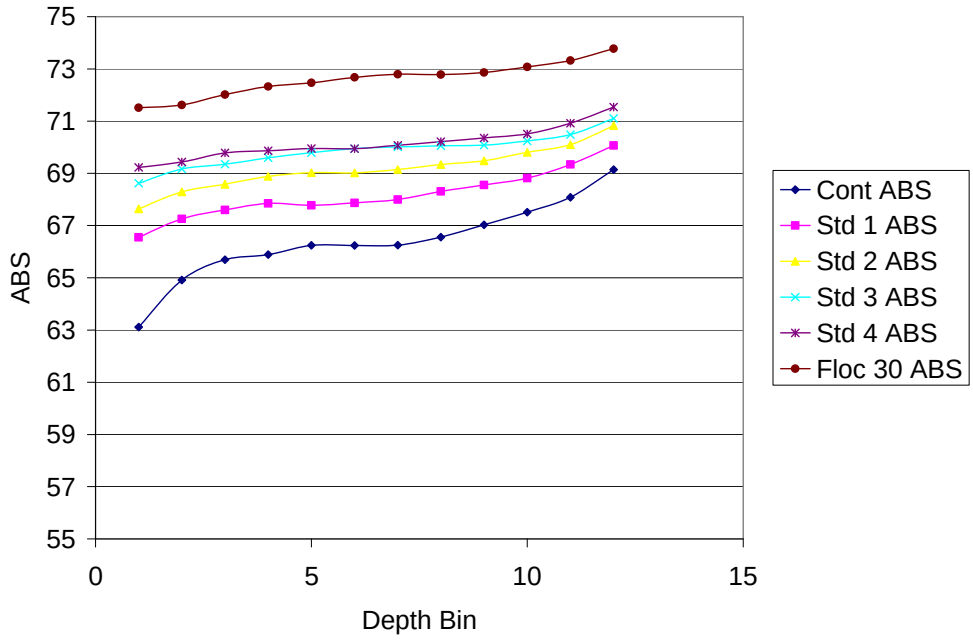

C)

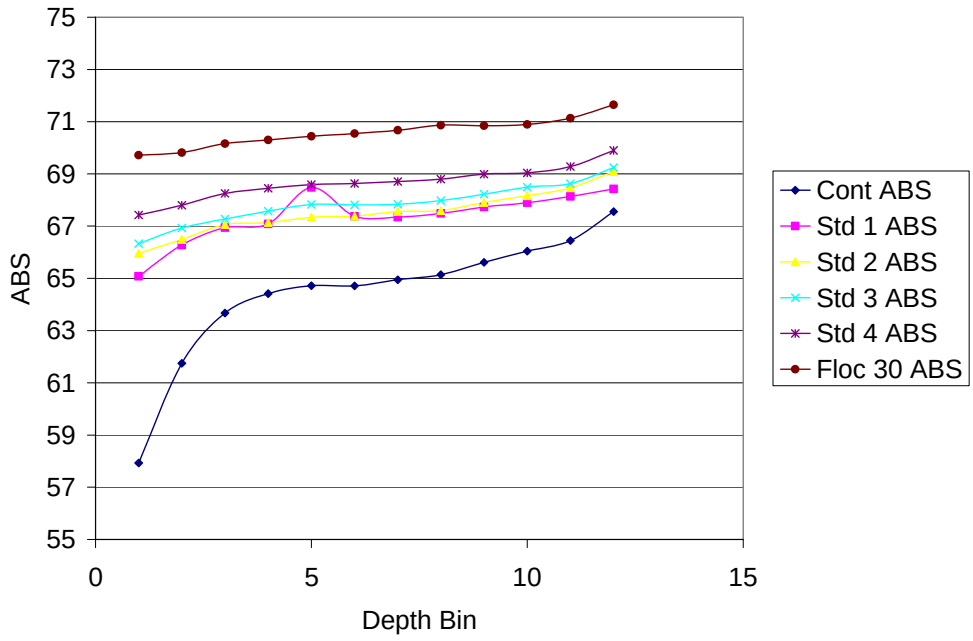

Fig. 5.9 continued

ABS response to SSC (mass basis)

Following procedures outlined by Wall et al. (2006) the ABS responses to the clay mass loads (including the Floc +30 minute) are plotted in Fig. 5.10. Initial inspection of Fig. 5.10 shows that Floc+30 treatments resulted in significantly elevated ABS without a corresponding increase in mass concentration in all replicates. However, linear ABS responses were demonstrated throughout all standard clay additions and Floc+30 treatments as indicated by the Pearson correlation coefficients shown in Table 5.3. Regression analysis also showed that both slope and y-intercept were reproducible between replicate tests and depth bins with covariances of 8 and 9%, respectively (Table 5.3). Substituting the slopes and y-intercepts into the respective coefficients A and B (Equation 5.3) allows the mass concentrations to be predicted with the measured ABS. The ratio of the predicted and measured mass concentrations for the lower and upper clay concentrations (i.e. Std 1 and Floc+30) were determined to evaluate the fit of the response factors (Table 5.3). These ratios ranged from 1.2 to 1.9, suggesting mass concentration acoustic backscatter calibrations can be used to provide suspended solids estimates within a factor 2 over a particle size distribution that varied within the Rayleigh region.

A)

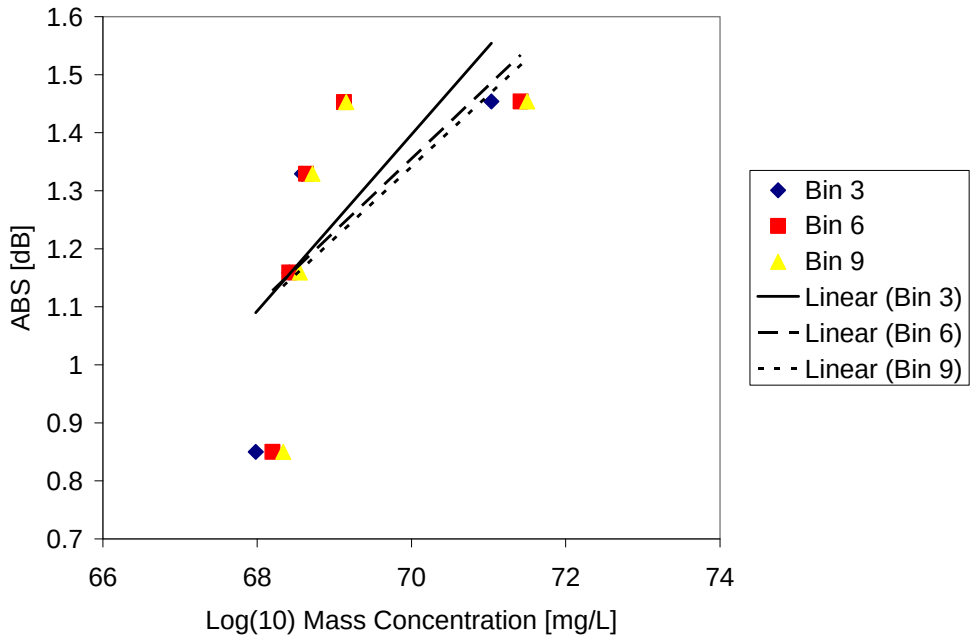

B)

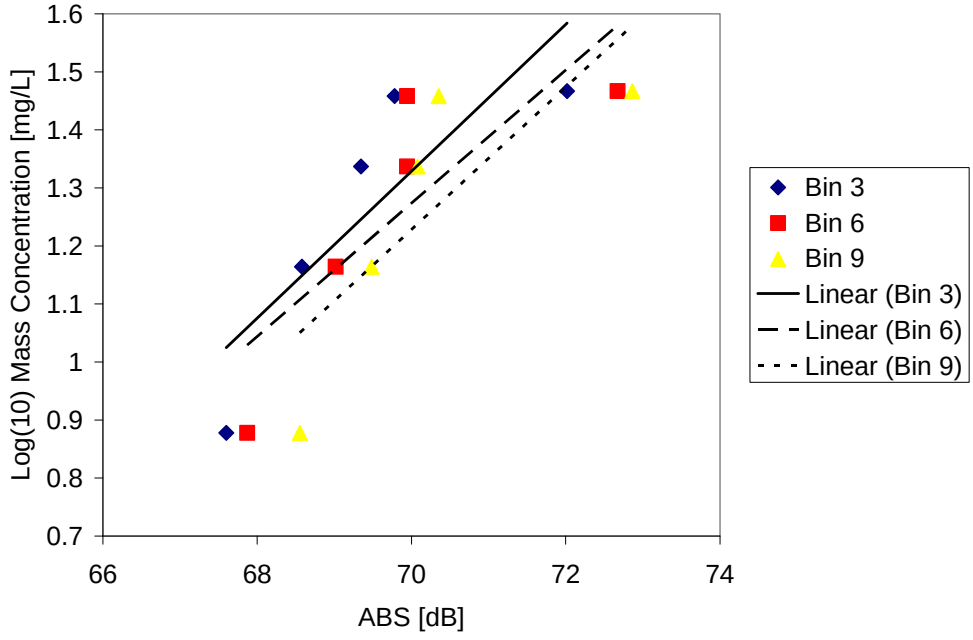

Fig. 5.10 ABS responses to standard clay mass loads, A) March 14, 2010, B) March 23, 2010, C) March 26, 2010.

C)

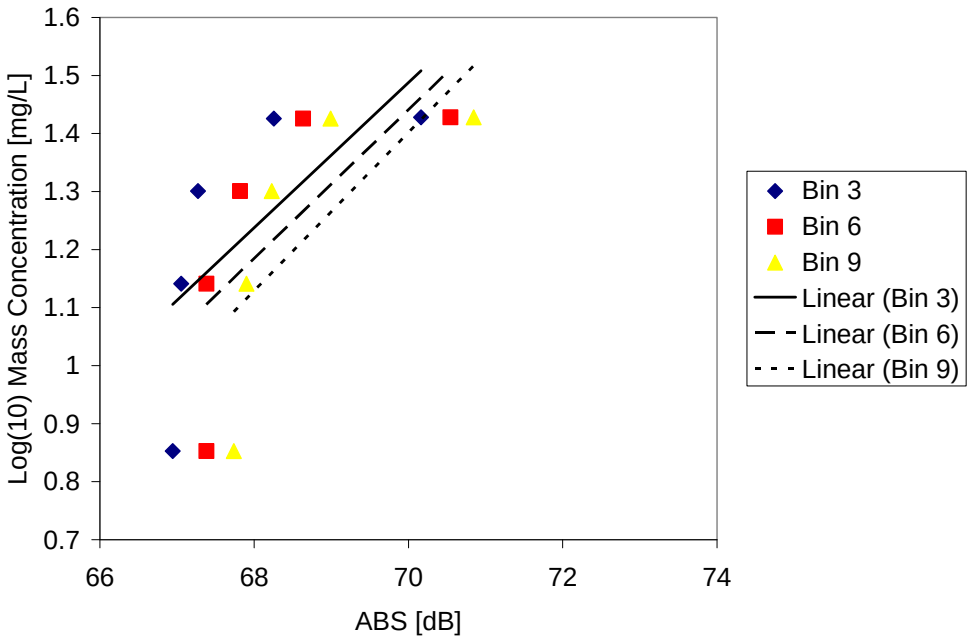

Fig. 5.10 continued

Table 5.3 Regression statistics from ABS-mass concentration response curves with ratios of predicted to actual mass concentrations.

	Slope	y-intercept	Pearson Correlation (r)	Ratio STD 1 [Predicted/Actual]	Ratio Floc + 30 [Predicted/Actual]
14-Mar-10					
Bin 3	0.15	-9.252	0.733	1.7	1.26
Bin 6	0.13	-7.48	0.691	1.9	1.21
Bin 9	0.12	-7.33	0.678	1.9	1.18
23-Mar-10					
Bin 3	0.13	-7.51	0.847	1.4	1.29
Bin 6	0.11	-6.76	0.826	1.4	1.30
Bin 9	0.12	-7.36	0.801	1.5	1.29
26-Mar-10					
Bin 3	0.13	-7.26	0.699	1.8	1.20
Bin 6	0.13	-7.52	0.705	1.8	1.20
Bin 9	0.14	-8.14	0.719	1.7	1.23
Average	0.13	-7.62	0.744	1.68	1.24
STDEV	0.01	0.707	0.063	0.203	0.0470
COVAR	8.20	-9.27	8.50	12.1	3.79

$r_{critical}$=0.648, n=5, $df = n$-2, α=0.05 (Johnson 1984)

ABS response to SSC (volume concentration basis)

Volume concentration response curves for depth bins 3, 6, and 9 for each test replicate are shown in Fig. 5.11. Log-linear acoustic backscatter responses to increasing particle volume concentration, including the 4 standard clay additions and the Floc+30 suspensions, for all depth bins and test replicates resulted. This observation is significant and demonstrates that ABS volume concentration calibrations are applicable over a varying PSD. Visual inspection of Fig. 5.11 also indicates that the ABS responses are comparable across the depth bins and test replicates and is confirmed by analysis of the regression statistics (Table 5.4) showing slope and y-intercept covariances of 18% and 22%, respectively. This apparently high covariance is due to the March 26, 2010, STD 1, which had elevated ABS with respect to the measured volume concentration which cannot be explained by the PSD. Substituting slopes and y-intercepts as the respective coefficients A and B in Equation 5.3, the predicted volume concentration for the STD 1 and Floc+30 were found to agree with the measured volume concentrations within 22% as indicated by average ratio of the predicted and measured values shown in Table 5.4. This is a substantial improvement over the values predicted by the mass concentration response curves and suggests that ABS responses are better suited to estimating volume concentrations than mass concentrations, especially when the particle suspensions have characteristically variable PSDs.

A)

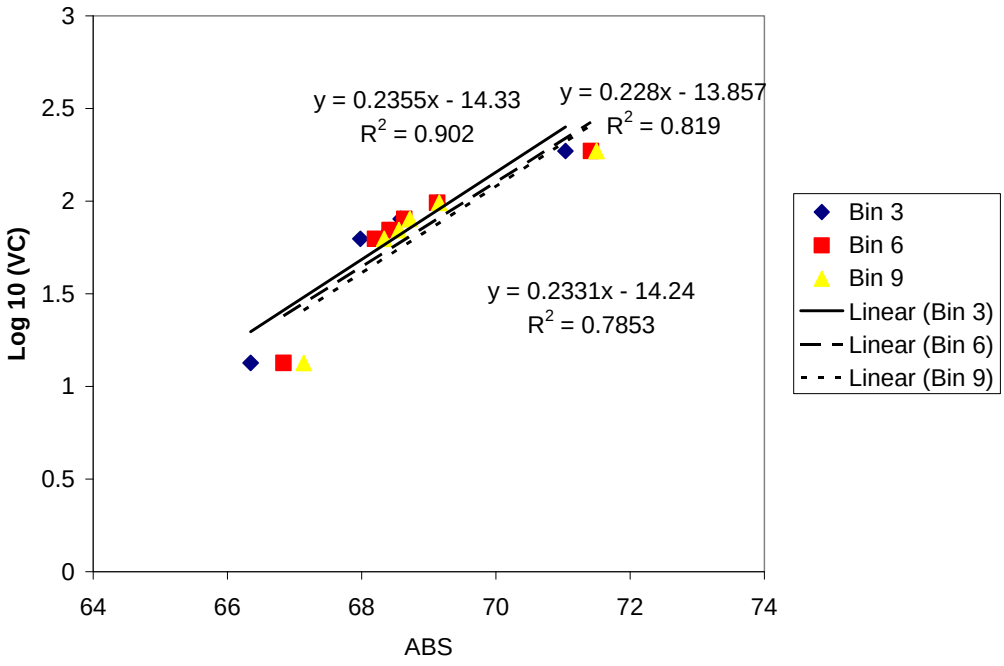

B)

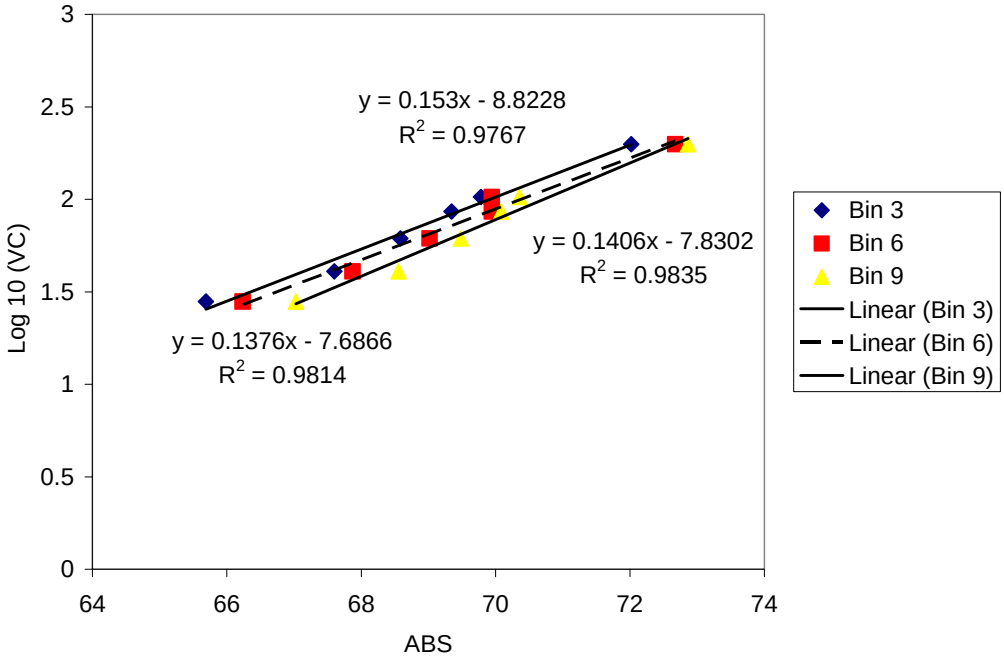

Fig. 5.11 ABS responses to standard clay volume concentrations, A) March 14, 2010, B) March 23, 2010, C) March 26, 2010.

C)

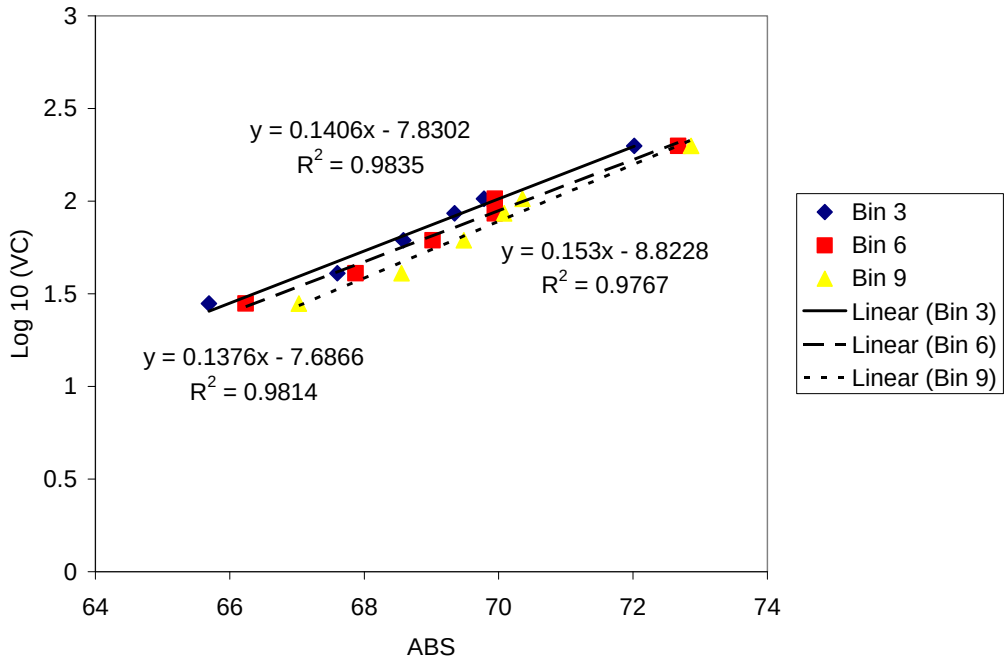

Fig. 5.11 continued

Table 5.4 Regression statistics for ABS-volume concentration response curves with ratios of predicted to actual volume concentrations.

	Slope	y-intercept	Pearson Correlation (r)	Ratio STD 1 [Predicted/Actual]	Ratio Floc + 30 [Predicted/Actual]
14-Mar-10					
Bin 3	0.16	-8.836	0.995	1.0	1.01
Bin 6	0.14	-7.857	0.993	1.1	1.03
Bin 9	0.14	-7.950	0.991	1.1	1.03
23-Mar-10					
Bin 3	0.15	-8.821	0.994	1.1	1.07
Bin 6	0.14	-8.049	0.985	1.1	1.08
Bin 9	0.16	-9.084	0.982	1.1	1.09
26-Mar-10					
Bin 3	0.20	-12.033	0.906	1.6	1.12
Bin 6	0.21	-12.378	0.910	1.6	1.12
Bin 9	0.22	-13.256	0.920	1.5	1.14
Average	0.17	-9.807	0.964	1.23	1.08
STDEV	0.031	2.128	0.039	0.241	0.0440
COVAR	19	21.7	4.09	19.6	4.09

$r_{critical}$=0.648, n=5, $df = n$-2, α=0.05 (Johnson 1984)

The primary incentive to conduct this study was to extend the capacity of the ADCP by developing ABS response factors that may be applied to estimate the volume concentration through the entire water column with variable particle size distribution. To make this evaluation, the ABS responses from all valid depth bins were plotted against the respective Log(10) Volume concentration (Fig. 5.12). A one-tail *t* test: Paired Two Sample for Means (Microsoft Excel) was performed to evaluate the error associated with predicting the volume concentration (dependent variable) from the ABS (independent variable). The null hypothesis was assumed (i.e. volume concentration is not dependent on ABS). The calculated t= 600 was within the critical region defined by $t_{critical}$=1.65 (α=0.05, df=179). Therefore, the null hypothesis was rejected indicating that it is appropriate to predict the volume concentration over the depth bins and particle size distributions evaluated by applying the acoustic backscatter response to the log-linear regression (Fig. 5.12).

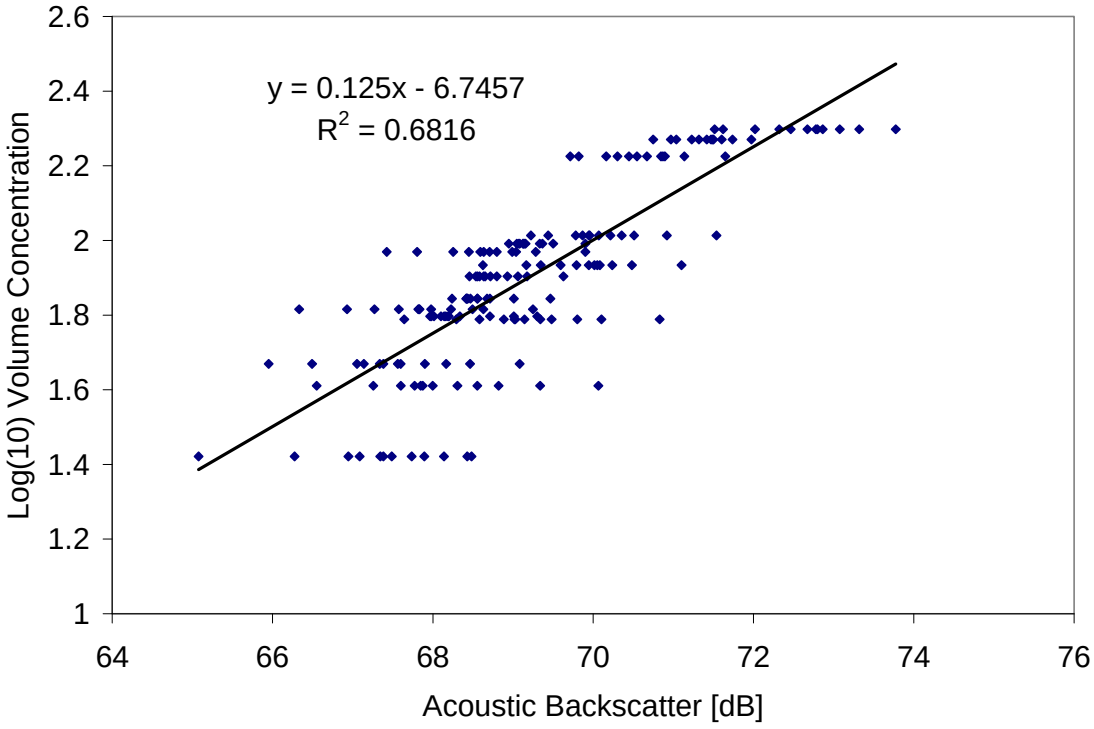

Fig. 5.12 Cumulative ABS responses from all replicate tests, depth bins, and standard clay loads.

The maximum SSC in this study was limited by the maximum detection limit of the LISST 100. Therefore it was not possible to empirically define the maximum SSC detection limit using the ABS response. However, the maximum ABS response of 93 dB was estimated as the sum maximum ABS value, obtained from the reflected signal off the tank bottom) plus the signal attenuation due to beam spreading and water absorption. Substitution of this estimated max ABS into linear the regression provided in Fig. 5.12 suggest a maximum acoustic backscatter SSC detection limit on the order of 10^5 µl/L , a 10% solids suspension. Minimum ABS responses obtained from no-clay controls averaged 62 dB at a mean volume concentration = 1.4 µl/L. These values suggest an ABS SSC detection range covering 5 orders of magnitude. However, at high

SSC concentrations signal attenuation due to sediment absorption would become significant, requiring additional corrections for signal attenuation. The increased signal attenuation resulting from elevated SSC concentrations would also reduce profiling range.

The correlation between the Rayleigh scattering model and the observed ABS with respect to increasing suspended clay volume concentrations was evaluated. This evaluation required that the target strength ABS (TS_R) be calculated with Eq. 5.1 using the particle size distribution data provide by the LISST 100. For this exercise, I_0 = intensity of source signal is assumed to be unity. The ensonified volume was calculated using Equation 5.17 for Bin 6. Plotting TS_R vs measured ABS for the representative bins, cumulative across all replicate tests, demonstrated a linear correlation in all depth bins evaluated (Fig. 5.13), as indicated by r=0.7928 - 0.8512 ($r_{\text{critical}} = 0.194$, $\alpha = 0.05$, $df = 13$, (Johnson 1984)), over a variable PSD that was characterized by doubling of the mean particle diameter. This shows that the Rayleigh scattering solution applies to ABS measurements and that it is applicable to estimating volume concentrations. Further, this correlation explains why ABS shows such a strong correlation to volume concentration over a variable PSD.

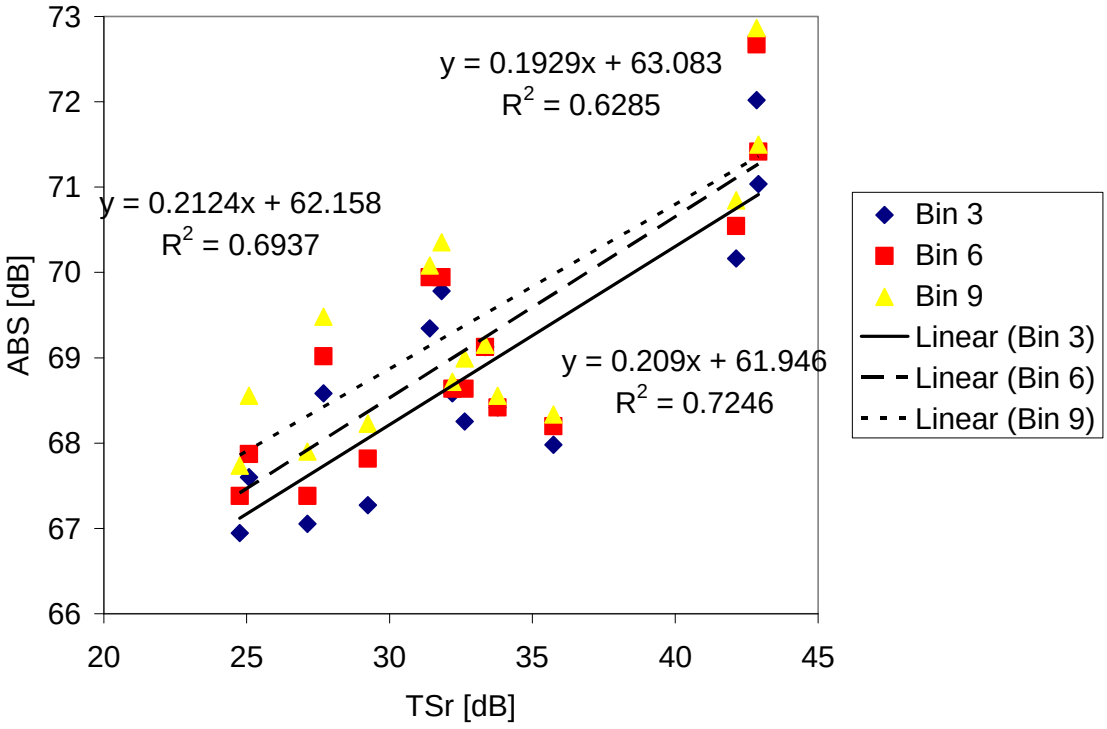

Fig. 5.13 Measured ABS vs Rayleigh scattering target strength.

The correlation between acoustic backscatter and volume concentration inferred from the LISST should be anticipated considering the theoretical similarities between the measurements. Acoustic backscatter is based on the Rayleigh scattering equation while the LISST utilizes the Mie scattering approximation to infer particle size distribution. Mie scattering applies to particles of all sizes, however when the particle circumference is less than the wavelength, the equation reduces to the Rayleigh equation. Mechanistically, the LISST utilizes the principle that small particles scatter light energy in an angular range unique to that size (Agrawal and Pottsmith 1994). The contribution to scattering from an ensemble of particles of a particular angle (i.e. particle radius) may be expressed as the sum intensity contributed by all particles at the specified radius *a*.

Therefore, the LISST particle size distributions and the ADCP echo intensities are generated using analogous principles and further suggest that suspended solid estimations based on echo intensity are better suited to estimate particle volume concentrations.

The analysis presented above demonstrates that a correlation between ABS and volume concentration is conserved over a variable PSD assuming that the particle density and compressibility remain constant. Using a modified Rayleigh equation allows TS_R to be calculated for particles not adhering to the assumptions of the general equation (i.e. dense rigid spheres). As given in Urick (1983), Rayleigh provided the expression

$$\left[1-\frac{k'}{k}+\frac{3\left(p'/p-1\right)}{1+2\,p'/p}\mu\right]^2 \tag{5.19}$$

to replace the term $\left(1+\frac{3}{2}\mu\right)^2$ found in Equation 5.1 where, k and p are the compressibility and density of water, respectively and prime denotes the same qualities for the particle. To evaluate the effect of the clay properties on the observed response, the modified TS_R was calculated using p'= 2.5 and assumed the clay particle compressibility was similar to sand with a k'≈0.1 as evaluated in Urick (1983). Using these value for p' and k', the modified TS_R values were found to be approximately 3.5 dB less than predicted by the standard TS_R equation. Considering the average slope of 0.2, generated from the regression of the measured ABS vs TS_R (Fig. 5.13), a TS_R difference of 3.5 dB would translate to about 0.7 dB difference in the measured ABS

with the StreamPro, or about 10% of the ABS range.

Conclusions

Log linear acoustic backscatter responses to both mass and volume concentrations were observed with a 2400 kHz ADCP over PSD's that varied within the Raleigh region. However, ABS responses to volume concentrations produced higher linear correlation coefficients with a corresponding improvement in the concentrations predicted by the linear regressions, compared to the response curves generated with mass concentration. This observed correlation between ABS and volume concentration is due to a shared dependence on the particle size distribution as defined by Rayleigh and Mie scattering assumptions, respectively. These findings suggest that volume concentration is more appropriate than mass concentration for developing ABS suspended solids response factors.

Despite the strong correlation between ABS and volume concentration, care must be taken when inferring volume concentrations from ABS measurements. Many environmental factors can adversely affect the observed ABS. During preliminary testing, much effort was focused on obtaining reproducible echo intensity profiles for given particle mass concentrations and it was observed that environments with elevated background noise could easily swamp out the signal due to the presence of scattering particles. The source of the background noise was found to be associated with elevated bubble concentrations and also observed on very windy days, which can induce bubble formation in the water column. Increased acoustic backscatter intensity has previously

been associated with high shear zones due to temperature and salinity variability related to oceanic mixing (Orr et al. 2000). Another study showed that increased acoustic backscatter can result in high shear zones when bubbles are mixed downward from surface turbulence (De Marco et al. 1995). Other interference sources that were experienced included elevated noise floor that was found to be coincident with pump operations.

In the event of boat based deployments, operators must first ensure that vessel noise originating from engines, prop wash, propeller signature, etc., does not interfere with the acoustic backscatter measurements. Additionally, care must be taken to characterize the weather conditions at the time measurements are being taken. In the event of high winds, precautions must be taken to ensure that echo intensity is not due to the formation of bubbles.

CHAPTER VI

ESTIMATING SUB-SURFACE DISPERSED OIL CONCENTRATION USING ACOUSTIC BACKSCATTER RESPONSE

Overview

The recent *Deepwater Horizon* resulted in a dispersed oil plume at an approximate depth of 1000 meters. Several methods were used to characterize this plume with respect to concentration and spatial extent including surface supported sampling, *in-situ* analysis with autonomous underwater vehicle AUV mounted instruments, and remote detection with echo sounders, demonstrating the potential for remote detection using acoustic backscatter (ABS). This study evaluated use of an Acoustic Doppler Current Profiler (ADCP) to quantitatively detect oil-droplet suspensions from the ABS response in a controlled laboratory setting. Results from this study showed log-linear ABS responses to oil-droplet volume concentration. However, the inability to reproduce ABS response factors suggests the difficultly in developing meaningful calibration factors for quantitative field analysis. Evaluation of theoretical ABS intensity derived from the particle size distribution provided insight regarding method sensitivity in the presence of interfering ambient particles.

Introduction

In April 2010, the *Deepwater Horizon* blowout resulted in the largest off-shore oil spill in history, releasing nearly 5 million barrels of oil into the Gulf of Mexico

(Lubchenco 2010). The blowout occurred at the well head at a depth of 1500 m, where the oil dispersant Corexit 9500 was injected (Hazen et al. 2010). This sub-surface spill produced a suspended oil plume between 1030 and 1300 m depth that was identified using autonomous underwater vehicles (AUV) and cable-lowered sampling rosette (Camilli et al. 2010). Additionally, sonar surveys showed acoustic signatures attributed to oil plumes near the well head (Smith et al. 2010) demonstrating the capacity to use acoustic backscatter to detect sub-merged oil plumes. Acoustic backscatter (ABS) obtained using Acoustic Doppler Current Profilers (ADCP) has previously been evaluated as a surrogate method to quantify suspended solids concentration (Wall et al. 2006; Gartner 2004; Gray and Gartner 2009; Hamilton et al. 1998). It has also been clearly demonstrated that oil dispersed in the water occurs predominantly as a droplet suspension (Page et al. 2000b; Sterling et al. 2004a, 2004b, 2004c, 2005). Thus, suggesting that ABS techniques may also be employed to quantify dispersed oil plumes.

ABS signal strength is a function of the particle size distribution and concentration as defined by the Rayleigh scattering (Equation 5.1) (Urick 1983; Reichel and Nachtnebel 1994). This expression assumes small spherical particles where the circumference is much less than the acoustic wavelength. Sterling et. al. (2004a) previously showed that dispersed oil suspensions generated at mean shears typical of marine and estuarine systems were composed of spherical droplets with circumferences on the order of 75 μm, thus satisfying the conditions required for Rayleigh scattering with 2400 kHz signal. While the primary condition suggesting that ABS can be used to measure sub-surface dispersed oil plumes is satisfied, there are two principles that can

negatively affect this application. First, sound absorption causes acoustic backscatter intensity to decay exponentially with range and the level of absorption increases proportionally to the frequency (Urick 1983). Thus, lower frequency signals are required for more distant (i.e. deeper) ABS measurements. For example, the nominal range of the 2400 kHz StreamPro is 2 meters (RD Instruments 2006) while the nominal range of the 76.8 kHz ADCP is 700 meters (RD Instruments 1996). This limitation restricts surface detection of deep sub-surface oil plumes to acoustic instruments with frequencies on the order of 38 kHz with a range of 800-1000 m (Teledyne RD Instruments 2010). The second principle affecting remote dispersed oil plume detection with ABS technology is a function of the Rayleigh target strength equation which indicates that the ABS intensity is proportional to the fourth power of the droplet radius and inversely proportional to the sixth power of the acoustic wavelength (Urick 1983). Therefore, the ABS intensity from a droplet of a given size would be significantly less when measured with a longer wavelength (lower frequency) instrument compared to shorter wavelength instrument. For example, the theoretical Raleigh target strength from a single 100 micron diameter droplet at 2400 kHz and 38 kHz would be 0.63 dB and -71 dB, respectively. One beneficial result of decreasing the frequency is an increase in the maximum droplet diameters responsible for Rayleigh scattering, defined as when the ratio of droplet circumference to wavelength is unity (Urick 1983). Applying this convention dictates that the maximum droplet diameters for 2400kH and 38 kH signals are approximately 200 and 12,000 μm, respectively. The lower frequency ADCPs are capable of detecting sub-surface oil plumes consisting of large droplets, but would be

limited in detecting plumes consisting of small droplets. These conflicting processes must be balanced to effectively apply ABS as a viable remote oil sensing methodology.

Camilli et al. (2010) found that the sub-surface oil plume resulting from the Deepwater Horizon spill persisted for months indicating that the plume resided in a stable strata within the water column. The strength of this stratification, is a function of the density and shear gradient and may be described using the Richarson number (*Ri*) (Islam et al. 2010a). When the density is much stronger than shear gradient, the stratification will be well defined and the diffusion of the small oil droplets into the surrounding strata will be limited. Similarly, the presence of shear-structure within the water column has been shown to result in elevated diffusivity values compared to relative diffusivity values determined for turbulence alone (Ojo et al. 2006a). Therefore, plume persistence over extended periods indicates that shear within the plume was minimum. Droplet collision efficiency is dominated by shear (Sterling et al. 2004a), implying that droplet aggregation would be minimized, and a stabilized suspension of characteristically small particles would result. Furthermore, in shear dominated systems, droplet aggregation would be enhanced leading to the formation of larger droplets with increases in both vertical settling velocities and diffusion (Sterling et al. 2004a; Ojo et al. 2006a). From the perspective of using ABS intensity to quantify stable sub-surface oil-droplet suspensions, this analysis suggests that the ABS response may be limited within deep water structures where low frequency (long wavelength) acoustic signals are required. Conversely, 38 kHz echo sounders have been proven useful to track sub-surface oil releases (Adams and Socolofsky 2005).

The goal of this study was to evaluate if ABS intensity measured with an ADCP can quantitatively measure oil droplet suspensions in a controlled laboratory setting with measured dispersed oil concentrations. The measured ABS response to these variable dispersed oil loads was compared against the theoretical ABS response to evaluate method efficacy and potential interferences.

Materials and Methods

Experimental design

A 2400-kHz Teledyne RD Instruments StreamPro ADCP was used to collect echo intensity depth profiles resulting from standard oil suspensions generated in a laboratory test tank (Fig. 6.1). The SteamPro was mounted to a rigid support in a down-looking orientation in the center of the tank with transducer depth set at 5 cm below the water surface. Real time data collection was made with WinRiverII (Teledyne RDI) via a Bluetooth serial connection to a Dell Laptop computer with a Window XP operating system. The StreamPro was configured in WinRiverII to collect echo intensity ensembles (samples) with the following settings; 6 pings/ensemble, ping rate=2 Hz, depth bin size = 10 cm, number of depth bins=15, first depth bin=0.16m). A separate ensemble file was collected for each standard oil concentration with at least 60 ensembles collected per file. To alleviate variations in incident signal strength resulting from power fluctuations as described by Wall et al. (2006), the StreamPro was connected to a laboratory power supply with operating voltage set to 12.5 VDC.

All echo intensity (*EI*) values were normalized with respect to Beam 1 using

Equations 5.3-5.4. The *EI* values were then converted to acoustic backscatter (ABS) in decibel [dB] units as the product of the *EI* and RSSI (Equation 5.13). The RSSI factor was determined as the slope of the line generated by plotting the normalized *EI* against the sum of the beam spreading and water absorption attenuation values, with respect to depth as described in Chapter V. The ABS values were then corrected for attenuation due to beam spreading and water absorption by using Equations 5.5-5.10b. Corrections for sediment attenuation were calculated from the oil droplet PSDs using Equation 5.11b. Sediment attenuation at the highest oil droplet concentration was found to be negligible. Therefore, sediment attenuation corrections were omitted from ABS data processing.

Test tank configuration

All tests were conducted in an open-top fiberglass tank (Inside Diameter 3.7m x Depth 1.7m) (Fig. 6.1). The tank bottom was lined with rubber mats (1.9 cm thick) to minimize acoustic signal reflection and subsequent interference with the StreamPro. The tank was filled with salt water with a salinity = 30 psu verified with a refractometer. The salt water was prepared by filling the tank to capacity with potable water to which 1,000 lbs of NaCl (Morton Purex All Purpose, food grade) was added (Fig. 6.1). The tank was then allowed to mix-continuously until salt was completely dissolved. Tank mixing was provided by a 1-Hp pool pump that was plumbed to an octagonal PVC distribution manifold installed on the tank bottom (Fig. 5.1). The manifold contained 32 equally spaced distribution ports (diam-0.7 cm) oriented to direct the water toward the

tank center and along the tank bottom. This configuration results in an upwelling at the tank center with a down current around the tank circumference. Pump intake was through a 3.7 cm (I.D.) plumbing fixture located 5 cm above the tank bottom. Pump flow rate was set at 0.17m^3/sec resulting in a tank turn over time of 92 minutes.

Fig. 6.1 Test tank just prior to salt addition.

To allow the salt water to be recycled between experimental replicates the mixing pump was plumbed into a 2 stage filtration system. The first filtration stage was provided by a diatomaceous earth filter (Hayward Progrid, Model 3620). Second stage filtration was provided by a sand type filter (Hayward Pro Series, Model S166T) charged with granular activated carbon. To prevent algal growth in tank, the water was treated

with an algaecide (Leslie's Swimming Pool Supplies, LPM 14-025) at the recommended dosage.

Mixing shear determination

The oil-droplet size distribution is dependent on the energy dissipation rate (i.e. shear) (Li et al. 2008; Sterling et al. 2004a). Therefore it is necessary to control the mixing power used to generate the oil-droplet suspensions so that realistic droplet size distributions can be generated. Following the procedure presented by Sterling et al. (2004a), the experimental test tank was mixing was scaled to the mean shear rate, G_m, determined with the Camp and Stein (1943) equation

$$G_m = \left(\frac{Po}{\mu V} \right)^{1/2} \tag{6.1}$$

where, G_m= s^{-1}, Po=watts, μ=1.002E-3 kg-m^{-1}-s^{-1}, V=reactor volume=16 m^3. Power injected into the test tank by the 1 Hp pump was calculated using Bernoulli's equation (De Nevers 1991)

$$\frac{-dW_{a.o}}{dm} = \Delta\left(\frac{P}{\rho} + gz + \frac{U^2}{2} \right) \tag{6.2}$$

where $W_{a.o.}$ is pump work [kg m^2s^{-2}], m is fluid mass [kg], P is pressure [kg $m^{-1}s^{-2}$], ρ is water density [kg m^{-3}], g is gravity [m s^{-2}], U is fluid velocity [m s^{-1}], and z is the water surface height [m]. Given that ΔP and Δz are zero, Equation 6.2 may be simplified to

$$\frac{-dW_{a.o}}{dm} = \Delta\left(\frac{U^2}{2} \right) \tag{6.3}$$

This expression may be converted to units of power by multiplying both sides of the equation by the mass flow rate [kg s^{-1}]. *Po* input to the system was calculated as a function of mass flow rate and water velocity, which were determined using an inline paddle wheel flow meter (Omega Engineering, Inc., Model # FP2020-R) that was installed between the pump and water discharge into the tank. The resultant power values were then substituted into Equation 6.1 to determine the respective G_m. All tests were conducted with at G_m=25 s^{-1}, which was within the ranges evaluated in oil droplet coalescence studies by Sterling et al. (2004a, 2004b, 2004c, 2005).

Dispersed oil

Artificially-weathered Arabian medium crude oil was used to prepare all crude oil suspensions in this study. The natural weathering of the crude oil was simulated by air stripping the volatile fractions which reduced the oil volume by 30-35%. The weathered oil has a specific gravity of 0.9129, kinematic viscosity of 102.4 centistokes at 20 C, and a Reid vapor pressure of 2.1 kPa at 37.8 C. This oil was premixed with the dispersant Corexit 9500A (Nalco, Sugar Land Texas) at a 10:1 oil mass to dispersant mass ratio. Standard oil concentrations of 6, 12, 18, 24, 30, and 36 µl/L (nominally) were made by injecting 95 ml of the oil-dispersant mixture (neat) with two 50-ml syringes directly into below the waters surface. For Replicate 1, the oil-dispersant mixture was added at the tank center, in the up-welling current. Visual observations combined with the low total volume concentrations indicated that substantial oil volumes remained at the tank surface (i.e. not entrained in the water column). For Replicates 2

and 3, oil injection location was moved from the tank center to a location adjacent to the tank wall to take advantage of the down-welling current which provided additional oil residence time in the water column, thereby enhancing overall oil dispersant efficiency as indicated by a higher percentage of the initial oil volume being dispersed. Also, for Replicates 2 and 3, one additional oil standard was added to evaluate the ABS response over the full linear detection limit of the LISST-100. Each standard oil-dispersant injection was allowed to mix in the tank for 10-min prior to collecting StreamPro ABS and LISST-100 particle size samples. To prevent acoustic interference, the LISST-100 was removed from the tank during ABS sampling with the StreamPro. Thus, sample collection was conducted sequentially, first the StreamPro followed by the LISST-100.

Volume concentration measurements

Oil droplet volume concentrations and particle size distributions were measured *in-situ* with a LISST 100, Type B (Sequoia Scientific, Bellevue, Wa. U.S.A.) that measures 32 log-normally-distributed particle size classes with diameters ranging from 1.2 to 250 microns. The LISST was configured to collect 1 sample/ensemble using the LISST MFC Application (Version 1.0.0.1). It was suspended on a chain in a horizontal orientation to reduce settling of suspended particles on optical surfaces (Fig. 6.2). All measurements were taken at 0.65 meters below the water surface. All volume concentrations and particles size distributions reported in this study are the mean of 30 ensembles. No attempt was made to quantify the amount of oil adsorbed to the tank surfaces as this study was designed only to evaluate the ABS response to the entrained

oil droplet concentration.

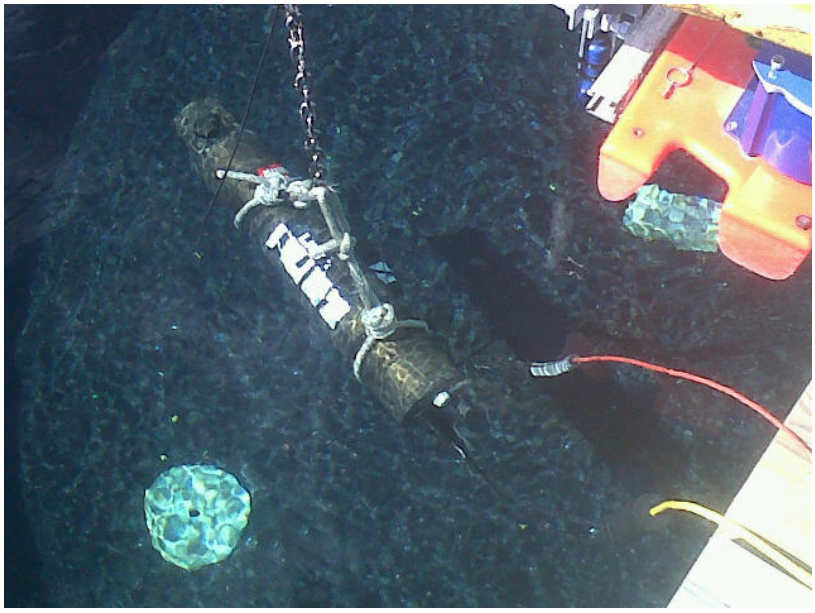

Fig. 6.2 LISST-100 suspended in test tank for volume concentration measurements. Clear water is representative of no-oil control conditions.

Results

Total volume concentrations

The LISST-100 total volume measurements were determined from response to all particles entrained within the water column including oil-droplets, suspended sediments, and bubbles. All measurements were made using a background scatter file collected during the Replicate 1 control (i.e. clean water no oil conditions). This was done to directly measure any variations in the experimental droplet distributions between replicates with respect to total volume concentrations and size distribution. Total oil volume concentration was linear with nominal oil loads as indicated by R^2>0.99 for all three replicates (Fig. 6.3). Changing the oil injection location from the tank center in

Replicate 1 to near the tank wall in Replicates 2 and 3 resulted in more efficient oil dispersion as indicated by the respective increase in the linear regression slopes (Fig. 6.3). Replicate 2 (red squares) showed an elevated ambient particle concentration of 5 µl/L at Nominal Oil Load [µl/L] = 0, compared to Replicates 1 (blue diamonds) and 3 (purple triangles) which both show ambient particle concentrations less than 1 µl/L (Fig. 6.3).

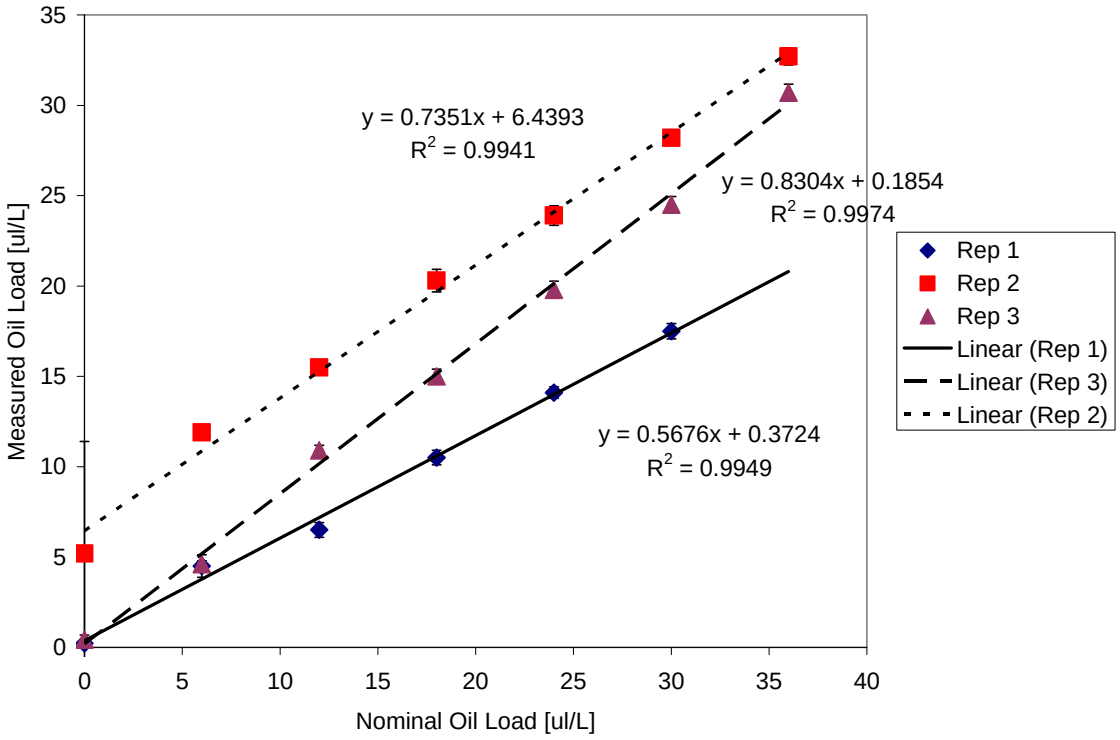

Fig. 6.3 Nominal vs measured oil load. Error bars represent standard deviation of mean (*n*=30).

Particle size distribution

The particle size distributions and their concentration from each experimental replicate were plotted Fig. 6.4. All particle size distributions were collected using the background scatter file collected in the test tank for Replicate 1 so that any PSD changes in the no-oil controls could be characterized. Note that the droplet size distribution for Replicate 2 (Fig. 6.4B) showed an elevated ambient particle load (i.e. no-oil control) with particle diameters greater that 150 μm being retained in all Replicate 2 standard oil concentrations. Inspection of Replicates 1 and 3 PSDs (Figs. 6.4A and 6.4C) showed elevated large droplet concentrations only with the Replicate 1, Std 1 (6 µl/L, nominal). Neglecting the presence of ambient particle loads, the oil-droplet PSDs were similar to the oil droplet PSDs generated at G_m=20s^{-1} as presented by Sterling et al. (2004a) with most of the droplets being distributed between 10 and 100 µm. However, one obvious difference is the presence for the large peak occurring at 1.3 microns, which is not present in the PSDs presented by Sterling et al. (2004a). This difference may be due the scale effects resulting from differences in reactor volume, configuration, and/or mixing method. For clarification, Sterling et al. (2004a) used a rectangular, 32 l reactor, agitated by rotating an impeller with four cylindrical rods evenly staggered throughout the water column. While the mean shear determined for both reactors were similar, localized volumes with high shear in the current reactor configuration, including centrifugal pump, plumbing fixtures, and distribution manifold, may have contributed to the presence of the small oil droplets.

A)

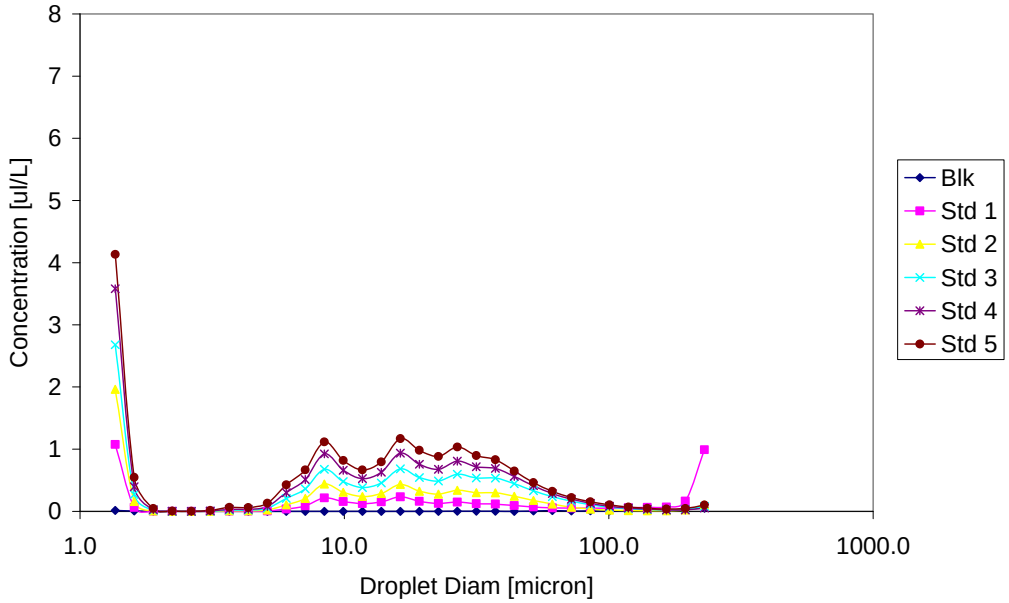

B)

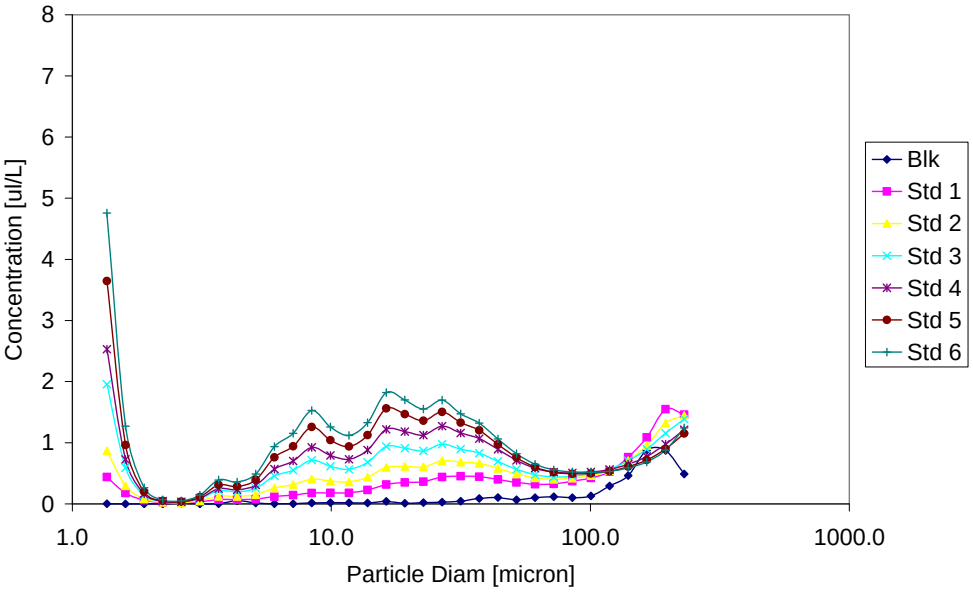

Fig. 6.4 Oil droplet size distributions measured with LISST-100, A) Replicate 1, B) Replicate 2, C) Replicate 3.

C)

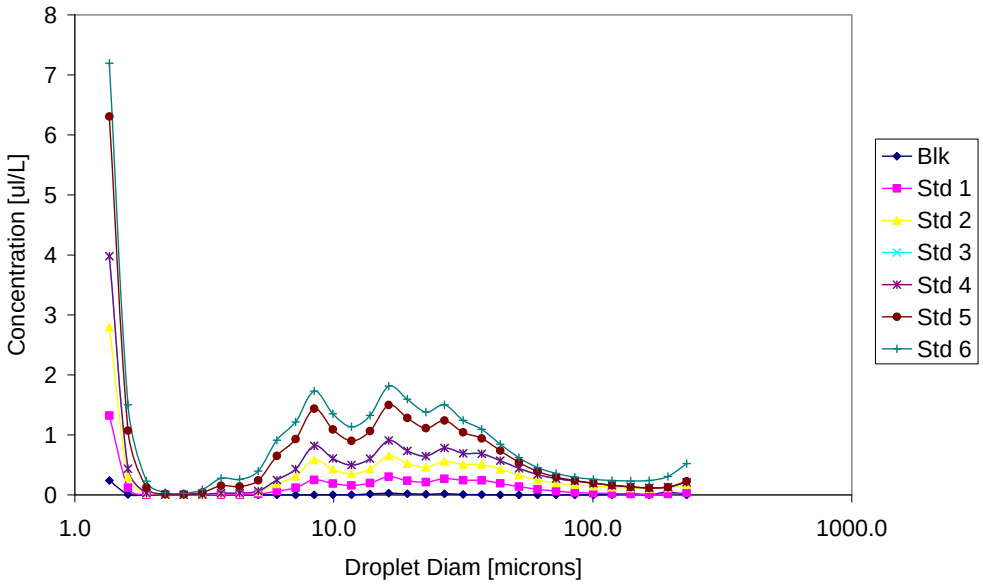

Fig. 6.4 continued

The mean droplet diameter is calculated from the particle size distribution as

$$d_{mean} = \frac{\sum C_i d_i}{C_{total}} \tag{6.4}$$

where C_i is the particle (droplet) concentration with a diameter d_i and C_{total} is the total volume concentration. To alleviate ambient particle contributions to the mean droplet diameter, the no-oil control PSD from each replicate was subtracted from the respective PSD obtained for each standard oil suspension. Elevated ambient particle loads in Replicate 2 occurred for particle diameters greater than 100 μm (Fig. 6.4) Maximum oil droplet diameters in all replicates were less than 100 μm and suggests that particles with diameters greater than 100 μm do not contribute to the mean droplet diameter. Omitting particles with diameters greater than 100 μm from the mean droplet diameter

calculations is justified by evaluating the ratio

$$\frac{VC_{<100um}}{VC_{oil}} \tag{6.5}$$

where $VC_{<100um}$ is the volume concentration inferred from the PSD < 100 μm, and

$$VC_{oil} = VC_i - VC_{no-oil} \tag{6.6}$$

i is the standard oil addition, and *no-oil* represents the no-oil control. The mean ratio (Equation 6.5) for all oil standard additions of all 3 replicates was 0.98 (STDEV=0.072), indicating that 98% of the oil-droplets had diameters less than 100 μm. The mean droplet diameters for each experimental replicate and condition indicate that the oil droplet diameters were conserved between both experimental replicates and conditions (Fig. 6.5). The mean droplet diameter for all replicates and experimental conditions was 18 (+/- 1) μm and is comparable to the mean droplet diameters of 17(+/-6) μm reported by Sterling et al. (2004a) indicating the test tank mixing was scaled appropriately with mean shear (G_m) . From the perspective of an ABS evaluation, the reproducible droplet suspensions suggest that the observed ABS responses in each experimental replicate should be similar.

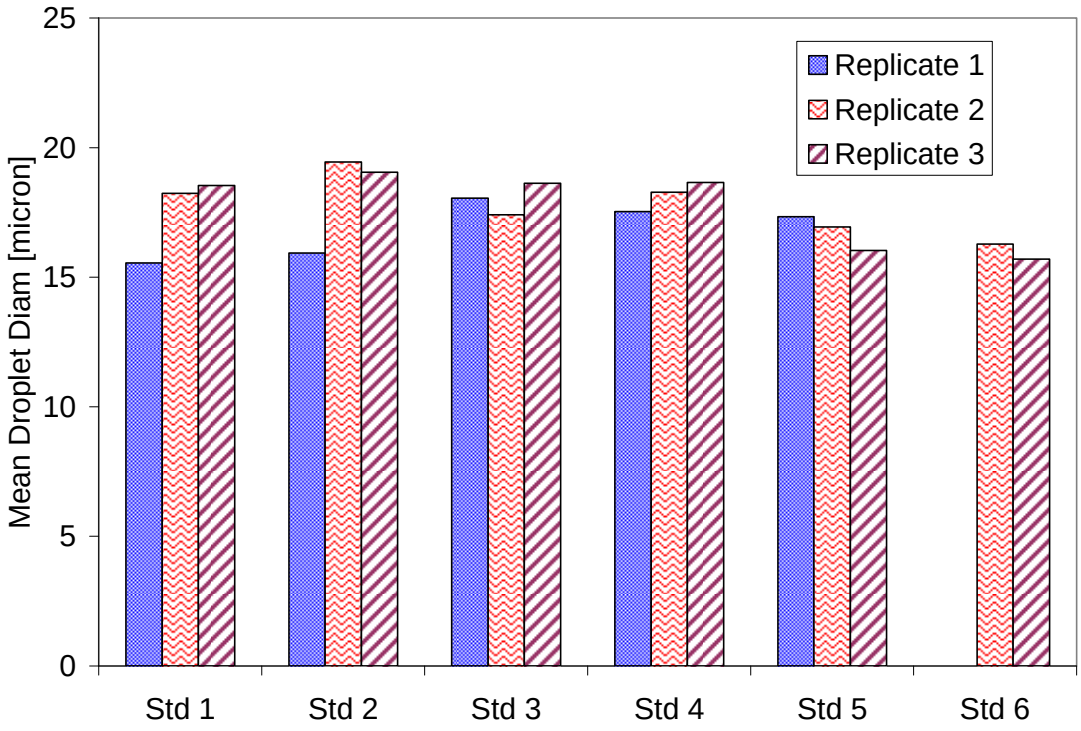

Fig. 6.5 Mean droplet diameter calculated from PSD less than 100 microns and with ambient particle load subtracted.

ABS depth profiles

ABS depth profiles were generated by first correcting the measured ABS for beam spreading and water absorption attenuation by application of Equations 5.5-5.10b. ABS profiles for no-oil controls were omitted as clean water conditions (i.e. lack of adequate acoustic scattering) resulted in high percentage (on the order of 90%) of bad ADCP ensembles. Addition of the lowest oil concentration standard, 6 µl/L nominal, in each replicate resulted in nearly 100% good echo intensity ensembles in all valid depth bins. A valid depth bin was defined in this study as the first eleven depth bins, representing depths from 0.16 to 1.16 meters, not showing elevated echo intensities resulting from incident signal reflection off tank surfaces. A positive relation is

indicated between oil-droplet concentration and the observed ABS (Fig. 6.6). However, in Replicates 2 and 3 (Figs. 6.6B and C, respectively) maximum oil loads (36 µl/L, nominal) resulted in no appreciable change in the ABS response relative to the previous oil load (30 µl/L, nominal). Error associated with the ABS corrections for beam spreading and water absorption is apparent in the ABS depth profiles generated for each standard oil addition in all replicates (Fig. 6.6). Assuming that the oil droplet suspensions were homogenously distributed throughout the tank volume, the corrected ABS depth profiles would exist as a horizontal line under ideal conditions. All profiles deviate from horizontal with a corrected ABS decline (~0.5-1 dB) between the 0.16 and 0.36 m depth bins and a gradual corrected ABS increase (~0.5 -1 dB) between the 0.36 and 1.16 m depth bins (Fig. 6.6) Despite this error, some inferences may be made from the ABS profiles.. The highest ABS (~62 dB) occurred at the highest Replicate 1 oil concentration of 17 µl/L (Fig. 6.6A). However, this oil load is approximately one-half the maximum oil concentration measured in Replicates 2 and 3 that resulted in maximum ABS responses on the order of ~58-59 dB (Figs. 6.6B-C). This observation suggests the inherent variability of the ABS intensity measurement despite efforts to maintain reproducible conditions by ensuring stable and consistent power to the ADCP and transducer mounting configuration between replicates.

A)

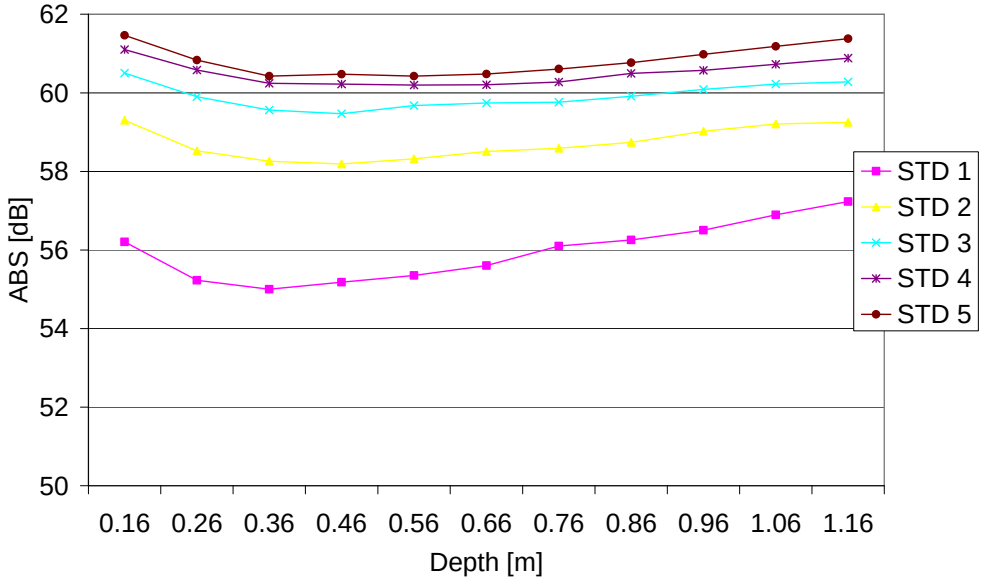

B)

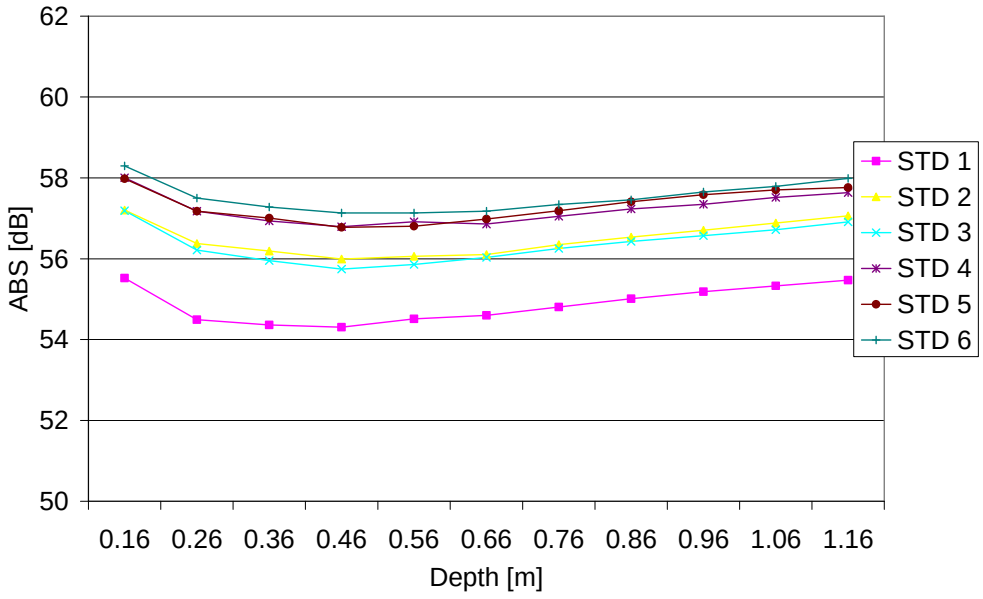

Fig. 6.6 Corrected ABS depth profiles for each standard addition. Profiles for no-oil controls omitted. A) Replicate 1, B) Replicate 2, C) Replicate 3.

C)

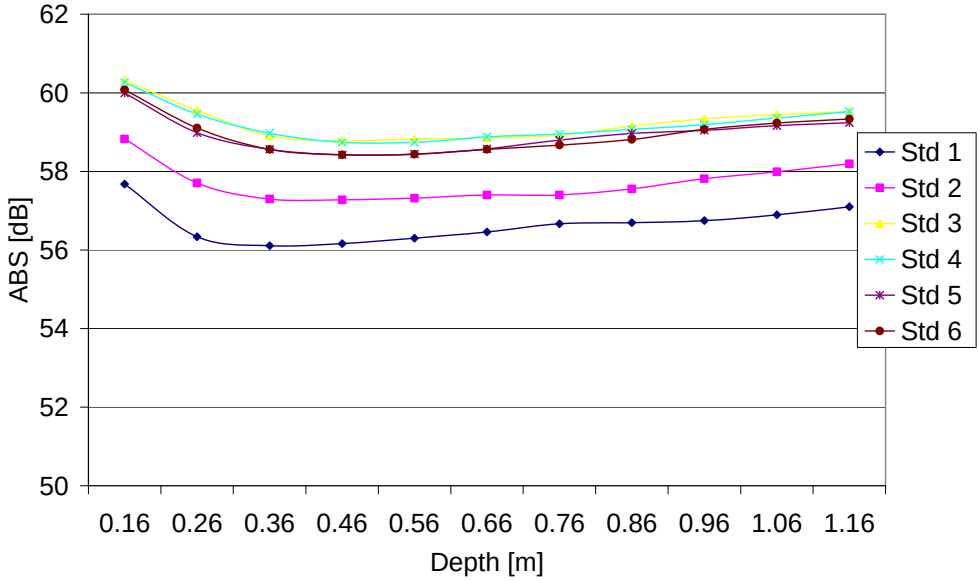

Fig. 6.6 continued

ABS response curves

No-oil control responses were omitted from all ABS response curves (Fig. 6.7) due to the lack of sufficient scattering particles required for valid echo intensity measurements. For all experimental replicates, log-linear relationships between ABS and volume concentration were observed as indicated by the Pearson coefficient (r) values of greater than $r_{critical}$ (α=0.05) = 0.805 (Replicate 1) and 0.729 (Replicates 2 and 3). Despite the log-linearity, response slopes varied appreciably, between 0.11 and 0.27, suggesting the difficultly associated with obtaining valid calibration coefficients for dispersed oil concentration determinations. Response curves for other valid depth bins (data not shown) were similar to respective replicate depth bin 6 responses.

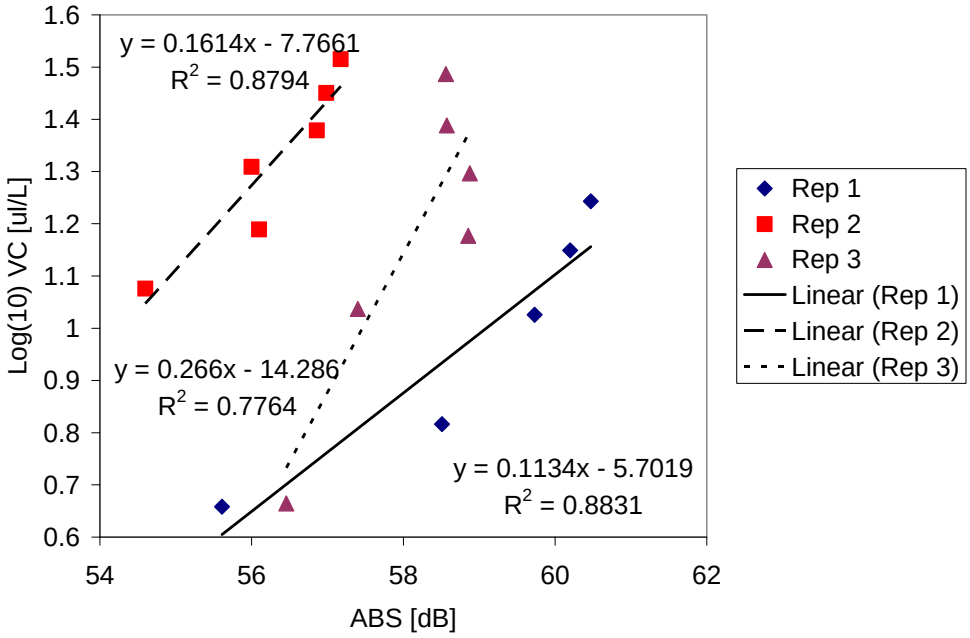

Fig. 6.7 Depth bin 6 ABS responses to dispersed oil Log(10) volume concentration.

The oil-droplet characterization indicated that the droplet size distributions were, for the most part conserved, between replicates, with the exception of the ambient concentration of relatively large particles in Replicate 2 (Fig. 6.4). Assuming that ABS response follows the Raleigh scattering equation (Equation 5.1) would predict that the measured responses would be proportional to theoretical values determined with the particle size distribution. However, when the measured ABS responses from all replicates are combined (no-oil control values omitted) and plotted against the respective Raleigh target strength (TS_R) the relationship is shown to be inversely proportional as indicated by the negative slope (Fig. 6.8). Furthermore, no correlation was indicated between the Rayleigh target strength and measured ABS response as indicated with students T-test (α=0.05) with p=1.45 x 10^{-11}. This suggests that the observed response

variability is not a function of the PSD. ABS measured by the ADCP is directly proportional to the transmit power and transmit length which can vary over time. When possible, ABS should be corrected for variable transmit power and length using instrument-provided data for transmit current, voltage, and transmit length as described by Wall et al. (2006). However, with the StreamPro ADCP, such corrections are not possible as these parameters are not provided in the data output. The primary measure exercised to reduce such variability in the study was the use of a laboratory power supply to alleviate the possibility of variable power associated with operation with the standard battery pack. Finally, the ADCP can determine water velocities once a minimum echo intensity level is achieved, by measuring the Doppler shift which is independent of echo intensity (Personal Communication, Dan Murphy, Teledyne RD Instruments, October 17, 2010). As such, it is not specifically intended to measure echo intensity.

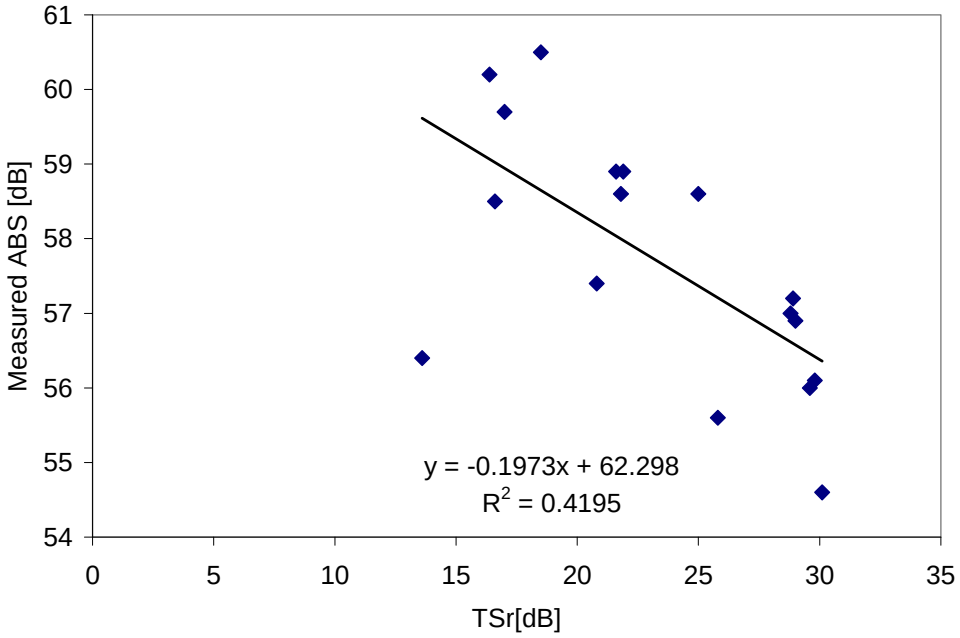

Fig. 6.8 Rayleigh target strength vs measured ABS (depth bin 6) for all experimental conditions and replicates. No-oil control responses omitted.

While the theoretical TS_R does not help explain replicate variability it can be useful to determine potential interferences. Plotting the ABS responses from each replicate separately against the respective TS_R values (Fig. 6.9) allows potential interferences to be evaluated. Only Replicate 3 showed an expected positive relationship between TS_R and measured ABS (Fig. 6.9). Inspection of Replicate 1 (Fig. 6.9, blue diamonds) shows an elevated TS_R at the lowest measured ABS. This data point corresponds to Replicate 1, standard 1 which was characterized with an elevated concentration of droplets at the largest size category = 230 μm (Fig. 6.4A). This observation indicated the presence of a transient (i.e. not present in latter oil droplet standard) scatterer population contributing to the unexpectedly high TS_R value. Similarly, Replicate 2 PSD (Fig. 6.4B) showed elevated concentrations at the upper end

of the size distribution in all experimental conditions (i.e. no-oil control and all dispersed oil standards). Fig. 6.9 also shows a negative relationship between Replicate 2 (red squares) TS_R and the measured ABS. It is important to notice the small absolute difference in maximum and minimum TS_R values determined for Replicate 2. Considering that TS_R is proportional to the 6^{th} power of the droplet radius as defined by Equation 5.1, indicates that that the modeled TS_R is being affected by the relatively high ambient particle load with diameters predominantly greater than 100 µm.

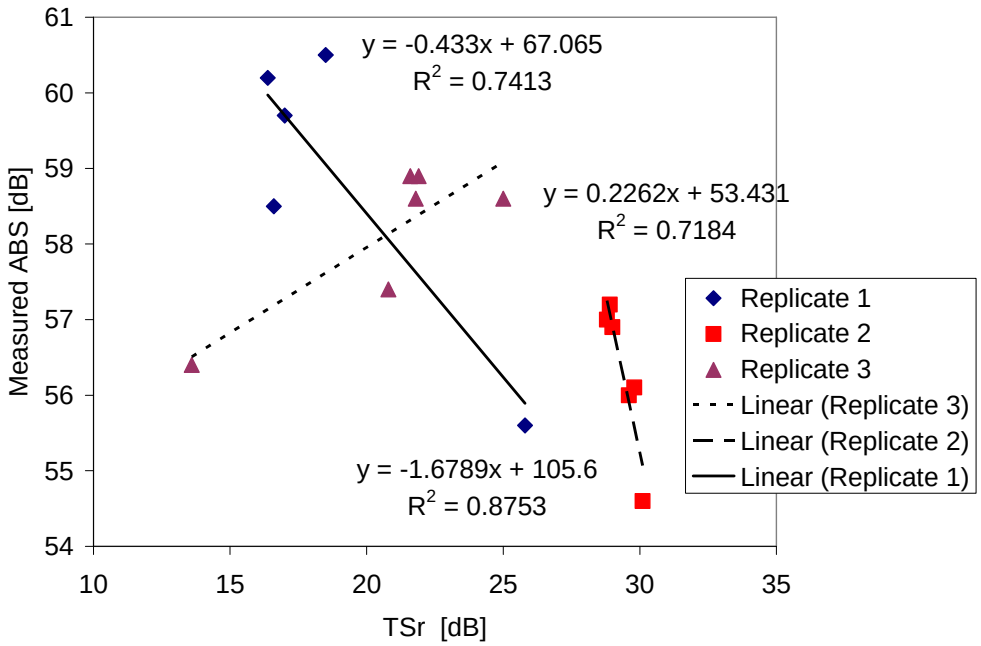

Fig. 6.9 Measured ABS (depth bin 6) vs calculated Rayleigh target strength for each replicate. No-oil control responses omitted.

To evaluate the effect of the ambient particles on the TS_R required that the TS_{Roil} be calculated from the PSD less than <100 µm, where TS_{Roil} is the Raleigh target strength resulting from the oil droplet suspension. Neglecting the PSD>100μm in the TS_{Roil}

calculations was justified by the previous evaluation of Equation 6.6. Plotting TS_{Roil} against the respective measured ABS responses shows positive linear correlations with R^2>0.87 for all three replicates (Fig. 6.10). Considering the ambient particle load to be constant within each replicate, this analysis demonstrates that the observed ABS intensity is changing with respect to variable oil-droplet concentrations. This further implies that this methodology has sufficient sensitivity to detect oil-droplet concentration variations even in the presence of relatively large ambient particles with characteristically elevated TS_R compared to the smaller oil-droplets.

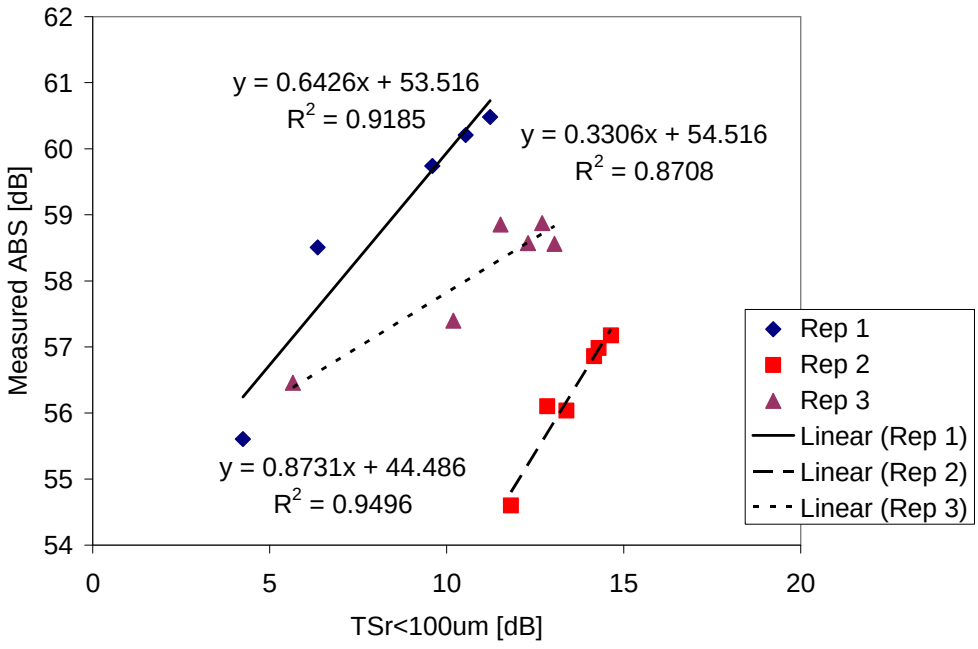

Fig. 6.10 Measured ABS response (depth bin 6) vs TS_{Roil} calculated with PSD < 100μm.

Conclusions

The observed log-linear ABS responses to oil-droplet volume concentration each experimental replicate suggest that ABS is a potentially viable remote sensing tool to

quantitatively and spatially characterize sub-surface dispersed oil plumes. The inability to generate reproducible slopes demonstrates method variability and indicates the difficultly associated with producing meaningful response factors required to make field measurements with any precision. However, the strong linear correlations between the observed ABS response and the TS_{Roil} demonstrate that this methodology has the sensitivity required to detect relative changes in the oil-droplet concentrations in the presence of potentially interfering ambient particles. These findings illustrate ABS intensity as a potentially viable technology for quantitative remote detection of sub-surface oil-droplet suspensions. However, further development is required to improve response reproducibility. Until this goal is achieved, these finding indicate that ABS can be an effective screening tool to remotely locate potential areas with high oil concentrations for more thorough analysis using alternative methods (i.e. fluorescence coupled with an AUV and/or discrete sampling).

CHAPTER VII

SUMMARY AND CONCLUSIONS

Oil spills continue to threaten our coasts and oceans as recently demonstrated in the Deepwater Horizon oil spill. Major concerns raised during this event included the environmental safety and effectiveness of dispersants used to treat the spill on the surface and its unprecedented application at the source 1.5 km below the surface. Addressing these concerns requires that the toxicity of the various components, such as oil, dispersant, and dispersed oil, be well understood. To assess both the potential environmental impact of the incident and effectiveness of the remedial response, the extent and concentration of the resultant dispersed oil plume must be characterized.

The research presented in this dissertation attempted to address these issues. Bioassays were performed to evaluate the acute toxic effects of dispersant, crude oil, and crude oil plus dispersant relative to standard indicator organisms representing potentially impacted environmental compartments including water column, inter-tidal sediments, and sub-tidal sediments. The performance of *in-situ* instruments used to measure dispersed oil was evaluated for the purpose of improving field monitoring protocols used to assess dispersant and *in-situ* burn operations. This evaluation showed that dispersed oil could be measured as a particulate suspension and suggests the basis for alternative detection methods. Acoustic backscatter intensity was studied as a potential surrogate technology to quantify suspended solids (i.e. clay flocs) *in-situ.* Finally, the applicability of acoustic backscatter response to quantify oil-droplet suspensions was evaluated.

The underlining theme connecting these apparently disparate topics is that oil, in particular chemically dispersed oil, exists predominantly as a droplet suspension in aqueous media. This property affects the oil's physical transport to the various environmental compartments and therefore affects its ecological impact in each. Recognizing chemically dispersed oil as a particulate suspension revealed greater insight into its transport and environmental fate and effects. This discovery led to developing the basis for detection methods using the alternative technologies of laser *in-situ* scattering and acoustic backscatter.

A toxicity study was conducted on inter- and sub-tidal sediment samples impacted with oil-only and oil-plus-dispersant suspensions as part of a comprehensive meso-scale fate and effects study. Results from this study showed that dispersant use reduced the accumulation of oil in the inter-tidal zone compared to no dispersant use with a subsequent reduction in the observed toxicity to sediment dwelling amphipods. Similarly, the Microtox sediment elutriate assay demonstrated a significant toxic response only in samples collected from oil-only treatment tanks. Evaluation of both petroleum chemistry and toxicity data suggest that dispersant treatments can reduce oil-accumulation and subsequent toxicity in inter-tidal beach sediments. Evaluation of sub-tidal sediment petroleum chemistry and amphipod toxicity observations demonstrated no correlation. However, amphipods exposed to samples collected from both oil-only and oil-plus-dispersant treatments demonstrated similar toxic effects (i.e. percent mortality and mortality + sub-lethal effects) and were elevated compared no-oil-control exposures. These observations suggest ambient-particle oil-droplet aggregation as a possible

mechanism resulting in the heterogeneous deposition of oil and oil-plus-dispersant in the sub-tidal zone at concentrations sufficient to cause a toxic response.

It is recognized that additional research is warranted to evaluate oil particle aggregation as a potential mechanism for oil deposition on sub-tidal sediments and subsequent ecological impact. Possible improvements to future experimental designs may include the use of sediment traps to quantify sedimentation and sediment bound petroleum hydrocarbons in the sub-tidal zone. Additional monitoring for suspended solids mass concentration and particle size distribution would provide the fundamental parameters required to characterize ambient particle-oil droplet interactions.

The toxicity of dispersant, oil, and oil-plus-dispersant media were compared in a laboratory study using standard water quality indicator macroorganisms (i.e. fish and shrimp) and with Microtox. Macroorganism assays included standard continuous and non-standard declining exposure regimes. The toxicity of media prepared with both fresh oil (i.e. unweathered) and weathered oil were compared. Results from both macroorganism and Microtox assays indicated that dispersant toxicity was negligible compared to the oil and oil-plus-dispersant toxicity. The relative toxicity of weathered-oil-plus-dispersant and weathered-oil-only was found to be similar on a non-volatile hydrocarbon basis when evaluated with both macroorganisms and Microtox. Macroorganism observations demonstrated that declining exposures resulted in reduced toxicity compared to standard continuous exposures. Finally, macroorganism testing with unweathered crude oil showed that soluble aromatic fractions were responsible for the observed toxicity, not the colloidal oil fractions. These results demonstrate the

importance of recognizing dispersed oil as a droplet suspension which affects its bio-availability and subsequent environmental impact.

Several *in-situ* sensors were evaluated for their respective abilities to quantify crude oil suspensions. All *in-situ* fluorescence instruments tested produced linear responses to crude oil suspensions over concentrations ranging up to 4 orders of magnitude (10 – 20,000 ppb), demonstrating their suitability to measure dispersed oil concentrations that have previously been shown to produce toxic responses to marine species in laboratory bioassays. Optical transmittance and volume concentration inferred from optical forward scattering also responded linearly to the crude oil suspensions at concentrations ranging from 1,000-30,000 ppb. The significance of this observation is demonstrated in the applicability of surrogate detection methods that measure dispersed oil as a droplet suspension, as opposed to relying on analytical petroleum chemistry.

Acoustic backscatter was evaluated as a surrogate method to quantify suspended sediments in aqueous environments. Log-linear acoustic backscatter responses to suspended solids mass and volume concentration over variable particle size distributions were observed. However, ABS responses to volume concentration, measured with a LISST-100, showed higher linear correlation coefficients. Agreement between measured suspended solids concentration and estimates determined with ABS-volume concentration regressions was better than estimates based on ABS-mass concentration regressions. The correlation between acoustic backscatter and volume concentration is due to the dependence of both measures on the particle size distribution as defined by the

Rayleigh and Mie assumptions, respectively. Thus, it was shown that acoustic backscatter, corrected for beam spreading and water absorption attenuation, can provide reasonable suspended solids volume concentration estimates throughout the water column within the acoustic range of the specific instrument (ADCP) over a range of particle sizes.

The use of acoustic backscatter intensity was evaluated as a potential method to quantify sub-surface oil droplet suspensions. This study demonstrated log linear acoustic backscatter intensity responses to oil droplet concentrations. However, generating reproducible response factors indicated the difficulty associated with generating valid calibrations. Evaluation of droplet size distribution data, theoretical acoustic backscatter intensity, and measured acoustic backscatter intensity provided insight with respect to method sensitivity. Despite the inability to generate reproducible response factors, it was shown that ABS can be used to determine relative oil droplet concentrations in the presence of interfering ambient particles.

It is recognized that measuring suspended solids and/or dispersed oil droplets using the acoustic methods developed in this work lacks the specificity inherent in conventional analytical methods and is subject to errors associated with variable particle characteristics (i.e. particle density, geometry, compressibility, interstitial water). However, acoustic methods are well suited for *in-situ* and remote detection of episodic events as part of continuous or event based monitoring operations requiring intensive sampling at high temporal and spatial resolutions. Such monitoring programs are often limited by the unit data cost. Developing surrogate detection methods, including

acoustic suspended solids/droplet measurements, effectively extends the capability of existing sensor infrastructure thereby, reducing operating costs allowing establishment and operation of monitoring networks.

This research showed that acoustic methods can provide reasonable suspended solids/droplet concentration measurement under controlled laboratory settings. However, more work is needed to demonstrate the technology in field applications characterized by dynamic environmental conditions. Additionally, implementation and/or development of an acoustic backscatter instrument intended to measure echo intensity, as opposed to Doppler shift, should also be investigated.

REFERENCES

Abel, P. D. (1974). Toxicity of synthetic detergents to fish and aquatic invertebrates. *Journal of Fish Biology*, *6*, 279 – 298.

Adams, E. E., & Socolofsky, S. A. (2005). Review of: Deep oil spill modeling activity supported by the DeepSpill JIP and Offshore Operators Committee. http://www.boemre .gov/tarprojects/377/Adams%20Review%204.pdf. Accessed 5 January 2010.

Agrawal, Y. C., & Pottsmith, H. C. (1994). Laser diffraction particle sizing in STRESS. *Continental Shelf Research*, *14*(10/11), 1101-1121.

Agrawal, Y. C., Whitmire, A., Mikkelsen, O. A., & Pottsmith, H. C. (2008). Light scattering by random shaped particles and consequences on measuring suspended sediments by laser diffraction. *Journal of Geophysical Research*, doi: 10.1029/ 2007JC004403.

Anderson, J. W., Neff, J. M., Cox, B. A., Tatem, H. E., & Hightower, G. M. (1974). Characteristics of dispersions and water-soluble extracts of crude and refined oils and their toxicity to estuarine crustaceans and fish. *Marine Biology, 27*, 75 – 88.

ASTM (American Society for Testing and Materials) (1997). Standard guide for conducting 10-day static sediment toxicity tests with marine and estuarine amphipods. E-1367-92. In *Annual book of ASTM standards, 11.05* (pp. 1161-1186). Philadelphia, PA: American Society for Testing and Materials.

Atkins, P. W. (1990). *Physical chemistry*. New York, NY: W.H. Freeman and Company.

Banerjee, S. (1984). Solubility of organic mixtures in water. *Environmental Science and Technology*, *18*, 587-591.

Barataria-Terrebonne National Estuary Program (2010) Oil spill cleanup in a marsh environment. http://www.btnep.org/client_files/editor_files/Spill_Cleanup_ in_Marsh.pdf. Accessed 15 November 2010.

Bauguss, J. L. (1997). *Accelerated solvent extraction of petroleum contaminated sediments.* M.S. Thesis. Texas A&M University. College Station.

Bent, C., Gray, J., Smith, K., & Glysson, G. (2003). A synopsis of technical issues for monitoring sediment in highway and urban runoff: National highway runoff data and methodology synthesis. USGS Open-File Report 00-497. http://ma.water. usgs.gov/fhwa/products/ofr00497.pdf. Accessed 16 December 2010.

Bizzell, C., Townsend, R. T., Bonner, J. S., & Autenrieth, R. L. (1999). Shoreline cleaner evaluation on a petroleum impacted wetland. In A. Leeson and B. Alleman (Eds.), *Fifth international in-situ and on-site bioremediation symposium, phytoremediation and innovative strategies for specialized remedial applications* (pp. 57-62). San Diego, CA: Battelle Press.

Boehm, P. D., & Quinn, J. G. (1976). The effect of dissolved organic matter in sea water on the uptake of mixed individual hydrocarbons and number 2 fuel oil by a marine filter-feeding bivalve (*Mercenaria mercenaria*). *Estuarine Coastal Marine Science*, *4*, 93-105.

Bonner, J. S., Kelly, F. J., Michaud, P. R., Page, C. A., Perez, J., Fuller, C., Ojo, T., & Sterling, M. (2003a). Sensing the coastal environment, building the European capacity in operational oceanography. In H. Dahlin, N.C. Flemming, N. Nittis, and E. Petersson (Eds.), *Building the European capacity in operational oceanography: Proceedings of the third international conference on EuroGOOS* (pp. 353-541). San Diego, CA: Elsevier.

Bonner, J., Page, C., & Fuller, C. (2003b). Meso-scale testing and development of test procedures to maintain mass balance. *Marine Pollution Bulletin*, *47*, 406-414.

Booksh, K. S., Muroski, A. R., & Myrick, M. L. (1996). Single-measurement excitation/emission matrix spectrofluorometer for determination of hydrocarbons in ocean water. 2. Calibration and quantitation of naphthalene and styrene, *Analytical Chemistry*, *68*, 3539-3544.

Bragin, G., Clark, J., & Pace, C. (1994). *Comparison of physically and chemically dispersed crude oil toxicity to both regional and national test species under continuous and spiked exposure scenarios.* Marine Spill Response Corporation, MSRC Technical Report Series 94-015, Washington, DC.

Bragin, G., & Clark, J. (1995). *Chemically dispersed crude oil: Toxicity to regional and national test species under constant and spiked exposures.* Marine Spill Response Corporation, MSRC Technical Report Series 95-023, Washington, DC.

Bragin, G., Coelho, G., Febbo, E., Clark, J., & Aurand, D. (1999). Coastal Oilspill Simulation System comparison of oil and chemically dispersed oil released in near-shore environments : biological effects. In *Proceedings of the 22nd Arctic and Marine Oilspill Program (AMOP) technical seminar, Calgary, AB, Canada, 1999* (pp. 671-683). Environment Canada.

Bryce, S., Larcombe, P., & Ridd, P. V. (1998). The relative importance of landward-directed tidal sediment transport versus freshwater flood events in the Normanby River estuary, Cape York Peninsula, Australia. *Marine Geology*, *149*, 55-78.

Bugden, J., Yeung, C., Kepkay, P., & Lee, K. (2008). Application of ultraviolet fluorometry and excitation-emission matrix spectroscopy (EEMS) to fingerprint oil and chemically dispersed oil in seawater. *Marine Pollution Bulletin, 56*, 677-685.

Cabioch, L., Dauvin, J., & Gentil, F. (1978). Preliminary observations on pollution of the sea bed and disturbance of sub-littoral communities in northern Brittany by oil from the Amoco Cadiz. *Marine Pollution Bulletin*, *9*(11), 303-307.

Camilli, R., Reddy, C. M., Yoerger, D. R., Van Mooy, B. A. S., Jakuba, M. V., Kinsey, J. C., McIntyre, C. P., Sylva, S. P., & Maloney, J. V. (2010) Tracking hydrocarbon plume transport and biodegradation at Deepwater Horizon. *ScienceExpress*, doi:10.126/science.1195223.

Camp, T. R., & Stein, P. C. (1943). Velocity gradients in laboratory and full-scale systems. *Journal Boston Society of Civil Engineering ASCE, 30*, 219-237.

Chen, R. F., & Bada, J. L (1992). The fluorescence of dissolved organic matter in seawater. *Marine Chemistry*, *37*, 191-221.

Christensen, R. (1990), *Log-linear models*. New York, NY: Springer.

Coble, G. C. (1996). Characterization of marine and terrestrial DOM in seawater using excitation-emission matrix spectroscopy. *Marine Chemistry, 51*, 325-346.

Cohen, A., Gagnon, M., & Nugegoda, D. (2003). Biliary PAH metabolite elimination in Australian bass, *Macquaria novemaculeata* following exposure to Bass Strait crude oil and chemically dispersed oil. *Bulletin of Environmental Contaminants and Toxicology*, *70*, 394-400.

Couillard, C. M., Lee, K., Legare, B., & King, T. L. (2005). Effect of dispersants on the composition of the water-accommodated fraction of crude oil and its toxicity to larval marine fish, *Environmental Toxicology and Chemistry*, *24*(6), 1496-1504.

Cracknell, A. P. (1999). Remote sensing techniques in estuaries and coastal zones – An update. *International Journal of Remote Sensing*, *19*(3), 485 -496.

Crosset, K. M., Culliton, T. J., Wiley, P. C., & Goodspeed, T. R. (2004). Population trends along the coastal United States: 1980-2008. NOAA coastal trends report series. National Oceanic and Atmospheric Administration.http://oceanservice.noaa.gov/programs/mb/pdfs/coastal_pop_trends_complete.pdf. Accessed 5 March 2010.

Deines, K. L. (1999). Backscatter estimation using broadband acoustic Doppler current profilers. http://www.commtec.com/Library/Technical_Papers/RDI/echopaper.pdf. Accessed 22 February 2011.

De Marco, S., Kelly, F., Zhang, J., & Guinasso, N., (1995). Directional wave spectra on the Louisiana-Texas shelf during Hurricane Andrew. *Journal of Coastal Research*, *Special Issue 21*, 217-233.

De Nevers, N. (1991). *Fluid mechanics for chemical engineers*. Boston, MA: McGraw-Hill.

Downing, A., Thorne, P. D., & Vincent, C. E. (1995). Backscattering from a suspension in the near field of a piston transducer. *Journal of the Acoustical Society of America*, *97*(3), 1614-1620.

Edwards, K. R., Lepo, J. E., & Lewis, M. A. (2003). Toxicity comparison of biosurfactants and synthetic surfactants used in oil spill remediation of two estuarine species. *Marine Pollution Bulletin*, *46*, 1309-1316.

Etkin, D. (1999). *Oil spill dispersants: From technology to policy*. Arlington, MA: Cutter Information.

Finney, D. (1971). *Probit analysis.* London, UK: Cambridge University Press.

Flammer, G. H. (1962). *Ultrasonic measurement of suspended sediment.* US Geological Survey, Bulletin 1141-1, Washington, DC: U.S. Government Printing Office.

Fuller, C., Bonner, J., McDonald. T., Bragin, G., Clark, J., Aurand, D., Hernandez, A., & Ernest, A. (1999). Comparative toxicity of simulated beach sediments impacted with both whole and chemical dispersions of weathered Arabian medium crude oil. In *Proceedings of the 22nd Arctic and Marine Oilspill Program (AMOP) technical seminar, Calgary, AB, Canada, 1999* (pp. 659-670). Environment Canada.

Fuller, C., Bonner, J., Page, C., Ernest, A., McDonald, T., & McDonald, S. (2004). Comparative toxicity of oil, dispersant, and oil plus dispersant to several marine species. *Environmental Toxicology and Chemistry*, *23*(12), 2941-2949.

Fuller, C., Bonner, J., Kelly, F., Page, C., & Ojo, T. (2005). Real time geo-referenced detection of dispersed oil plumes. *In Proceedings of the 2005 International Oil Spill Conference (IOSC).* http://www.iosc.org/papers/IOSC%202005%20a356.pdf. Accessed 22 February 2011.

Gartner, J. W. (2004). Estimating suspended solids concentrations from backscatter intensity measured by acoustic Doppler current profiler in San Francisco Bay, California. *Marine Geology*, *211*, 169-187.

Garton, L. S., Bonner, J. S., Ernest, A. N., & Autenrieth, R. L. (1996). Fate and transport of PCBs at the New Bedford Harbor Superfund site. *Environmental Toxicology and Chemistry*, *15*(5), 736-745.

Gearing, P. J., Gearing, J. N., Pruell, R. J., Wade, T. L., & Quinn, J. G. (1980). Partitioning of No. 2 fuel oil in controlled estuarine ecosystems. Sediments and suspended particulate matter. *Environmental Science and Technology*, *14*(9), 1129-1136.

Gibbs, R. (2010). The response to the oil spill: 5/1/10. The White House Blog. http:// www.whitehouse.gov/blog/2010/05/01/response-oil-spill-5110. Accessed 28 June 2010.

Gray, J. R. (2002). The need of sediment surrogate technologies to monitor fluvial-sediment transport. In *Proceedings of the federal interagency sedimentation workshop on turbidity and other sediment surrogates. U. S. Geological Survey*. http://water.usgs. gov/osw/techniques/TSS/gray/pdf. Accessed 16 December 2010.

Gray, J .R., & Gartner, J. W. (2009). Technological advances in suspended-sediment surrogate monitoring, *Water Resources Research*, *45*, W00D29, doi:10.1029/2008 WR007063.

Guilbault, G. G. (Ed.) (1990). *Practical fluorescence.* New York, NY: Marcel Dekker, Inc.

Hall, W. S., Patoczka, J. B., Mirenda, R. J., Porter, B. A., & Miller, E. (1989). Acute toxicity of industrial surfactants to *Mysidopsis bahia. Archives of Environmental Contaminants and Toxicology, 18*, 765 – 772.

Hamilton, L. J., Shi, Z., & Zhang, S. Y. (1998). Acoustic backscatter measurements of estuarine suspended cohesive sediment concentration profiles. *Journal of Coastal Research, 14*(4), 1213-1124.

Hargrave, B. T., & Phillips, G. A. (1975). Estimates of oil in aquatic sediments by fluorescence spectroscopy. *Environmental Pollution*, *8*, 193-215.

Harris, B. C., Bonner, J. S., & Autenrieth, R. L. (1999). Nutrient dynamics in marsh sediments contaminated by an oil spill following a flood. *Environmental Technology*, *20*, 795-810.

Harris, B. C., LaRiviere, D. J., Autenrieth, R. L., Dimitriou,-Christidis, P., McDonald, T. J., & Bonner, J. S. (2001). Assessment of petroleum biodegradation potential with alternative electron acceptors. In A. Leeson, E. Foote, K. Banks, and V. Magar (Eds.), *Proceedings of the sixth international in-situ and on-site bioremediation symposium, phytoremediation and wetlands for remediation of contaminated areas.* (pp. 17-24).

http://serf.clarkson.edu/Publications/Peerreviewed/Harris%20et%20al%20Sixth%20Intl%20In%20Situ%202001.pdf. Accessed 22 February 2011.

Harris, B. C. Bonner, J. S., McDonald, T. J., Fuller, C. B., Page, C. A., Dimitriou-Christidis, P., Sterling, M. C., & Autenrieth, R. L. (2002a). Nutrient effects of the biodegration rates of chemically-dispersed crude oil. In *Proceedings of the 25th Arctic and Marine Oilspill Program (AMOP) technical seminar, Calgary, AB, Canada, 2002* (pp. 877-893). Environment Canada.

Harris, B. C. Bonner, J. S., McDonald, T. J., Fuller, C. B., & Page, C. A. Dimitriou-Christidis, P., Sterling, M.C., Autenrieth, R.L. (2002b). Bioavailability of chemically dispersed crude oil. In *Proceedings of the 25th Arctic and Marine Oilspill Program (AMOP) technical seminar, Calgary, AB, Canada, 2002* (pp. 895-905). Environment Canada.

Hazen, T., Dubinsky, E., DeSantix, T., Andersen, G., Piceno, Y., Singh, N., Jansson, J., Probst, A., Borglin, S., Fortney, J., Stringfellow, W., Bill, M., Conrad, M., Tom, L., Chavarria, K., Alusi, T., Lamendella, R., Joyner, D., Spier, C., Baelum, J., Auer, M., Zemla, M., Charkraborty, R., Sonnenthal, E., D'haeseleer, T., Holman, H., Osman, S., Lu, A., Van Nostrand, J., Deng, Y., Zhou, J., & Mason, O. (2010). Deep-sea oil plume enriches indigenous oil-degrading bacteria, *Sciencexpress*, doi:10.1126/science.1195979.

Hirsch, R., & Costa, J. (2004). U.S. Stream flow measurement and data dissemination improve. *EOS Transactions, American Geophysical Union, 85*(20), 197-203.

Hoitink, A. J. F., & Hoekstra, P. (2005). Observations of suspended sediment from ADCP and OBS measurements in a mud-dominated environment. *Coastal Engineering*, *52*, 103-118.

Howard, H., & Meylan, W. M. (1997). *Handbook of physical properties of organic chemicals*. Boca Raton, FL: CRC.

Islam, M. S., Bonner, J. S., & Page, C. A. (2010a). A fixed robotic profiler system to sense real-time episodic pulses in Corpus Christi Bay. *Environmental Engineering Science*, *27*(5), 431-440. doi:10:1089/ees.2010.0006.

Islam, M. S., Bonner, J., Ojo, T., & Page, C. (2011a). A mobile monitoring system to understand the processes controlling episodic events in Corpus Christi Bay. *Environmental Monitoring and Assessment*, *175,* 349-366. doi:10.1007/s10661-010-1536-y.

Islam, M. S., Bonner, J. S., Page, C., & Ojo, T. O. (2011b). Integrated real-time monitoring system to investigate the hypoxia in a shallow wind driven bay. E*nvironmental Monitoring and Assessment*, *172,* 33-50. doi:10.1007/s10661-010-1316-8.

Johnson, R. (1984). *Elementary statistics*. Boston, MA: PWS Publishers.

Kanga, S. A., Bonner, J. S., Page, C. A., Mills, M. A., & Autenrieth, R. L. (1997). Solubilization of naphthalene and methyl-substituted naphthalenes from crude oil using biosurfactants. *Environmental Science and Technology, 31*, 556-561.

Kepkay, P. E., Bugden, J. B. C., Lee, K., & Stoffyn-Egli, P. (2002). Application of ultraviolet fluorescence spectroscopy to monitor oil-mineral aggregate formation. *Spill Science and Technology Bulletin*, *8*(1)*,* 101-108.

Kepkay, P. E., Yeung, C. W., Bugden, B. C., Li, Z., & Lee, K., (2008). Ultraviolet fluorescence spectroscopy (UVFS): A new means of determining the effect of chemical dispersants on oil spills. In *International Oil Spill Conference (IOSC)* (pp. 639-643). Washington DC: American Petroleum Institute.

Khan, R. A., & Payne, J. F. (2005). Influence of a crude oil dispersant, Corexit 9527, and dispersed oil on Capelin (*Mallotus villosus*), Atlantic Cod (*Gadus morhua*), Longhorn Sculpin (*Myoxocephalus octodecemspinosus*), and Cunner (*Tautogolabrus adspersus*). *Bulletin of Environmental Contamination and Toxicology*, *75*, 50-56.

Kitchen, R., Bonner, J., Autenrieth, R., Donnelly, K., & Ernest, A. (1997). Introducing COSS: A new and unique oil spill research facility. In *Proceedings of the 20th Arctic and Marine Oilspill Program (AMOP) technical seminar, Vancouver, BC, Canada, 1997* (pp. 1327-1335). Environment Canada.

Kuwabara, J. S., Chang, C. C. Y., Cloern, J. E., Fries, T. L., Davis, J. A., & Luoma, S. N. (1989). Trace metal associations in the water column of South San Francisco Bay, California. *Estuarine*, *Coastal and Shelf Science*, *28*, 307-325.

Lakowicz, J. R. (1999). *Principles of fluorescence spectroscopy*. New York, NY: Kluwer Academic/Plenum Publishers.

Law, R. J., Marchand, M., Dahlmann, G., & Fileman, T. W. (1987). Results of two bilateral comparisons of the determination of hydrocarbon concentrations in coastal seawater by fluorescence spectroscopy. *Marine Pollution Bulletin*, *18*(9), 486-489.

Lee, D., Bonner, J., Garton, L., Ernest, N., & Autenrieth, R. (2000). Modeling coagulation kinetics incorporating fractal theories: a fractal rectilinear approach. *Water Research, 34*(7)*,* 1987-2000.

Le Floch, S., Guyomarch, J., Merlin, F. X., Stoffyn-Egli, P., Dixon, J., & Lee, K. (2002). The influence of salinity on oil-mineral aggregate formation. *Spill Science and Technology*, *8*(1), 65-71.

Li, Z., Lee, K., King, T., Boufadel, M., & Venosa, A. D. (2008). Assessment of chemical dispersant effectiveness in a wave tank under regular non-breaking and breaking wave conditions. *Marine Pollution Bulletin, 56*, 903-912.

Liu, B., Romaire, R. P., Delaune, R. D., & Lindau, C. W. (2006). Field investigation on the toxicity of Alaska North Slope Crude oil (ANSC) and dispersed ANSC crude to gulf killifish, eastern oyster, and white shrimp. *Chemosphere*, *62*, 520-526.

Long, S. M., & Holdway, D. A. (2002). Acute toxicity of crude and dispersed oil to *Octopus pallidus* (Hoyle, 1885) hatchlings. *Water Research*, *36*, 2769-2776.

Lubchenco, J. (2010). Transcript- NOAA Administrator's Keynote Address on NOAA Science and the Gulf Oil Spill. http://www.restorethegulf.gov/release/2010/10/01 /transcript-noaa-administrator%E2%80%99s-keynote-address-noaa-science-and-gulf-oil-spill. Accessed 18 November 2010.

Lunel, T., Swannell, R., Rusin, J., Wood, P., Baily, N., Halliwell, C., Davies, L., Sommerville, M., Dobie, A., Mitchell, D., McDonagh, M., & Lee, K. (1995). Monitoring the effectiveness of response operations during the *Sea Empress* Incident: A key component of the successful counter-pollution response. *Spill Science and Technology Bulletin*, *2*(2/3), 99-112.

Lynch, J. F., Irish, J. D., Sherwood, C. R., & Agrawal, Y. C. (1994). Determining suspended sediment particle size information from acoustical and optical backscatter measurements. *Continental Shelf Research*, *14*(10/11), 1139-1165.

MacNaughton, S. J., Swannell, R., Daniel, F., & Bristow, L. (2003). Biodegradation of dispersed Forties crude and Alaskan North Slope oils in microcosms under simulated marine conditions. *Spill Science and Technology Bulletin*, *8*(2), 179-186.

Marchetti, R. (1965). The toxicity of nonyl phenol ethoxylate to the developmental stages of the rainbow trout, *Salmo gaidnerii Richardson. Annals of Applied Biology*, *5*, 425-430.

Mearns, A., Doe, K., Fisher, W., Hoff, R., Lee, K., Siran, R., Mueller, C., & Venosa, A. (1995). Toxicity trends during an oil spill bioremediation experiment on a sandy shoreline in Delaware, USA. In *Proceedings of the 18th Arctic and Marine Oilspill Program (AMOP) technical seminar, Edmonton, AB, Canada, 1995* (pp. 1133-1145). Environment Canada.

Merlin, F. X. (2008). French sea trials on chemical dispersion: DEPOL 04 & 05. In Davidson, W.F., & Lee, K., Cogswell (Eds.), *Oil spill response: a global perspective* (pp. 119-140). Netherlands: Springer, doi:10.1007/978-1-4020-8565-17.

Microbics (1992). *Microtox manual: A toxicity testing handbook.* Carlsbad, CA: Microbics.

Mills, M., McDonald, T., Bonner, J., Simon, M., & Autenrieth, R. (1999). Method for quantifying the fate of petroleum in the environment. *Chemosphere*, *39*(14), 2563-2582.

Mills, M. A., Bonner, J. S., McDonald, T. J., Page, C. A., & Autenrieth, R. L. (2003). Intrinsic bioremediation of a petroleum-impacted wetland. *Marine Pollution Bulletin*, *46,* 887-899.

Mills, M. A., Bonner, J. S., Page, C. A., & Autenrieth, R. L. (2004). Evaluation of bioremediation strategies of a controlled oil release in a wetland. *Marine Pollution Bulletin*, *49*, 425-435.

MMS (Minerals Management Service) (2008). *Deepwater Gulf of Mexico 2008: America's offshore energy future.* U.S. Department of the Interior Minerals Management Service Gulf of Mexico OCS Region, OCS Report MMS 2008-013, New Orleans, LA.

Montagna, P., & Kalke, R. (1992). The effect of freshwater inflow on meiofaunal and macrofaunal populations in the Guadalupe and Nueces estuaries, Texas. *Estuaries, 15*, 307-326.

Montgomery, J., Harmon, T., Kaiser, W., Sanderson, A., Haas, C., Hooper, R., Minsker, B., Schnoor, J., Clesceri, N., Graham., W., & Brezonik, P. (2007). The WATERS network: An integrated environmental observatory network for water research. *Environmental Science and Technology*, *41*(19), 6642-6647.

Mueller, D. C., Bonner, J. S., McDonald, S. J., & Autenrieth, R. L. (1999). Acute toxicity of estuarine wetland sediments contaminated by petroleum. *Environmental Technology, 20*, 875-882.

Mueller, D. C., Bonner, J. S., McDonald, S. J., Autenrieth, R. L., Donnelly, K. C., Lee, K., Doe, K., & Anderson, J. (2003). The use of toxicity bioassays to monitor the recovery of oiled wetland sediments. *Environmental Toxicology and Chemistry*, *22*(9), 1945-1955.

Nalco (2005). Material Safety Data Sheet (MSDS), Corexit 9500. http://www.lmrk.org /corexit_9500_uscueg.539287.pdf. Accessed 12 December 2010.

Nalco (2010). Corexit ingredients. http://www.nalco.com/applications /4297.htm. Accessed 15 December 2010.

Nicolau, B., & Nunez, A. (2005). Coastal Bend Bays and Estuaries Program Regional Coastal Assessment Program (RCAP) RCAP 2002. Annual Report, Publication CBBEP-51, Project Number-0202, Sept. 2005 (p. 198). http://www.cbbep.org/publications /virtuallibrary/2008table/0202.pdf. Accessed 15 November 2010.

Nikora, V., Aberle, J., & Green, M. (2004). Sediment flocs: Settling velocity, flocculation factor, and optical backscatter. *Journal of Hydraulic Engineering*, *130*(10), 1043-1047.

NRC (2003). *Oil in the sea: inputs, fates, and effects*. Washington, DC: National Academies Press.

NRC (2005). *Oil spill dispersants efficacy and effects*. Washington, DC: National Academies Press.

NOAA (National Oceanic and Atmospheric Administration) (2010a). Integrated Ocean Observing System (IOOS). http://www.ioos.gov/about/basics.html. Accessed 12 December 2010.

NOAA (National Oceanic and Atmospheric Administration) (2010b). NOAA reopens more and 5,000 square miles of closed Gulf fishing area. http://www. noaanews.noaa.gov/stories2010/20100810_fishreopening.html. Accessed 7 September 2010.

Ojo, T. O. Bonner, J. S., & Page, C. (2006a). Observations of shear-augmented diffusion processes and evaluation of effective diffusivity from current measurements in Corpus Christi Bay. *Continental Shelf Research*, *26,* 788-803.

Ojo, T. O. Bonner, J. S., & Page, C. (2006b). Studies on turbulent diffusion processes and evaluation of diffusivity values from hydrodynamic observations in Corpus Christi Bay. *Continental Shelf Research, 26,* 2629-2644.

Ojo, T. O. Bonner, J. S., & Page, C. (2007a). A rapid deployment Integrated Environmental and Oceanographic Assessment System (IEOAS) for coastal waters: Design concepts and field implementation. *Environmental Engineering Science, 24*, 160-171. doi: 10.1089/ees.2006.0036.

Ojo, T. O., Bonner, J. S., & Page, C. (2007b). Simulation of constituent transport using a reduced 3D constituent transport model (CTM) driven by HFRadar: Model application and error analysis. *Environmental Modeling and Software*, *22*, 488-501.

OMLC (2007). Benzene. http://omlc.ogi.edu/spectra/Photochem CAD/html/benzene .html. Accessed 15 November 2010.

Orr, M., Haury, L., Wiebe, P., & Brisco, M. (2000). Backscatter of high-frequency (200 kHz) acoustic wavefields from ocean turbulence. *Journal of the Acoustical Society of America*, *108*(4), 1595-1601.

Pace, C. B., Clark ,J. R., & Bragin, G. E. (1995). Comparing crude oil toxicity under standard and environmentally realistic exposures. In *1995 International Oil Spill Conference.* http://www.iosc.org/papers/00327.pdf. Accessed 22 February 2011.

Page, C., Sumner, P, Autenrieth, R., Bonner, J., & McDonald, T. (1999). Materials balance on a chemically-dispersed oil and a whole oil exposed to and experimental beach front. In *Proceedings of the 22nd Arctic and Marine Oil Spill Program (AMOP) technical seminar, Calgary, AB, Canada* (pp. 645-658). Environment Canada.

Page, C. Bonner, J. S., Sumner, P. L., McDonald, T. J., Autenrieth, R. L., & Fuller, C. B. (2000a). Behavior of a chemically-dispersed oil and a whole oil on a near-shore environment. *Water Research*, *34*(9), 2507-2516.

Page, C. A., Bonner, J. S., Sumner, P. L., & Autenrieth, R. L. (2000b). Solubility of petroleum hydrocarbons in oil/water systems. *Marine Chemistry*, *70*, 79-87.

Page, C. A., Bonner, J. S., McDonald, T. J., & Autenrieth, R. L. (2002a). Behavior of chemically dispersed oil in a wetland environment. *Water Research*, *36*(15), 3821-3833.

Page, C., Bonner, J., Fuller, C., & Sterling, M. (2002b). Dispersant effectiveness in a simulated shallow embayment. In *Proceedings, 25th Arctic and Marine Oilspill Program (AMOP) technical seminar, Calgary, AB, Canada* (pp. 721-733). Environment, Canada.

Patra, D., & Mishra, A. (2002). Total synchronous fluorescence scan spectra of petroleum products. *Analytical and Bioanalytical Chemistry, 373*, 304-309. doi: 10.1007/s00216-002-1330-y.

Price, W. W., Heard, R. W., & Stuck, L. (1994). Observations on the genus *Mysidopsis Sars.* 1564 with the designation of a new genus, *Americamysis,* and descriptions of *Americamysis alleni* and *A. stuck* (Pericardia:Mysidacea:Mysidae), from the Gulf of Mexico. *Proceedings of Biological Society Washington*, *107*, 680-698.

Ramachandran, S .D., Hodson, P. V., Khan, C. W., & Lee, K. (2004). Oil dispersant increases PAH uptake by fish exposed to crude oil. *Ecotoxicology and Environmental Safety*, *59*, 300-308.

RD Instruments (1996). *Acoustic Doppler current profiler, principles of operation, a practical primer.* San Diego, CA: RD Instruments.

RD Instruments (2006). *StreamPro ADCP operation manual*. *P/N 95B-6003-00.* Poway, CA: RD Instruments.

Reichel, G., & Nachtnebel, H.P. (1994). Suspended sediment monitoring in a fluvial environment: advantages and limitations applying an acoustic Doppler current profiler. *Water Research*, *28*(4), 751-761.

Rodriguez, J. J., Garcia, J. J., Suarez, M. M. B., & Martin-Lazaro, A. B. (1993). Analysis of mixtures of polycyclic aromatic hydrocarbons in sea-water by synchronous fluorescence spectrometry in organized media. *Analyst*, *118*, 917-921.

RRT-6 (2001). FOSC dispersant pre-approval guidelines and checklist. US EPA Region-VI. http://www.losco.state.la.us/pdf_docs/RRT6_Dispersant_Preapproval_2001.pdf. Accessed 7 April 2011.

RRT-6 (2005). Nearshore Environment Dispersant Expedite Approval Process and Checklist. US EPA Region-VI. http://www.losco.state.la.us/pdf_docs/RRT6_Nearshore_Dispersant_EAP_031605.pdf. Accessed 5 January 2011.

SAS/STAT®. (1989). *User's guide.* Cary, NC: SAS Institute, Inc.

Scarlett, A., Galloway, T. S., Canty, M., Smith, E. L, Nilsson, J., & Rowland, S. J. (2005). Comparative toxicity of two oil dispersants, Superdispersant-25 and Corexit 9527, to a range of coastal species. *Environmental Toxicology and Chemistry*, *24*(5), 1219-1227.

Schulkin, M., & Marsh, H. W. (1962). Sound absorption in sea water. *Journal of the Acoustical Society of America*, *32*(6), 864.

Simon, M., Bonner, J., McDonald, T., & Autenrieth, R. (1999). Bioaugmentation for the enhanced bioremediation for petroleum in a wetland. *Polycyclic Aromatic Compounds, 14 & 15,* 231-239.

Simon, M., Bonner, J., Page, C., Townsend, R., Mueller, D., Fuller, C., & Autenrieth, R. (2004). Evaluation of two commercial bioaugmentation products for enhanced removal of petroleum from a wetland. *Ecological Engineering, 22*, 263-277.

Simpson, M. (2001). *Discharge measurements using a broad-band Acoustic Doppler Current Profiler.* Open-File Rep. 01-01. Washington, DC: U.S. Government Printing Office.

Singer, M. M., Smalheer, D.L.,Tjeerdema, R.S., & Martin, M. (1991). Effects of spiked exposure to an oil dispersant on the early life stages of four marine species. *Environmental Toxicology and Chemistry*, *10*, 1367 – 1374.

Singer, M., George, S., Benner, D., Jacobson, S., Tjeerdema, R., & Sowby, M. (1993). Comparative toxicity of two oil dispersants to the early life stages of two marine species. *Environmental Toxicology and Chemistry, 12*, 1855-1863.

Skidmore, J. F. (1970). Respiration and osmoregulation in rainbow trout with gills damaged by zinc sulphate. *Journal Experimental Biology*, *52*, 481-494.

Smith, S., Greenaway, S., Apeti, D., Mayer, L., Weber, T. C., De Robertis, A., Wright, D., Blankenship, M., & Cousins, J. (2010). NOAA ship Thomas Jefferson Deepwater Horizon response mission report, Interim project report-Leg 3, June 15-July 1, 2010. http://www.noaa.gov/sciencemissions/PDFs/TJ%20Deepwater%20Horizon%20Response%20Project%20Report%20Leg%203_final.pdf. Accessed 18 November 2010.

Sterling, M. C., Ojo, T., Autenrieth, R., Bonner, J., Page, C., & Ernest, A. (2002). Coalescence of dispersed oil in a laboratory reactor. In *Proceedings of the 25th, Arctic and Marine Oilspill Program (AMOP) technical seminar, Calgary, AB, Canada, 2002* (pp. 721-733). Environment Canada.

Sterling, M. C., Bonner, J.S., Ernest, A. N. S., Page, C. A., & Autenrieth, R. L. (2004a). Chemical dispersant effectiveness testing: influence of droplet coalescence. *Marine Pollution Bulletin*, *48*, 969-977.

Sterling, M. C., Bonner, J. S., Page, C. A., Fuller, C. B., Ernest, A. N., & Autenrieth, R. L. (2004b). Modeling crude oil droplet-sediment aggregation in nearshore waters. *Environmental Science and Technology*, *38*, 4627-4634.

Sterling, M. C., Bonner, J. S., Ernest, A. N. S., Page, C. A., & Autenrieth, R. L. (2004c). Characterizing aquatic sediment-oil aggregates using *in-situ* instruments. *Marine Pollution Bulletin*, *48*, 533-542.

Sterling, M. C., Bonner, J. S., Ernest, A. N. S., Page, C. A., & Autenrieth, R. L. (2005). Application of fractal flocculation and vertical transport model to aquatic sol-sediment systems. *Water Research, 39,* 1818-1830.

Swedmark, M., Braaten, B., Emanuelsson, E., & Granmo, A. (1971). Biological effects of surface active agents on marine animals. *Marine Biology*, *9*, 183-204.

Taylor, G. I. (1954). The dispersion of matter in turbulent flow through a pipe. *Proceedings of the Royal Society of London, Ser. A.*, *223*(1155), 446-467.

Teledyne RD Instruments (2010) Teledyne RDI's tech tips. http://www.rdinstruments.com/tips/tips_archive/pharray_0203.aspx. Accessed 18 October 2010.

Thorne, P. D. Agrawal, Y. C., & Cacchione, D. A. (2007). A comparison of near-bed acoustic backscatter and laser diffraction measurements of suspended sediments. *IEEE Journal of Oceanic Engineering*, *32*(1), 225-235.

Tissot, B. P., & Welte, D. H. (1978). *Petroleum formation and occurrence: A new approach to oil and gas exploration.* Berlin, Germany: Springer-Verlag.

Townsend, R., Bonner, J., & Autenrieth, R., (2000). Microbial dynamics during bioremediation of crude oil-contaminated coastal wetland. *Bioremediation Journal, 4*(3), 203-218.

Turner Designs (2007). Crude oil. http://www.turnerdesigns.com/t2/doc/appnotes/S-0079.pdf. Accessed 15 November 2010.

Turner Designs (2010). Detection of refined oils (fuels) in water. http://www.turnerdesigns.com/t2/doc/appnotes/S-0113.pdf. Accessed 15 November 2010.

Urick, R. J. (1983). *Principles of underwater sound.* New York, NY: McGraw-Hill Book Company.

USACE (US Army Corps of Engineers) (1984). *Shore protection manual.* Washington DC: U.S. Government Printing Office.

U.S. Coast Guard (2006) Special Monitoring of Applied Response Technologies (SMART). http://response.restoration.noaa.gov/book_shelf/648_SMART.pdf. Accessed 15 November 2010.

US EPA (US Environmental Protection Agency) (1993a). Use of chemical dispersants for marine oil spills. EPA-600/R93/195. Cincinnati, OH: IT Corporation.

US EPA (US Environmental Protection Agency) (1993b). Methods for measuring the acute toxicity of effluents and receiving waters to fresh water and marine organisms. EPA-600/4-90/027/F. Cincinnati, OH: US Environmental Protection Agency.

US EPA (US Environmental Protection Agency) (1994). Short-term methods for estimating the chronic toxicity of effluents and receiving waters to marine and estuarine organisms. EPA-600/4-91/003. Cincinnati, OH: US Environmental Protection Agency.

US EPA (US Environmental Protection Agency) (2000). The quality of our nation's waters. EPA-841-S-00-001. http://www.epa.gov/305b/98report/98brochure.pdf. Accessed 16 December 2010.

Von der Dick, H., & Kalkreuth, W. (1985). Synchronous excitation and three-dimensional fluorescence spectroscopy applied to organic geochemistry. *Advances in Organic Geochemistry, 10*, 633-639.

Wakeham, S. G. (1977). Synchronous fluorescence spectroscopy and its application to indigenous and petroleum-derived hydrocarbons in lacustrine sediments. *Environmental Science and Technology*, *11*(3), 272-276.

Wall, G. R., Nystom, E. A., & Litten, S. (2006). Use of an ADCP to compute suspended sediment discharge in the tidal Hudson River, New York: U.S. Geological Survey scientific investigations report 2006-5055. http://pubs.usgs.gov/sir/2006/5055/pdf/SIR2006-5055.pdf. Accessed 22 February 2011.

WATERs Network (2005). WATERs test bed site – Corpus Christi Bay. http://www.watersnet.org/wtbs/wtbs05/index.html. Accessed 15 November 2010.

Wood, T. M., Lehman, R. L., & Bonner, J. (1997). Ecological impacts of a wetland oil spill and bioremediation experiments. In *International Oil Spill Conference (IOSC)*. http://www.iosc.org/papers/00580.pdf. Accessed 6 January 2010.

Yamada, M., Takada, H., Toyoda, K., Yoshida, A., Shibata, A., Nomura, H., Wada, M., Nishimura, M., Okamoto, K., & Ohwada, K. (2003). Study on the fate of petroleum-derived polycyclic aromatic hydrocarbons (PAHs) and the effect of chemical dispersant using and enclosed ecosystem, mesocosm. *Marine Pollution Bulletin*, *47*, 105-113.

VITA

Name: Christopher Byron Fuller

Address: Clarkson University
8 Clarkson Ave.
Potsdam, New York 13699

Email Address: cfuller900@gmail.com

Education: B.S., Biology, Texas A&M University, 1989
M.S., Environmental Engineering, Texas A&M University-Kingsville, 1996
Ph.D., Civil Engineering, Texas A&M University, 2011